NUREG/CR-5258
Vol. 3

Georgia/Alabama Regional Seismographic Network

Annual Report
July 1987 – June 1988

Prepared by L. T. Long

School of Earth and Atmospheric Sciences
Georgia Institute of Technology

Prepared for
U.S. Nuclear Regulatory Commission

AVAILABILITY NOTICE

Availability of Reference Materials Cited in NRC Publications

Most documents cited in NRC publications will be available from one of the following sources:

1. The NRC Public Document Room, 2120 L Street, NW, Lower Level, Washington, DC 20555
2. The Superintendent of Documents, U.S. Government Printing Office, P.O. Box 37082, Washington, DC 20013-7082
3. The National Technical Information Service, Springfield, VA 22161

Although the listing that follows represents the majority of documents cited in NRC publications, it is not intended to be exhaustive.

Referenced documents available for inspection and copying for a fee from the NRC Public Document Room include NRC correspondence and internal NRC memoranda; NRC Office of Inspection and Enforcement bulletins, circulars, information notices, inspection and investigation notices; Licensee Event Reports; vendor reports and correspondence; Commission papers; and applicant and licensee documents and correspondence.

The following documents in the NUREG series are available for purchase from the GPO Sales Program: formal NRC staff and contractor reports, NRC-sponsored conference proceedings, and NRC booklets and brochures. Also available are Regulatory Guides, NRC regulations in the *Code of Federal Regulations*, and *Nuclear Regulatory Commission Issuances*.

Documents available from the National Technical Information Service include NUREG series reports and technical reports prepared by other federal agencies and reports prepared by the Atomic Energy Commission, forerunner agency to the Nuclear Regulatory Commission.

Documents available from public and special technical libraries include all open literature items, such as books, journal and periodical articles, and transactions. *Federal Register* notices, federal and state legislation, and congressional reports can usually be obtained from these libraries.

Documents such as theses, dissertations, foreign reports and translations, and non-NRC conference proceedings are available for purchase from the organization sponsoring the publication cited.

Single copies of NRC draft reports are available free, to the extent of supply, upon written request to the Office of Information Resources Management, Distribution Section, U.S. Nuclear Regulatory Commission, Washington, DC 20555.

Copies of industry codes and standards used in a substantive manner in the NRC regulatory process are maintained at the NRC Library, 7920 Norfolk Avenue, Bethesda, Maryland, and are available there for reference use by the public. Codes and standards are usually copyrighted and may be purchased from the originating organization or, if they are American National Standards, from the American National Standards Institute, 1430 Broadway, New York, NY 10018.

NUREG/CR-5258
Vol. 3
RA

Georgia/Alabama Regional Seismographic Network

Annual Report
July 1987 – June 1988

Manuscript Completed: August 1990
Date Published: September 1990

Prepared by
L. T. Long

School of Earth and Atmospheric Sciences
Georgia Institute of Technology
Atlanta, GA 30332

Prepared for
Division of Engineering
Office of Nuclear Regulatory Research
U.S. Nuclear Regulatory Commission
Washington, DC 20555
NRC FIN D1598
Under Contract No. NRC-04-85-122

EXECUTIVE SUMMARY AND ABSTRACT

OBJECTIVE:

The objective of this study is to contribute data and analyses conducive to the development of criteria for establishing earthquake hazard potential in the southeastern United States.

TASKS:

The first task is to install and maintain the Georgia/Alabama seismic network. The seismic network consists of about 21 stations in Alabama, Georgia, and adjoining regions of southeastern Tennessee and South Carolina. The seismic net includes three three-component short period stations and operates completely on solar power.

The second task is to monitor the seismic activity in southeastern Tennessee, northern Alabama, and Georgia. The data are to be used in appropriate topical studies.

RESULTS:

Four topical studies achieved notable conclusions or were completed during the reporting period of July 1987 to June 1988. The principal conclusions for these four topical studies are summarized below and presented in detail in the Appendices. In addition, we examined the rate of seismicity through time in southeastern Tennessee. A review of the historical seismicity of southeastern Tennessee suggests that the period of 1970 through 1988 was anomalously more active than before 1970. The greatest uncertainty relates to the uniformity of coverage and detection. If this period is indeed more active, then it represents a unique stress release event that would satisfy the model for major intraplate earthquakes proposed by Long (1988).

First motion data and SV/P amplitude ratios were used to determine 36 single event and two composite focal mechanism solutions for earthquakes in southeastern Tennessee. The dominant focal mechanism is strike slip; however, the focal mechanisms exhibited components of reverse and normal fault movement. Estimates of solution confidence suggest that the variation in focal mechanism is significant.

Coda Q is determined by the integrated effects of crustal parameters in the ellipsoidal volume of crust with the recording station and hypocenter as foci. Zones of anomalous crust will influence the computation of coda Q differently for different station and hypocenter pairs. We have linearized the relation between the measured apparent coda Q and an assumed constant coda Q for discrete zones of crust. Inversion of coda Q data near station CBT suggests an anomalously low coda Q region (Q=50) in a 300 kilometer region northeast of station CBT.

Fracture density was mapped in an area of induced seismicity in the Clarks Hill Reservoir area in sufficient detail to allow contouring of the

data. These contours suggest that areas of higher joint spacing correspond to zones of induced seismicity. The rock type typically described as granite gneiss has shown a spatial correlation with reservoir induced seismicity in this and other seismic reservoirs. Earthquakes tend to occur where jointing is sparse and the rock is strong. In contrast, seismic activity is not often observed in foliated schists and altered mafic rocks, in which stress may be released through creep or failure along the many foliations and fractures.

Earthquakes in the Lake Sinclair Reservoir area were relocated using a technique in which the origin time was computed independent of the location. The location residuals improved substantially with a velocity model which includes an abnormally high (6.6 km/s) crustal velocity at 2.0 km depth. The relocated activity suggests clustering of seismicity in five distinct zones.

TABLE OF CONTENTS

LIST OF FIGURES

List of Figures (continued)

List of Figures (continued).

Appendix D

LIST OF TABLES

GEORGIA/ALABAMA REGIONAL SEISMOGRAPHIC NETWORK

Objectives

The objective of this study is to contribute data and analyses conducive to the development of criteria for establishing earthquake hazard potential in the southeastern United States. The main tasks are to install and maintain a seismic network and monitor the seismic activity in eastern Tennessee, northern Alabama, and Georgia. The data are to be contributed to the southeastern U. S. regional bulletin. Also, available information will be used in appropriate topical studies.

* Specific objectives for network maintenance and seismic monitoring are as follows:

* Install or provide about 16 short-period seismograph stations deployed in Tennessee, Alabama, and Georgia. This network is to be operated with a maximum of 5 percent downtime.

* Obtain and/or reaffirm use permits and telemetry service to convey the data to a central recording point.

* Provide all seismic phase readings and hypocenter locations to the Southeast U. S. Seismographic Network Bulletin.

* Provide a recording medium with on-line digital recording at the Central Recording Facility.

* Report any significant earthquake within the study region to the Nuclear Regulatory Commission within 24 hours.

* Relocate and/or establish new seismograph stations as it becomes necessary after approval of the Nuclear Regulatory Commission.

Objectives for topical studies are as follows:

* Study the spatial and temporal distributions, including earthquake recurrence rates, of seismicity and relate them to structural features.

* Identify parameters that influence seismic processes within the network area and use these in defining seismogenic/tectonic provinces.

* Study crustal and upper mantle velocity structure in the United States based on the current data from the network.

* Study the magnitudes of historic events using magnitude-felt area relationships and obtain the magnitude-frequency relationships.

* Evaluate the relative significance of results obtained in each of the above analyses as they impact the determination of seismic hazards.

Summary of Results and Findings

Network maintenance and seismic monitoring

During the period of 1 July, 1987, to 30 June, 1988, the Georgia/Alabama regional Seismic Net consisted of 21 stations located as shown in Figure 1. The Clarks Hill Reservoir Area and the area of Lake Richard B. Russell were monitored by four stations. The State of Georgia is monitored by five additional stations. Seven stations are located in Alabama and five in southeastern Tennessee. The Alabama, Tennessee and northwest Georgia stations constitute coverage for the termination of the southern Appalachian seismic zone. Most of the time during July and August was consumed by trips to replace or fix field systems damaged by thunder storms. The efforts to replace or fix field systems damaged by thunder storms continues to require a significant portion of the work time during the summer quarter. Station CH6 will be taken down to allow lumbering on the station site during the winter months.

All stations in the Georgia/Alabama Regional Seismographic Network are monitored by a digital acquisition system. Triggered events are saved to disk and, if appropriate, saved on tape for later study. The digital system recorded the entire record of the Alaskan Earthquake and most smaller local events. The large Virginia mine collapse was recorded. A magnitude 2.7 event was detected near Knoxville. The Alabama quake was recorded in its entirety by the digital system. Two significant local events were recorded during December. One near our station TLT in southeastern Tennessee and the other in a swarm in the Richard B. Russell Reservoir, marking the first significant induced seismicity by that reservoir. Later, one additional small event was detected in the Richard B. Russell Reservoir area, suggesting continued reservoir induced seismicity.

With the cooperation of mine operators in Alabama, a digital event recorder in the area of recent large mine bumps is obtaining data on local events for the period of September, 1987 through mid-December, 1987. However, the expected Alabama mine collapse event caused only a swarm of activity that reached a peak March 20. We have a set of digital 3-component records of the swarm. The Alabama mine monitoring indicated an increase in activity at the time the longwall was in line with the previous large mine collapses.

One interesting aspect of the historical seismicity in southeastern Tennessee is the apparent increase in seismicity in the last 20 years. During this year an effort was made to test the stationarity of the seismicity by examination of the historical record. The study included a reevaluation of the ATL WWSSN records of southeastern Tennessee earthquakes to develop consistency in magnitudes. Reported felt area, duration magnitude and local body wave magnitudes were examined and recomputed where appropriate. Some minor adjustments in recently computed magnitudes were made; however, most historical events, before 1960, have magnitudes based on intensity data and no significant discrepancies were found. The resulting catalog was then used to compute strain release, energy release and event frequency in ten year increments.

Figure 2 shows frequency of occurrence of magnitude greater than three events and Figure 3 shows frequency of occurrence of magnitude greater than

four events. In both cases a dominant peak appears in the 1955 decade. The last 20 to 40 years are greater than the previous years. Figure 4 gives the strain release, which also shows a minor peak in 1955, but is dominated by the influence of the many small events reported in the last decade. The strain release mimics the number of magnitude greater than two events, which are susceptible to gaps in detection. The energy release, Figure 5, also shows an increase in the 1955 to present time span. Unfortunately, the normal tests for completeness do not work when testing for variations in activity with time. Two observations suggest that the recent increase in valid. First the magnitude four and larger events show a distance increase. These would be expected to be detected at least for the last 100 years. Second, the rate of seismicity from historical data in western North Carolina is greater than in the recent monitored data, suggesting that such events would have been noted and a change in activity is possible.

A review of the historical seismicity of southeastern Tennessee suggests that the period of 1970 through 1988 was anomalously more active than before 1970. The greatest uncertainty relates to the uniformity of coverage and detection. If this period is indeed more active, then it represents a unique stress release event that would satisfy the model for major intraplate earthquakes proposed by Long (1988).

Graphical representation of the operational status of the network

The high level of station down time in the late spring was caused by heavy thunder storm activity and lightening damage. The graphical representation of the operational status of the network is given in the form of the daily log of recording and is given in figure 6.

Plans for next year

Digital data accumulating for the southeastern Tennessee area is showing evidence of a highly variable coda Q. Plans for next year include the development of an inversion technique for coda Q in southeastern Tennessee. The first step will be the development of a computational model to generate synthetic coda.

The studies of seismicity and crustal structure in southeastern Tennessee have lead to the development of a theory for major intraplate earthquakes. The data from southeastern Tennessee will be examined for consistency with this model. In particular, we will look for evidence in coda Q and focal mechanisms.

Focal mechanisms will be compared to computed estimates of stress surrounding a weak zone in a plate in order to evaluate the consistency of focal mechanisms in southeastern Tennessee with a model for major earthquakes.

The rate of attenuation of Lg phase in Alabama will be examined for possible comparison with intensity data. Because earthquake data are sparse, the attenuation study will use blast data.

The Rg waves recorded from the many blasts in Alabama will be used to solve for the shallow crustal structure.

Abstracts of Presentations

The following are abstracts of talks which were made possible by data and research related to the Georgia/Alabama seismographic network.

A STUDY OF THE DISTRIBUTION OF FOCAL MECHANISM SOLUTIONS OF EARTHQUAKES IN SOUTHEASTERN TENNESSEE.

ZELT, K.-H. and LONG, L. T., School of Geophysical Sciences, Georgia Institute of Technology, Atlanta, Georgia 30332-0340.

The infrequent occurrence of earthquakes in the southeastern United States and sparse seismic station coverage limits the number and distribution of first motions and SV/P amplitude ratios available for the determination of focal mechanism solutions. Subsequently, only solutions from large MD > 3.0 earthquakes are well constrained. For most of the smaller events, the sparse coverage of the focal sphere introduces ambiguity to the focal mechanism. Consequently, the certainty of determining a local stress field or a deviation from the regional stress field is limited. In southeastern Tennessee, the pattern of seismicity is diffused and cannot be associated with a distinct single fault. The majority of large events (MD > 3.0) occur near the center of southeastern Tennessee activity and have a strike-slip mechanism with predominantly north-south striking nodal planes. Outside the central zone, smaller events which may be recorded on only a few stations show a spatial distribution of normal or reverse components in the predominant strike-slip component. A statistical treatment of the distribution of first motions on the focal sphere is used to establish a measure of confidence for the focal mechanism solution of the smaller events in southeastern Tennessee and to establish the validity of the special distribution of normal and reverse components.

Presented at the American Geophysical Union, Spring Meeting, Baltimore, Maryland, May 16, 1988.

A MECHANISM FOR MAJOR INTRAPLATE EARTHQUAKES

LONG, L.T., School of Geophysical Sciences, Georgia Institute of Technology, Atlanta, GA 30332.

The seismicity associated with a major intraplate earthquake is proposed to be a transient phenomenon triggered by a perturbation in the fluid and thermal regime of the lower crust. A major intraplate earthquake has a magnitude greater than 6, and a fault rupture of crustal dimensions; 20 km or greater. Regional plate stress provides the energy, and a perturbation in the fluid content, which decreases crustal strength, determines the location. The timing of a major earthquake and the characteristics of associated seismicity may be described by a sequence of five phases in the perturbation of crustal

strength. The five phases are: (1) initiation, (2) strength corrosion, (3) stress concentration, (4) failure, and (5) crustal healing. (1) A major intraplate earthquake is initiated by the underplating at Moho depths of a portion of the continental crust. (2) A corrosion in crustal strength follows the upward migration of fluids from the area of recent underplating. (3) As a weakened central zone deforms in response to tectonic plate stress, stresses are concentrated in the surrounding rigid crust. (4) A major earthquake occurs when the stress surrounding the weakened core exceeds the crustal strength, either because the concentrated stresses are anomalously high or because the dispersing fluids have spread beyond the core. (5) The final phase in the occurrence of a major intraplate earthquake is extended aftershock activity concentrated on the fault plane of the main event. The occurrence of a major intraplate earthquake as described above releases the strain energy in a perturbed area. Additional major events would not occur there again until the strength has recovered sufficiently for a repeat of the cycle.

Presented at the American Geophysical Union, Spring Meeting, Baltimore, Maryland, May 16, 1988.

PARADIGM FOR MAJOR INTRAPLATE EARTHQUAKES

LONG, L. T., Georgia Institute of Technology, School of Geophysical Sciences, Atlanta, Georgia, 30332.

Let us discard the traditional paradigms of continental seismicity. Let us assume, instead, that the seismicity associated with a major (magnitude 6 or larger) intraplate earthquake is a transient phenomenon triggered by a perturbation in the fluid and thermal regime of the lower crust. Regional plate stress may still provide the energy, but instead of high stress triggering an event, let us assume a decrease in crustal strength in the vicinity of the major earthquake. The timing of a major earthquake and the characteristics of the associated seismicity may be described by a sequence of five phases: (1) initiation, (2) strength corrosion, (3) stress concentration, (4) failure, and (5) crustal healing. (1) A major intraplate earthquake is initiated by the under-plating at Moho depths of a portion of the continental crust. (2) A corrosion in crustal strength follows the upward migration of fluids from the area of recent underplating. (3) As a weakened central zone deforms in response to tectonic plate stress, stresses are concentrated in the surrounding rigid crust. (4) A major earthquake occurs when the stress surrounding the weakened core exceeds the crustal strength, either because the concentrated stresses are anomalously high or because the dispersing fluids have spread beyond the core. (5) The final phase in the occurrence of a major intraplate earthquake is extended aftershock activity which is concentrated on the fault plane of the main event. The occurrence of a major intraplate earthquake as described above releases the strain energy in a perturbed area. Additional major events would not occur there again until the strength has recovered sufficiently for a repeat of the cycle.

Presented at the National Workshop on Seismogenesis in the Eastern United States, University of Illinois at Urbana-Champaign, Urbana, Illinois, April 12, 1988.

ZONES OF INDUCED SEISMICITY DEFINED BY ROCK QUALITY

SORLIEN, C. C., LONG, L. T., Georgia Institute of Technology, Atlanta, Georgia, 30332, and SCHMITT, T. J., Georgia Geologic Survey, 19 Dr. Martin Luther Dr., Atlanta, Georgia 30334.

Preliminary measurements of fracture density and rock quality have shown a relation with reservoir induced seismicity. Fracture density maps have been made at Clarks Hill Reservoir. The results show that areas of higher joint spacing correspond to zones of induced seismicity. Also, in other reservoirs, the rock type typically described as granite gneiss has shown a spatial correlation with reservoir induced seismicity. In reservoir induced seismicity, earthquakes occur by failure on pre-existing joints. Hypocentral depths of these earthquakes are typically less than 1 km, and it has been demonstrated that fracture density is not strongly dependent on depth in the first km. Therefore quantitative surface measurements of rock quality (which includes fracture density) can be extrapolated to the zone of induced earthquake nucleation. In contrast, stress may be released through creep on (foliated) schists and altered mafic rocks, explaining the lack of seismicity in those rock types. A complementary measurement of slickenside data can usually be collected on the same outcrops. Very fine scratches, and fresh slickensides in saprolite are both assumed to be related to the recent stress field. The striation data is then inverted for the local and regional stress field at time of movement. In this manner, rock quality measurements can be used to predict susceptibility to induced or natural shallow seismicity, so that important facilities can be properly sited an engineered.

Presented at the Association of Engineering Geologists, 30th Annual Meeting, Atlanta, Georgia, October 8-13, 1987.

FOCAL MECHANISM SOLUTIONS FOR NORTH GEORGIA AND SOUTHEASTERN TENNESSEE EARTHQUAKES (1982-1987).

ZELT, K.-H., and LONG, L. T., School of Geophysical Sciences, Georgia Institute of Technology, Atlanta, GA 30332-0340.

Seventy-one earthquakes recorded on the Georgia Tech Seismic Network and adjacent stations operated by the Tennessee Valley Authority and the Tennessee Earthquake Information Center were investigated to determine focal mechanism solutions. These events occurred during the period between January 1982 and December 1986 and have epicenters in North Georgia and southeastern Tennessee. First motion data and SV/P amplitude ratios were used to determine 36 single event and two composite focal mechanism solutions. The composite solutions were determined using data of two earthquakes. The solutions include four previously published focal mechanism solutions (Teague et al., 1984). The duration magnitude ranged from 0.7 to 3.8. Focal mechanism solutions of nine events could not be restricted to a unique domain. Including both unique and multiple domain solutions the results are divided into three categories of focal mechanism solutions: Twenty-two strike-slip, nine reverse and 18 normal. Twenty of the 38 earthquakes have data coverage over all four quadrants, 17 over three quadrants and one focal mechanism solution was determined from data coverage over two quadrants. The average depth of earthquakes investi-

gated equals 17.68 kilometers. The percent of the nodal planes that strike north-south is 59, 44.5, 27.7 and for those that strike northwest 41, 55.5, 61 for strike-slip, reverse and normal focal mechanism solutions respectively, The strike-slip, reverse and normal focal mechanism solutions have average depths of 18.4, 15.3 and 17.9 kilometers respectively.

Published as [(abs.) Seism. Res. Lettrs., Vol. 58, No. 4, 1987, p. 106]

Presented at the 59th Annual Meeting Eastern Section, Seismological Society of America, St. Louis University, St. Louis, Missouri, October 7-9, 1987.

A FINITE DIFFERENCE STUDY OF THE EFFECT OF AN OVERTHRUST ON THE PROPAGATION OF SEISMIC WAVES.

LIOW, J.-S. and LONG, L.T., School of Geophysical Sciences, Georgia Institute of Technology, Atlanta, GA 30332

A two-dimensional finite difference technique was developed to study the effect of an overthrust on the propagation of seismic waves. The structural model consists of a 3.5 km thick sedimentary layer over a crystalline basement. The P-wave velocity of the sedimentary layer and the basement are 4.5 km/s and 6.15 km/s respectively. A wedge-shaped overthrust zone with P-wave velocity of 6.05 km/s replaces part of the sedimentary layer on one side of the model. Synthetic seismograms are generated for a compressional line source at depths of 0.5 km and 7.0 km. The amplitude variation with distance of different phases are compared for waves traveling from the opposite direction. For a source at shallow depth, the existence of the high-velocity overthrust zone causes a more rapid decay of the amplitude of the direct wave. However, the overthrust zone does not affect the P and S reflections from the bottom of the sediments and the Rayleigh waves as strongly as it affects the direct wave. The amplitude of the secondary phases increase on traveling from the overthrust zone into the sediments. For the deeper source, the existence of the overthrust zone does not significantly affect the amplitude decay of either the direct wave or the other phases. For the deep source underneath the overthrust zone, the amplitude of the direct wave observed in the sediments within a short distance from the edge of the overthrust zone is enlarged by a factor of three. Also, more scattered phases are observed in the sediments.

Published as [(abs.) Seism. Res. Lettrs., Vol, 58, No. 4, 1987, p. 100]

Presented at the 59th Annual Meeting, Eastern Section, Seismological Society of America, St.Louis University, St. Louis, Missouri, October 7-9, 1987.

A TECHNIQUE FOR THE INVERSION OF CODA Q

LONG, L. T., LIOW, J.-S., School of Geophysical Sciences, Georgia Institute of Technology, Atlanta, Georgia 30332 and JONES, F. B., Georgia Southwestern, Department of Physics, Americus, Georgia 31709

Digital data from station CBT in southeastern Tennessee provide estimates of

coda Q with variations which depend on the direction to the earthquake. We interpreted this azimuthal variation to indicate a spatial variation of the properties of the crust that determine coda Q. Coda Q is a phenomenological parameter characterizing coda decay and it is determined by the integrated effects of crustal parameters in the ellipsoidal volume of crust with the recording station and hypocenter as foci. Zones of anomalous crust will influence the computation of coda Q differently for different station and hypocenter pairs. Through a sequence of approximations, we have linearized the relation between the measured apparent coda Q and an assumed constant coda Q for discrete zones of crust. Inversion of coda Q data from regional stations in the southeastern United States suggests a reduction in coda Q as one nears the coastal plane, consistent with the results of Singh and Herrmann (1983). Inversion of coda Q data near station CBT suggests an anomalously low coda Q region (Q=38) in a 300 square kilometer region northeast of station CBT.

Published as [(abs.) Seis. Res. Lettrs., Vol. 58, No. 4, 1987, p. 101]

Presented at the 59th Annual Meeting, Eastern Section, Seismological Society of America, St. Louis University, St. Louis, Missouri, October 7-9, 1987.

A Master's thesis by Jeff Ogilvie was completed on the generation of seismic coda and on the inversion of seismic coda for structure in the earth's crust.

Results of topical studies

Four topical studies achieved notable conclusions or were completed during the reporting period of July 1986 to June 1987. The principal conclusions are summarized below and presented in detail in Appendices A-D.

Appendix A summarizes the results of focal mechanism studies. First motion data and SV/P amplitude ratios were used to determine 36 single event and two composite focal mechanism solutions for earthquakes in southeastern Tennessee. The dominant focal mechanism is strike slip; however, the focal mechanisms exhibited components of reverse and normal fault movement. Estimates of solution confidence suggest that the variation in focal mechanism is significant. The unique and new approach of this analysis, which includes improved hypocentral precision, is the use of statistical parameters to quantify the confidence level of focal mechanism solutions. The confidence levels allow a rational comparison of focal mechanism solutions of differing quality with models of stress in the crust. For an individual event the distribution of first motions was quantified by the random probability factor, a measure of randomness of the distribution of take-Off points. The quality of first motions was quantified by confidence levels which were assigned by the interpreter to each reading and which were adjusted by a consideration of adjacent points. The quality of the fit of the focal mechanism solution was quantified by a confidence measure which was computed for the fit of the data to a focal mechanism solution by using a Chi-Square distribution test developed specifically for polarity data.

Appendix B describes the initial development of a technique to find regional variations in Coda Q. Coda Q is determined by the integrated effects of crustal parameters in the ellipsoidal volume of crust with the recording station and hypocenter as foci. Zones of anomalous crust will influence the computation of coda Q differently for different station and hypocenter pairs. We have linearized the relation between the measured apparent coda Q and an assumed constant coda Q for discrete zones of crust. Inversion of coda Q data near station CBT suggests an anomalously low coda Q region (Q=50) in a 300 kilometer region northeast of station CBT.

Appendix C gives the results of the analysis of field data on joint systems obtained in the seismic zone of the Clarks Hill Reservoir. Fracture density was mapped in an area of induced seismicity in the Clarks Hill Reservoir area in sufficient detail to allow contouring of the data. These contours suggest that areas of higher joint spacing correspond to zones of induced seismicity. The rock type typically described as granite gneiss has shown a spatial correlation with reservoir induced seismicity in this and other seismic reservoirs. Earthquakes tend to occur where jointing is sparse and the rock is strong. In contrast, seismic activity is not often observed in foliated schists and altered mafic rocks, in which stress may be released through creep or failure along the many foliations and fractures.

Appendix D gives the results of relocating earthquakes in the Lake Sinclair Area. Earthquakes in the Lake Sinclair Reservoir area were relocated using a technique in which the origin time was computed independent of the location. The location residuals improved substantially with a velocity model which includes an abnormally high (6.6 km/s) crustal velocity at 2.0 km depth. The relocated activity suggests clustering of seismicity in five distinct zones.

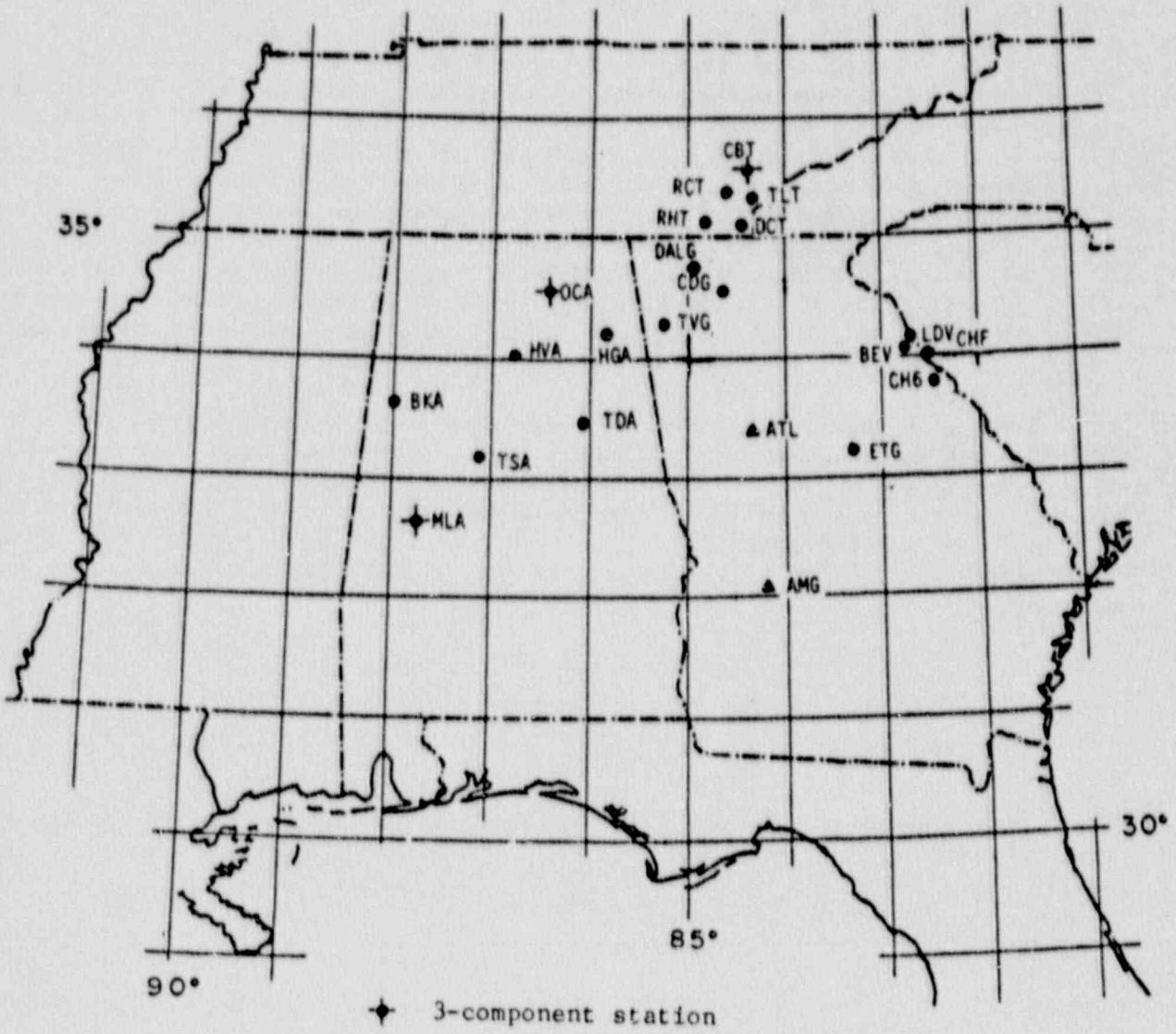

Figure 1. Distribution of seismic stations recorded during the period of 1 July, 1987 to 30 June, 1988.

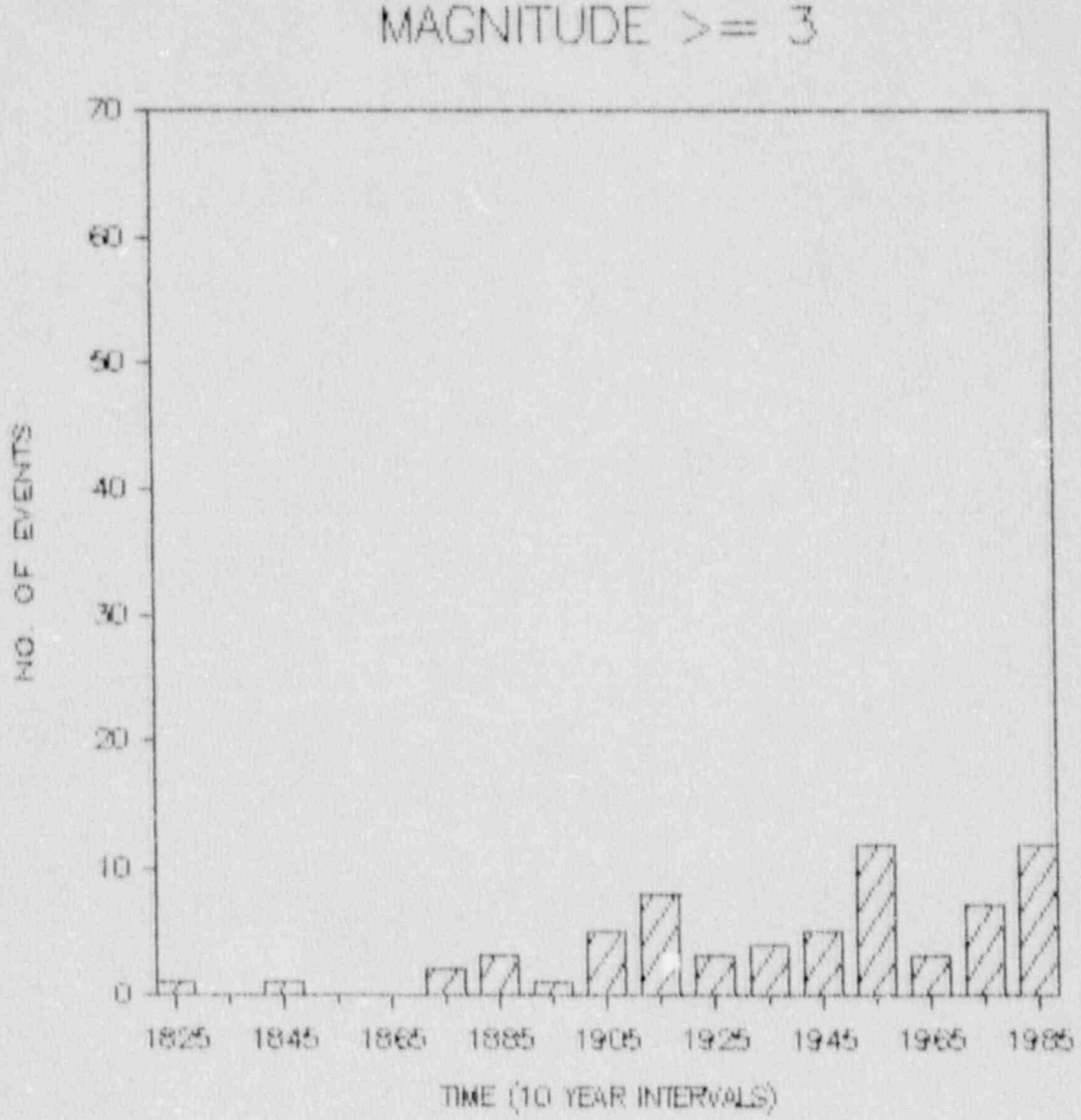

Figure 2. Frequency of occurrence of events with magnitude greater than three. The number of events is for ten year periods in southeastern Tennessee.

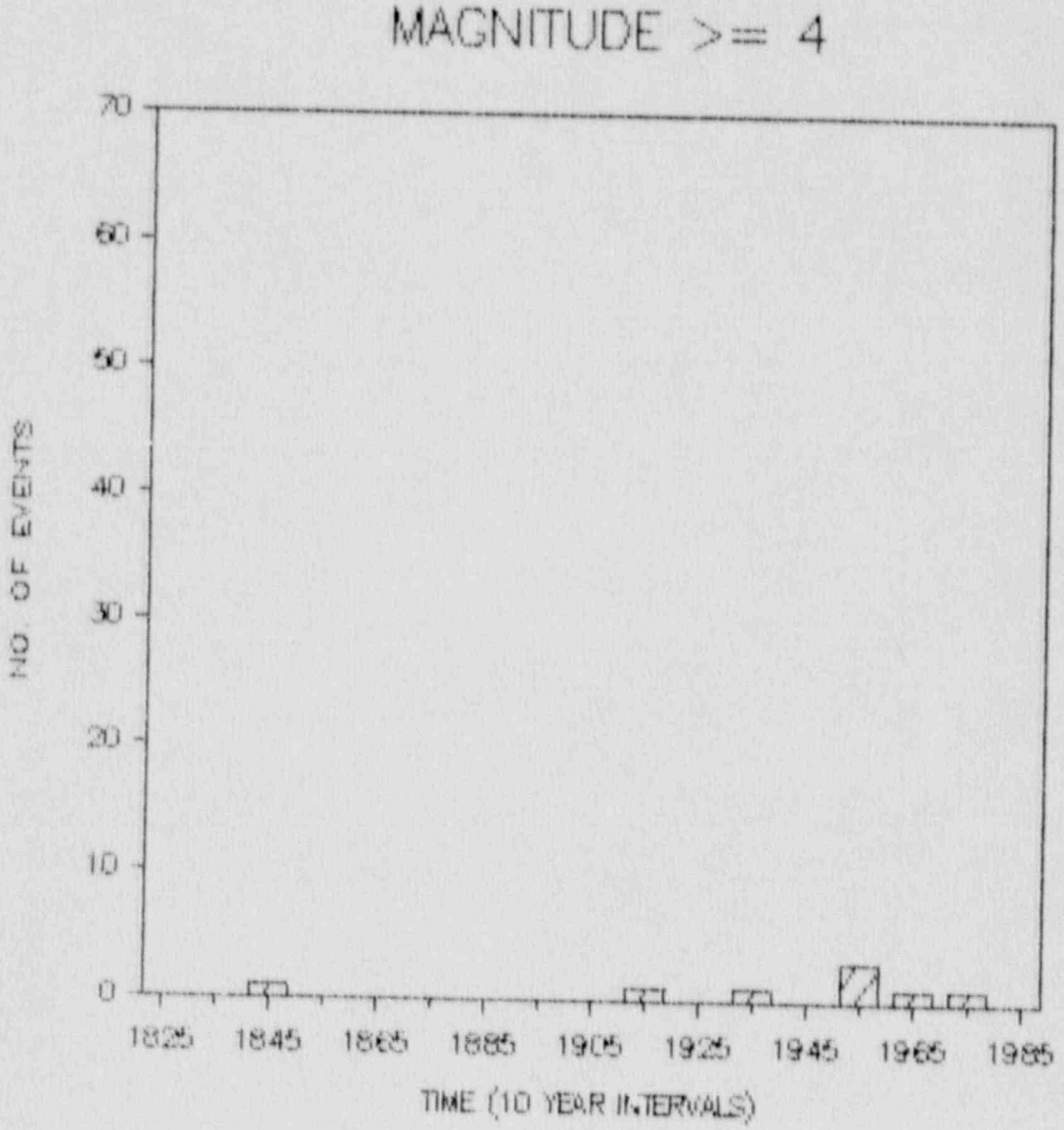

Figure 3. Frequency of occurrence of events with magnitude greater than four. The number of events is for ten year periods in southeastern Tennessee.

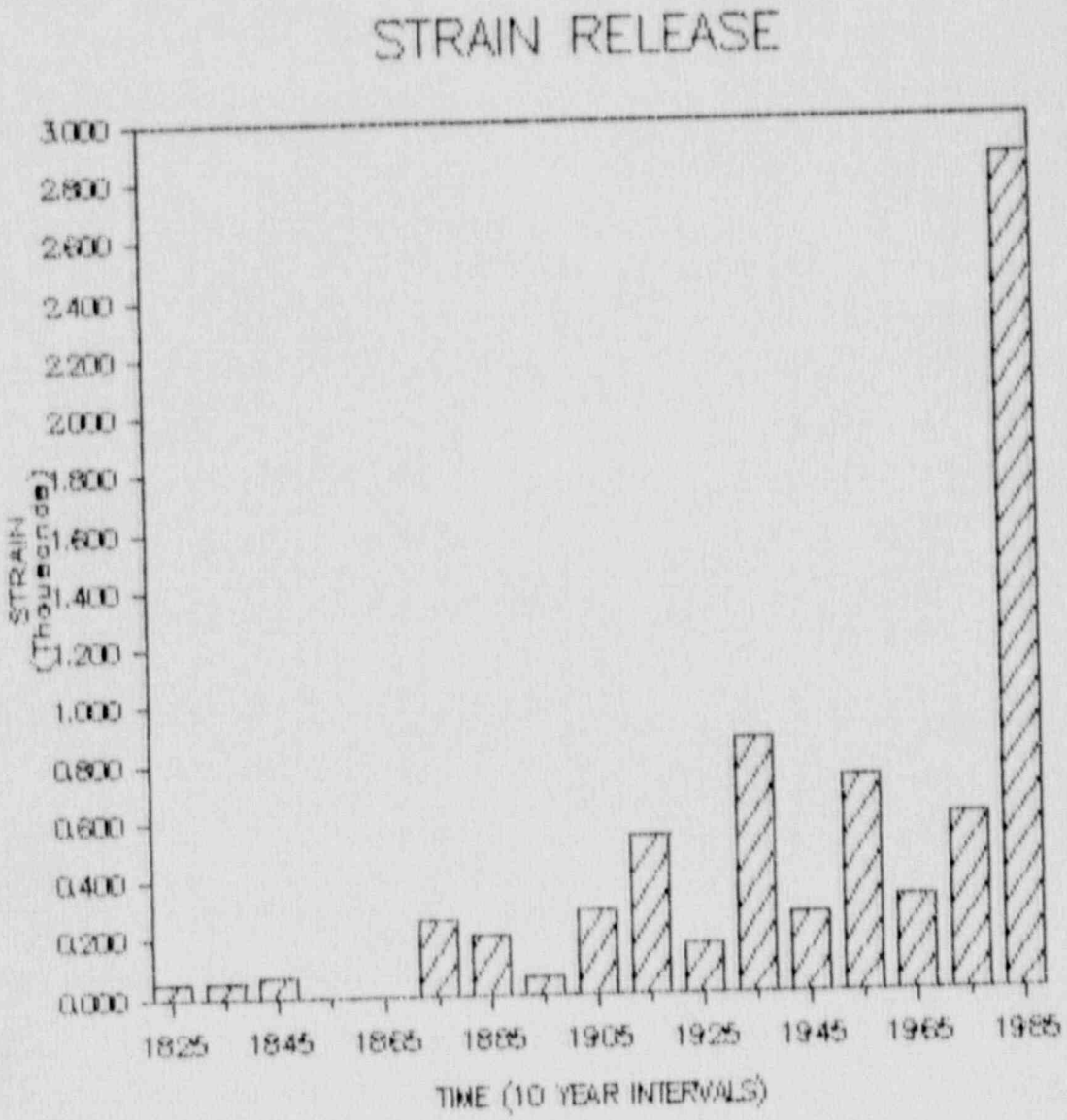

Figure 4. Strain release in ten year increments for recorded seismicity in southeastern Tennessee.

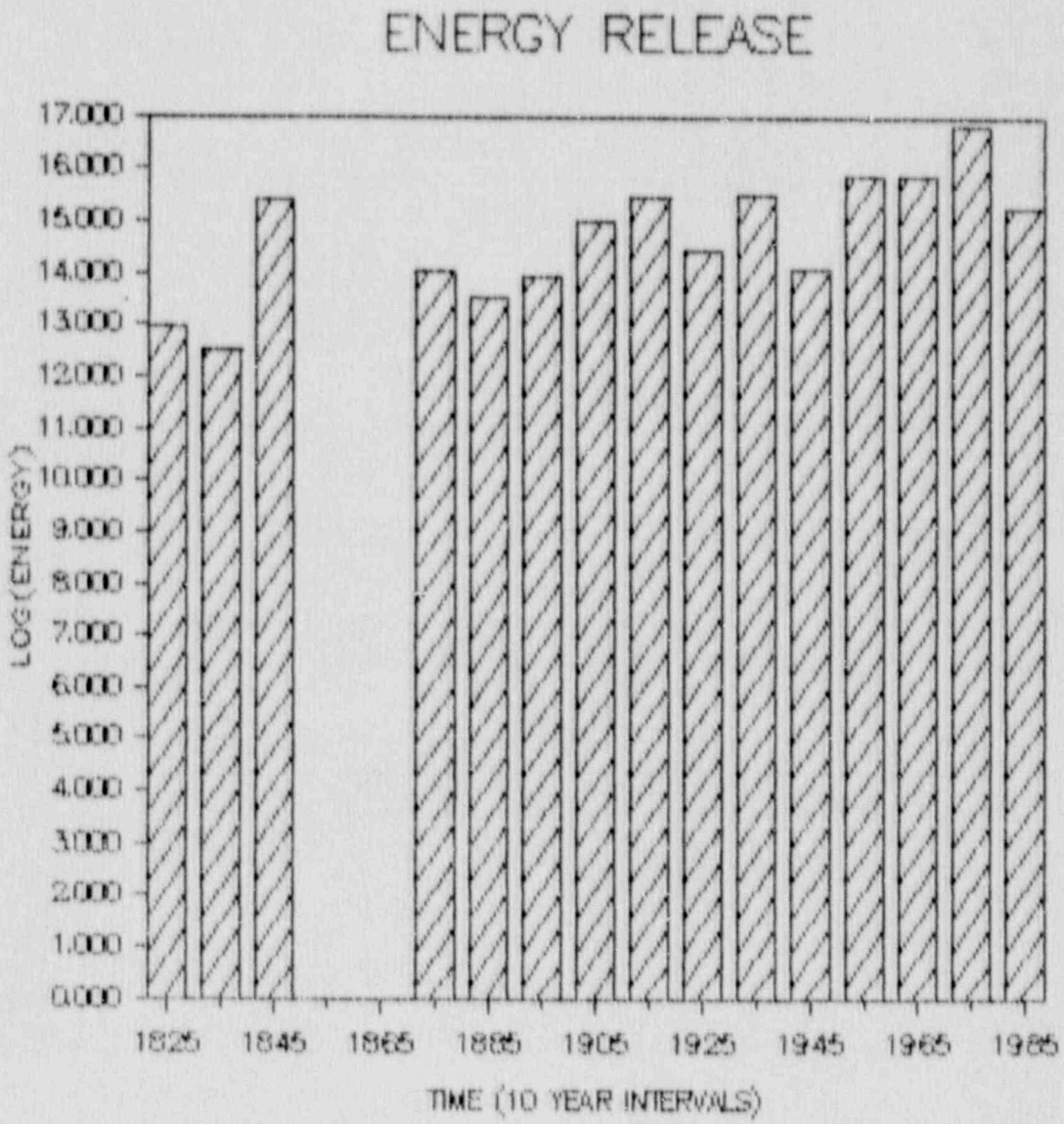

Figure 5. Energy release in ten year increments for southeastern Tennessee computed from magnitude.

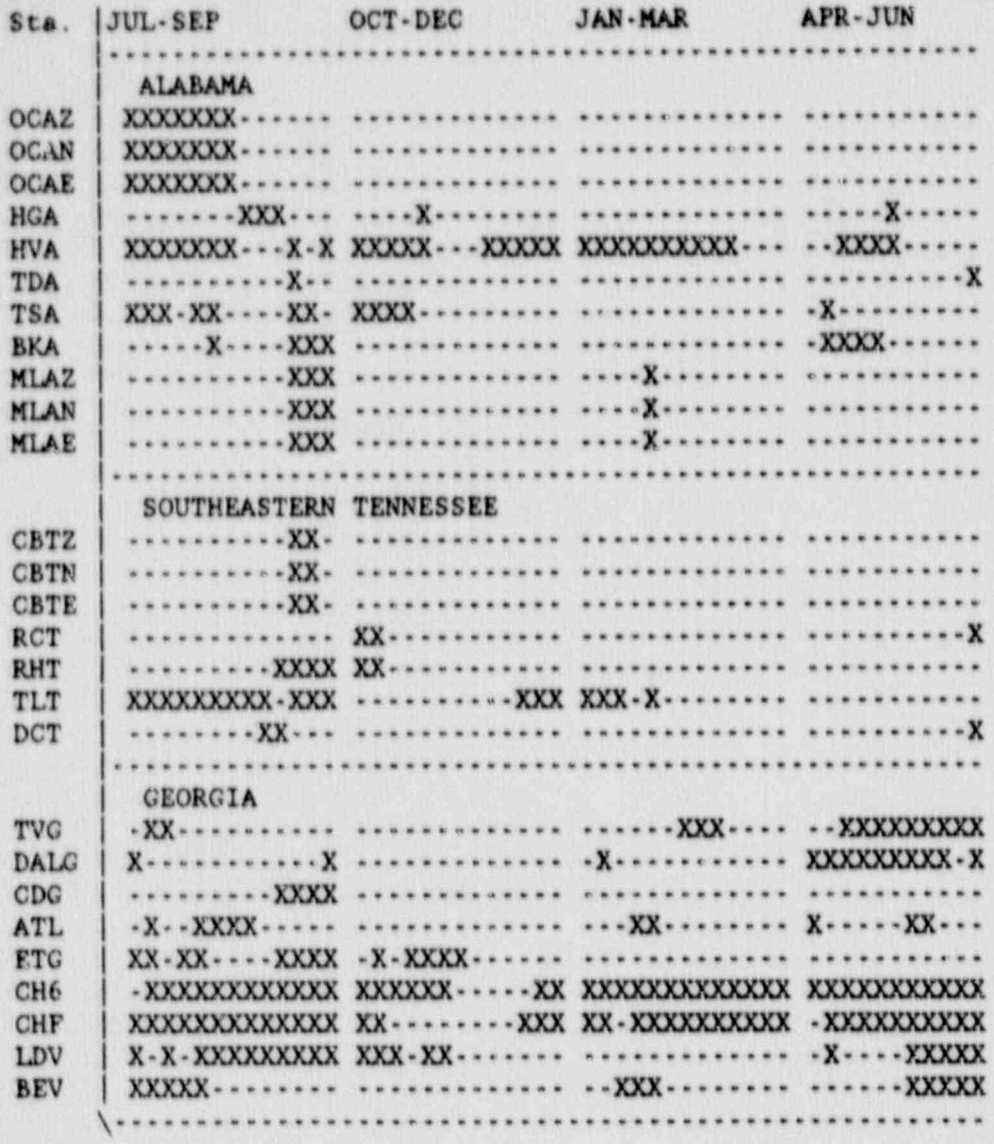

Figure 6. Graphical representation of the operational status of the Georgia/Alabama Seismographic Network.

APPENDIX A

Pattern of Earthquake Focal Mechanisms in Southeastern Tennessee

APPENDIX A

PATTERN OF EARTHQUAKE FOCAL MECHANISMS IN SOUTHEASTERN TENNESSEE

Karl-Heinz Zelt and Leland T. Long

ABSTRACT: In southeastern Tennessee earthquakes are located in a diffused pattern and cannot be associated with a single distinct linear structure. We have extended the data set of 14 published focal mechanism solutions for the period of 1977 to 1984 with 43 focal mechanism solutions for the period 1982 to 1987. In this study earthquake locations were computed by a method that uses the S-P times to isolate the origin time computation from the location computation. A statistical treatment of the distribution of first motions on the focal sphere is used to establish a measure of confidence for the focal mechanism solution of the smaller events in southeastern Tennessee. The majority of events with magnitude greater than three occur near the center of southeastern Tennessee activity and have a strike-slip mechanism with predominantly north striking nodal planes. Outside the central zone, smaller events which may be recorded on only a few stations show a spatial distribution of normal or reverse components in the predominant strike-slip component. The validity of the spatial distribution is investigated using a statistical treatment as a measure of confidence in each focal mechanism solution.

INTRODUCTION

As of 1985, earthquake focal mechanism solutions had been published for 14 earthquakes in southeastern Tennessee and northern Georgia (see Table 1 for published focal mechanism solutions). The Maryville, Tennessee, earthquake of 30 November 1973 provided the first estimate of the principle stress directions; however, the results were ambiguous. Bollinger et al. (1976) with regional P-wave first motions determined two equally possible solutions: normal faulting on either a northeast or a southeast striking nodal plane or reverse faulting with northwest striking nodal planes. First motion data obtained during the aftershock survey suggested a strike-slip or horizontal thrust motion incompatible with the solution for the main shock. Herrmann (1979) using surface waves obtained a solution with predominantly strike-slip faulting on north-northeast or east-southeast striking nodal planes for the Maryville event. Guinn (1980) and Guinn and Long (1977) introduced the concept of domains of valid P, T and B axes as a means of evaluating focal mechanism solutions in cases of limited data. The domains of valid principle axes for first motions for the 30 November 1973 Maryville earthquake contained both focal mechanism solutions published by Bollinger et al. (1976). In condition, Guinn (1980) found domains of valid P, T and B axes suggesting reverse fault movement with northwest striking nodal planes for both the 4 February 1976 Conasauga, and the 27 July 1977 Englewood, Tennessee, earthquake. Reinbold and Cornwell (1983) using first motion data determined a composite solution suggesting strike-slip fault motion with a north-northeast and a nominally east striking nodal plane for the Greenback, Tennessee, earthquakes on 24 September 1982.

The first analysis of focal mechanisms from data recorded through 1983 by a regional network installed in 1980 (Teague, 1984) found 11 single event and 11 composite focal mechanism solutions. The Teague et al. (1986) analysis used the technique of Guinn and Long (1977) as extended by Tzeng (1982) to include both first motions and SV/P amplitude ratios and as rewritten in program FOCMEC by Snoke et al. (1984). The dominant focal mechanism solution obtained by Teague et al. (1986) was strike-slip with north or east striking nodal planes. Many of Teagues (1984) results are based on data sets of less than 10 points and thus the domains of valid principle axes can be large Johnston et al. (1985) extended the focal mechanisms from the seismic network data through 1984 to include a focal mechanism solution for the 14 February 1984 earthquake occurring north of Knoxville near Mascot, Tennessee. This well-constrained solution was strike-slip on a north or east striking nodal plane. The focal mechanism solutions are shown in Figure 1.

The total of 14 published focal mechanism solutions did not suggest that a single type of focal mechanism would apply to all southeastern Tennessee and northern Georgia earthquakes; however, for all of the 14 solutions the principle compressive stress direction strikes northeast. Focal mechanism solutions range from pure strike-slip to events with large components of reverse or normal fault movement (see Figure 1). Nine of the 14 solutions were composite solutions because the single events had usable arrivals at less than 10 stations which were distributed so as to require additional data from nearby events to limit the size of the domains of valid principle axes. In addition to sparse data, uncertainty in depth of focus could contribute to the uncertainty in direction of the principle axes. Johnston et al. (1985) discussed the issue of hypocentral depth for earthquakes in southeastern Tennessee and concluded that the most critical factor in depth determination is distance to the nearest recording station. They found that only 57 percent of 101 events satisfied this criteria for reliable depth computation. Eight of the 14 events for which focal mechanisms were presented satisfied the criteria for reliable depth estimate.

In this study we present 43 new or reinterpreted focal mechanism solutions. Within the central seismic zone (see inset, Figure 1)., the number of focal mechanism solutions is increased from 10 to 24, allowing interpretation of the spatial distribution of focal mechanisms. The earthquakes were located using a velocity gradient model (Propes, 1985) and a fixed origin time (Long et al., 1986). The gradient velocity model and fixed origin time provides a ±5 kilometer confidence in the depths of earthquakes is southeastern Tennessee and northern Georgia with the existing seismic array. The individual focal mechanism data sets were evaluated for randomness of distribution on the focal sphere. This unique test was used to qualify the sampling of the focal sphere as determined by the location of seismic monitoring stations and the hypocenter of the event. Each first motion reading was assigned a confidence value expressing the estimated probability that the reading is correct. this confidence value was then adjusted, according to the distribution of polarities of adjacent data points. Focal mechanism solutions ere then found using the adjusted or conditional probability values as a measure of consistency with a possible solution. A centroid solution is obtained from the domain of valid principle axes at a given confidence level. This centroid solution is then used to compute a Chi-Square estimate of confidence in the focal mechanism.

RELOCATION OF EARTHQUAKES

The linear dependence of origin time and depth is a well known problem in using P-wave data to locate earthquakes recorded at a few unevenly distributed stations. In this study, earthquake locations were computed by a method that uses the S-P times to isolate the origin time computation from the location computation. The method requires only a constant Poisson's ratio. The origin time is first fixed on the basis of the S-P times. Anomalous readings are corrected in the process and the epicenter is found by the traditional iterative least squares method of Geiger (1910). Then the epicenter is held constant and the depth is found by the iterative least squares method. The epicenter and depth are obtained alternately until convergence to a solution is achieved. The distributed method has two advantages; first, computation of the origin time, epicenter and depth are uncoupled, and second, separate weights can be used for epicenter and depth computations (Liow et al., 1985). A weighting scheme which combines the reading accuracy and the scatter in the P- and S-wave arrivals in the Southern Appalachian area is taken into consideration while finding the epicenter and depth. An additional distance weight is incorporated into the weights for the depth computation since only stations within a distance comparable to the focal depth can realistically constrain the depth (Johnston et al., 1985).

A gradient velocity crustal model is used in order to compute the theoretical travel times. Recent seismic refraction data (Propes, 1985) indicate that one gradient velocity model will satisfy variations in apparent velocity observed in the granitic crust of the southeastern United States. The model simultaneously satisfies the observed 6.05 km/s P-wave velocity of the Georgia Piedmont, the 6.14 km/s velocity of central Alabama and a 6.2 km/s velocity observed for the 10 kilometer deep North Georgia earthquake of October 9, 1984 (Long et al., 1986). Figure 2 compares the observed crustal refraction velocities and velocity gradients as a function of depth. The data suggest that the crust can be modelled by a constant velocity gradient from 5.95 km/s at the surface to 6.3 km/s at 15 kilometer depth. A velocity of 6.7 km/s could exist below 15 kilometer. Velocity structure below 20 km is not needed for the relocation of these events. The greatest variation in velocity exists near the surface and can be related to variations from mafic to sedimentary structural units. A 6.5 km/s rock unit could exist in the remnants of a rift zone in eastern Tennessee centered north-northeast of the central active zone. The Paleozoic sediments in Tennessee and Alabama for simplicity were assumed to satisfy a velocity gradient from 5.5 km/s to 5.7 km/s in the top two kilometers. However, the sediments in some areas may extend to depths of 6 km and in other areas the velocity could be as low as 4.5 km/s. An area of 6 by 7 kilometers in a zone northwest of seismic station CBT provided measurable velocity delays of 0.1 to 0.2 seconds (Tie, 1986) which were corrected for in the relocation of all events.

STATISTICAL EVALUATION OF FOCAL MECHANISMS

Focal mechanism solutions generally assume a random distribution of data coverage over the focal sphere. Non-random distributions can affect the solution. For the distribution of first motion readings and their amplitudes the focal sphere is a continuous function. The pattern of available

observation on the focal sphere are dependent on the location of seismicity and terrain available for installation of seismic stations. Subsequently, the distribution of points is dependent on many factors and neither uniform nor random. Although the occurrence of a non-random distribution can be demonstrated, the significance of differences in the pattern of two or more populations is hard to evaluate. The distance between nearest neighbors, first used by Dice (1952), measures the departure from randomness. Clark and Evans (1954) used the distance between nearest neighbors to define randomness as a spatial concept, providing the possibility of searching for randomness in sub-populations or smaller areas of interest. The distance between nearest neighbors is applied in this study. If

$$R_A = \frac{\sum_{n} r_n}{N} \tag{1}$$

where R_A = mean of the series of distances to nearest neighbor

r_n = distance to nearest neighbor

N = total number of points

and

$$R_E = \frac{1}{\sqrt{2\rho}} \tag{2}$$

where R_E = mean distance to the nearest neighbor expected in an infinity large random distribution of density ρ

ρ = density (points/ km^2)

then

$$R = \frac{R_A}{R_E} \tag{3}$$

is a measure of the degree to which the observed distribution departs from random expectation with respect to the distance to the nearest neighbor. Subsequently, for a random distribution, R = 1, for a maximum aggregation R = 0, where all the data occupy the same locus and for a perfectly uniform data set R = 2.1491, where all the data are equidistant from each other. The random probability factor can be interpreted as a measure of expected deviation from randomness. For instance, for a R value of 0.5, on the average, the nearest neighbors are half as far apart as expected under conditions of randomness. Figure 3 shows the direct correspondence between the random probability factor and the conventional measure of station coverage, the maximum azimuthal gap. It can be seen that as the maximum azimuthal gap decreases and the data trends towards maximum aggregation, the

value of the random probability factor trends towards zero. Also, the maximum azimuthal gap increases with increasing random probability factor. Data sets with no regularity in azimuthal spacing tend to have one or two large (greater than 90 degrees) azimuthal gaps and their associated random probability factor values are scattered.

Each individual data point in this study was assigned a confidence value following the criteria listed in Table 2. In addition, these user-assigned confidence values are modified by a conditional probability based on consistency with neighboring points. For each data point, the nearest data are tested for similarity of polarity, resulting in a lower adjusted probability if data of different polarity are nearby, a higher adjusted probability value if data nearby is of the same polarity and a constant value if no data are nearby. In the case of an obvious inconsistency of a low user confidence value surrounded by first motions of opposite polarity, the confidence value can be changed to a value less than 0.5 (random) by this consistency test. Nearest neighbors are determined by searching a circular area with a 10 degree radius around the point tested. If no points are found within this area, the radius is increased by 10 degrees. Beyond a circular radius of 30 degrees the data point tested is considered independent and no adjustments to the confidence value is made.

Focal mechanism solutions are found using the search technique on the focal sphere and using cumulative probability as criteria for valid solutions instead of the number of correct points as used by Guinn and Long (1977), Tzeng (1982) and Snoke (1984). The computational details using cumulative probability to determine a focal mechanism solution area s follows. All assigned probabilities of the polarity data are changed so that all polarities are considered compressive. The mean probability for both polarities and SV/P amplitude ratios is used as a threshold value. If a polarity fits the stress axes orientation tested then a cumulative probability value is incremented by the polarity's probability value. If the cumulative value for all p9olarity data is greater than the threshold value a solution has been found. the SV/P amplitude ratios the probability value is the measure of deviation from the theoretical SV/P amplitude ratio value and a separate cumulative probability value is found. If both the polarity and the SV/P amplitude ratio threshold value is exceeded a valid solution has been found.

Once the domain of the pressure and the tension axes are known, the centroid solution is found and the distribution of data points is evaluated with respect to that solution using the Chi-Square test (Sachs, 1982). The Chi-Square distribution is expressed as (Sachs, 1982, page 139, equation 1.130)

$$\chi^2 = (n-1)\,\frac{s^2}{\sigma^2} \qquad (4)$$

where s^2 = variance of random sample data set

σ^2 = variance of parent data set (theoretical)

By definition,

$$s^2 = \frac{1}{(n-1)} \Sigma(x_i - \mu)^2 \qquad (5)$$

where x_i = probability values

μ = mean of probabilities

The probability data are adjusted to provide only two distinct cases for evaluation; -1, compressive or -1, dilatational. Therefore the mean of observed p9olarities from the estimates of conditional probability is the probability value, if compressive, multiplied by n cases minus the probability value, if dilatational, multiplied by n cases and this value divided by n cases, or

$$\mu = \frac{x_i n - (1-x_i)n}{n} = 2\,x_i - 1 \qquad (6)$$

Assuming that each probability value was derived from a large number of readings

$$s^2 = \frac{1}{(n-1)} (\rho_1^2 + \ldots + \rho_i^2 + \ldots + \rho_n^2 \qquad (7)$$

where $\rho_i^2 = \frac{1}{k} \Sigma(x_i - \mu)^2$

$$= \frac{1}{k} (kx_i(1-\mu)^2 + k(1-x_i)(-1 - \mu)^2)$$

$$= 4(1-x_i)x_i$$

Thus, $s^2 = \frac{1}{(n-1)} \Sigma\, 4(1-x_i)x_i \qquad (8)$

For the parent distribution

$$\sigma^s = \frac{1}{(n-1)} \Sigma(x_i-\mu)^2$$

$$= \frac{1}{(n-1)} \Sigma(\pm 1 - \mu)^2 = \frac{n}{(n-1)} \qquad (9)$$

as $\mu = 0$ for all four quadrants. Therefore

$$\chi^2 = \frac{(n-1)}{n} \Sigma\, 4(1-x_i)x_i \qquad (10)$$

To take care of adjusted probabilities less than random, i.e. < 0.5,

$$\rho_i^2 = 2 - 4(1-x_i)x_i \qquad (11)$$

The complete function ρ^2 is plotted in Figure 4. Confidence levels for a focal mechanism solution are read from a χ^2 distribution table (Sachs, 1982, p. 140).

RESULTS

The distribution of the random probability factor for the earthquake data set (see Figure 5) indicates that the individual data sets are all nearly random, as the distribution is centered around R=1. The distribution of the random probability factor is dependent on the number of data points per data set. Large data sets have lower values of R or maximum aggregation, whereas smaller data sets show more uniformity. This is indicated in Figure 6. The random probability factor also shows no dependence on duration magnitude of the events. Earthquakes greater or smaller than duration magnitude 2.75 show a broad range of values of R, centered around R=1. For all determined values of R, see Table 3.

The Chi-Square distributions were transformed to significance (or confidence values) using statistical tables (Sachs, 1982). The resulting values are listed in Table 3. Confidence values were determined for polarity data, SV/P amplitude ratio data and all data separately. The results are shown in Figure 7a through 7c. In each of these figures, the data are further separated into earthquakes greater or less than duration magnitude 2.75. The confidence values are not different when comparing small and large magnitude earthquakes for all three cases. In general, confidence values range from 0.4 to 0.99, with the majority between 0.75 and 0.99. Also, confidence values are higher for polarity data only compared to SV/P amplitude ratio data only. Confidence values show no correlation with the number of data points per data set. For both data points greater or less than 10, the range of confidence values is from about 0.5 to 0.99.

We examined 77 events between January 1982 and August 1987 to determine focal mechanism solutions. The directions of first motions and SV/P amplitude

ratios were used to determine 41 single event and two composite focal mechanism solutions for earthquakes in southeastern Tennessee and northern Georgia. the composite solutions were determined using data of two earthquakes. The solutions include reinterpretation of four of the 11 single event focal mechanisms determined by Teague et al. (1986). All four events have consistent P-axis trends when compared with Teague et al.,'s (1984) results, which are all strike-slip solutions. Only one result is different in that our data analysis also allows a normal component. These events were detected by all three major seismic networks in the southeastern Tennessee area (Georgia Tech Seismic Network, Tennessee Valley Authority Seismic Network and the Center for Earthquake Research and Information Seismic Network) between 1982 and 1987. The dates, epicenter location, duration magnitude, depth and origin time are listed in Table 3. Figure 8 shows the location of the earthquakes and their depths along a northeast profile.

The 43 solutions can be divided into three categories which are listed in Table 4. Twentyfour solutions could be considered pure strike-slip, six strike-slip with a normal or reverse component, six normal, two normal with strike-slip component and five reverse with strike-slip component. The average depth for all events is 16.9 ± 4.8 kilometers. The average depth for strike-slip fault earthquakes is 17.3 ± 4.6 kilometers. The normal fault earthquakes and reverse fault earthquakes had similar average depths of 15.9 ± 5.7 kilometers and 15.7 ± 3.1 kilometers respectively.

Pure strike-slip solutions are confined to three distinct areas: A central zone between 84.2W and 84.5W and 35.5N and 35.8N, a zone at Knoxville and a southern zone in northern Georgia (Long et al., 1986, and Zelt and Long, 1987). Earthquakes with normal and reverse components generally surround areas of strike-slip mechanisms.

The focal mechanism solutions were divided into different categories of quality. Each statistical parameter was divided into four quality categories, as shown in Table 5. The quality of a solution thus is ultimately derived from 12 different categories, the highest quality solution being defined by a (S1, R1, P1) quality combination and the lowest quality solution by a (S4, R4, P4) quality combination.

Figures 9a through 9k show our focal mechanism solutions. Their statistical qualifications in the form of the random probability factor, number of data points and significance are listed in Table 3. Each diagram shows the polarity readings, domains of the pressure, tension and null axes and the nodal planes of the central solution. Each of the solutions has its distinct character with respect to the performed statistical analysis.

Figure 9a shows a solution where R = 0.982, the number of data points = 35 and the significance value equals 0.99. Figure 9b shows a solution where R = 1.09, the number of data points = 16 and the significance value equals 0.96. The statistics indicate near-random, equally distributed data sets and therefore solutions of (S1, R1, P1) quality. Every statistical parameter evaluated provides a measure of confidence in the solution. Lack of data in one or two quadrants can result in non-random values of R and near-random (random equals 0.5) significance. Examples of this case are seen in Figure 9c and 9d, where the values of the random probability factor are 1.273 and 0.702

respectively. The solutions of Figure 9c and 9d are of (S2, R2, P2) quality. Figure 9e shows a solution where 11 out of 22 data points are SV/P amplitude ratios. In general, user assigned probabilities are lower for SV/P amplitude ratios than for polarities (see Table 3). Although the value of R = 1.005 (near random) the significance value is only 0.78 because of the abundance of SV/P amplitude ratios in the data set. The result is only a S3, R1, P1) quality. Figure 9f and 9g are examples of focal mechanism solutions that are not strike-slip but rather normal and normal with a large strike-slip component respectively. The statistics for the solution of Figure 9f (Significance = 0.78, R = 0.918, number of data points = 13) and the solution of Figure 9g (Significance = 0.67, R = 1.241, number of data points = 14) indicate qualities of (S3, R1, P2) and S4, R2, P2) respectively. This shows that focal mechanism solutions other than strike-slip with north striking nodal planes are possible solutions for southeastern Tennessee and northern Georgia earthquakes as some of the determined qualities are high, but such solutions may be ambiguous. Figure 9h shows a strike-slip solution found in southeastern Tennessee for 9 events. The nodal planes here trend northwest or northeast. The number of data points available for this solution equals only 8 and their distribution makes this a low quality solution of (S3, R2, P3). Figures 9i through 9k show more focal mechanism solutions of non-strike-slip character. The first two shows normal fault plane solutions, whereas the third shows a reverse fault plane solution with a strike-slip component. Significance values for all three events are rather low (S = 0.68, 0.53 and 0.66), resulting in qualities of (S4, R3, P3), (S4, R1, P2) and (S4, R1, P2).

Significance values and other statistical results show that not just strike-slip solutions are valid for southeastern Tennessee and northern Georgia, but that solutions with large normal and reverse components are acceptable.

Pure strike-slip solutions are confined to three distinct areas: A central zone between 84.2W and 84.5W and 35.5N and 35.8N, a zone at Knoxville and a southern zone in northern Georgia (Long et al., 1986, and Zelt and long, 1987). Earthquakes with normal and reverse components generally surround areas of strike-slip mechanism.

The focal mechanism solutions of the central zone of seismicity were used to investigate a possible regional pattern of characteristic stress release in earthquakes. Figure 10 shows a contoured map of the dip of the null-axis for the central seismic zone in southeastern Tennessee. Three distinct areas of near-vertical dip, corresponding to strike-sl[illegible] regions are apparent. First, a central region centered at 35.55N and 84[illegible] second a region towards the east and third a region in the northwest [illegible] the study area. The central region is of greatest interest, because it is surrounded by regions of low B-axis dips, thus regions of normal and reverse components.

The following method was used to determine which of the low B-axis dip regions corresponds to a normal or a reverse fault component region. The dip of the tension axis was subtracted from the dip of the pressure axis for each solution. This results in a range of values from -90 to +90, where -90 corresponds to a pure reverse fault and +90 to a pure normal fault. Values close to zero correspond to strike-slip fault solutions. Figure 11 shows the result of this evaluation. All three non-strike-slip areas can still be

distinguished, but only the southwestern and southeastern zones surrounding the central zone show a large normal component. The northeastern zone is broken up into zones of either normal or reverse character.

DISCUSSION AND CONCLUSION

The random probability factor and significance values for each of the earthquake polarity and SV/P amplitude ratio data sets indicate no distinct difference in quality between small and large magnitude earthquakes. Both small and large magnitude earthquakes can have random and non-random R values and low and high significance values. It is important to note that a large magnitude earthquake ($M_D > 2.75$) usually has a large and well distributed data set (more than 15 data points), which in turn has significance values greater than 0.9 and near-random R values. Events with magnitudes less than 2.75 can have a large data set resulting in a near-random R and a high confidence value, but most of the time the data set is small, resulting especially in lower confidence values. A well-determined focal mechanism solution can therefore be classified as one with a data set consisting of more than 15 data points, near-random R and a significance value greater than 0.9. Throughout the examined data set the strike-slip solutions with north trending nodal planes exemplify this classification. Strike-slip solutions with normal or reverse components, considered anomalous focal mechanism solutions also exemplify this classification. Fifteen anomalous focal mechanism solutions indicate confidence values of less than 0.85 (see Table 3), R values not close to one and have data sets of less than 10 points. The results indicate that the statistical analysis provides an additional tool in the standard focal mechanism analysis (Guinn and Long, 1977; Tzeng, 1982; and Snoke et al., 1984) and is a measure of confidence in each solution. The statistics enhance the interpretation of the stress regime in southeastern Tennessee and northern Georgia. Good results were obtained for solutions other than strike-slip solutions with north trending nodal planes. The anomalous seismic zone hypothesis can therefore not be discounted.

Three major areas where strike-slip mechanisms dominate in southeastern Tennessee have been delineated. they are the northern Georgia seismic zone, the Knoxville seismic zone and a central seismic zone centered around Madisonville. These three areas are also the zones of largest seismic activity, as can be seen in Figure 16 where all 296 relocated events within the southeastern United States that occurred between 1982 to 1987 are shown. The central seismic zone is surrounded by areas where focal mechanisms with normal or reverse components dominate. These areas gave less seismic activity. The northern Georgia seismic zone is connected with the central seismic zone by two seismic lineations trending northeast (see Figure 8). The mean depth of strike-slip events indicates that they generally occur at greater depths than the surrounding reverse or normal events.

The central zone corresponds to an area near a proposed Precambrian rift zone (McKeown, 1978). Shear wave reflections from the Moho (Liow and Long, 1985) and the time-term analysis of refraction data (Long and Liow, 1986) suggests a 5 to 10 kilometer deeper Moho in this zone when compared with the surrounding areas of southeastern Tennessee. A thickening of the crust is consistent with the regional gravity gradient (Winester, 1984). The average depth of strike-slip fault earthquakes in this zone of 17.29 kilometers

correlates with deeper Moho because the depth is deeper than the average depth of the surrounding events. This may suggest that the brittle ductile transition zone (BDT) is deeper in the central zone of seismicity. Bollinger et al. (1985) already have described a difference in depth of the BDT when comparing the Piedmont area with southeastern Tennessee. A further zoning of the BDT therefore is possible. The seismicity of the central zone has also been related to a possible zone of weakness in the lower crust (Long, 1988), where fluid injection from the upper mantle may be a further mechanism for seismicity in southeastern Tennessee and northern Georgia. The zone is also the area of greatest seismic activity in southeastern Tennessee.

Earthquakes with normal or reverse fault components generally surround the central zone of seismicity. Some of these events are located on the southern edge of the central seismic zone, which correlates to a northwest trending seismic boundary (see Figure 16). The nodal planes determined for these events strike north-northwest to northwest. McKeown (1978) relates different types of focal mechanisms in a region to the complex system of geologic discontinuities due to mafic intrusives which in turn could be responsible for local changes in the level of stress. Mareschall and Kuang (1986) have found high enough levels of stress due to topographic loading to accommodate seismicity in southeastern Tennessee and northern Georgia.

Long (1988) correlates the strike-slip focal mechanism solutions of the central zone with the surrounding normal or reverse focal mechanism solutions. Zones of weakness could explain areas of high density seismicity and the majority of strike-slip mechanisms within. Earthquakes with normal or reverse components could be explained by stress release on the edges of such a zone. Such events would subsequently be shallower as has been determined here. The two linear seismic features connecting the North Georgia seismic zone with the central seismic zone are similar to features described by Long's (1988) proposed model for major intraplate continental earthquakes.

In summary, the density of focal mechanism solutions for southeastern Tennessee and northern Georgia has been increased by 43 new or revised focal mechanism solutions. A statistical measure has been introduced to provide a measure of confidence in each solution. The derived spatial distribution of focal mechanism solutions indicates zones where strike-slip mechanisms dominate and surrounding zones of focal mechanism solutions with large normal or reverse components. The spatial distribution provides new speculation on the origin of seismicity in the southeastern Appalachian area and makes it clear that focal mechanism studies in this area should continue. Also, seismic modelling of the stress regime would be a future step in providing answers to the seismic origin of earthquakes in southeastern Tennessee and northern Georgia.

REFERENCES

Bollinger, G.A., C.J. Langer and S.T. Harding, April 1976. The Eastern Tennessee Earthquake Sequence of October through December, 1973, BSSA, Vol. 66, No. 2., pp. 525-547.

Bollinger, G.A., M.C. Chapman, M.S. Sibol and J.K. Costian, 1985. An analysis of earthquake focal depths in the southeastern U.S., Geophysical Research Letters, Vol. 12, No. 11, pp. 785-788.

Clark, P.J. and F.C. Evans, 1954. Distance to Nearest Neighbor as a measure of spatial relationships in populations, Ecology, Vol. 35, No. 4, pp. 445-453.

Dice, L.R., 1952. Measure of the spacing between individuals within a population, Contrib. Lab. Vert. Biol. Univ. Mich., 55, p. 1-23.

Geiger, L., 1910. Herdbestimmung bei Erdbeben aus den Ankunftszeiten, K. Gesell. Wiss. Goettingen, 4, pp. 331-349.

Guinn, S.A. and L.T. Long, 1977. A computer method for determination of valid focal mechanism solutions using P-wave first motions applied to southeastern United States earthquakes, Abstract, Earthquake Notes, Vol. 48, No. 3., p. 16.

Guinn, S.A., June 1980. Earthquake Focal Mechanisms in the Southeastern United States, NUREG/CR-1503.

Herrmann, R.G., July 1979. Surface wave focal mechanisms for Eastern North American Earthquakes with Tectonic Implications, Journal of Geophysical Research, Vol. 84, No. B7, pp. 3543-3552.

Johnston, A.C., D.J. Reinbold and S.I. Brewer, 1985. Seismotectonics of the Southern Appalachians, BSSA, Vol. 75, pp. 291-312.

Liow, J.-S, An Tie, L.T. Long, 1985. Earthquake Location: A Consideration of independent computation of origin time, epicenter and depth, Abstract, Earthquake Notes, Vol. 56, No. 3, p. 77.

Liow, J.-S and L.T. Long, 1985. Analysis of reflections from the base of the crust in southeastern Tennessee, in Summary Report for contract GSA-80-3053, Geological Survey of Alabama; A Study of Seismicity and Earthquake hazard in northern Alabama and adjacent parts of Tennessee and Georgia, Georgia Institute of Technology, School of Geophysical Sciences, Atlanta, GA 30332, 16 pp.

Long, L.T. and J.-S. Liow, 1986. Crustal Thickness, velocity structure, and the isostatic response function in the southern Appalachians, in Reflection Seismology: The Continental Crust, Geodynamics Series, Vol. 14, AGU, pp. 215-222.

Long, L.T., J.-S. Liow, An Tie and K.-H Zelt, May 1986. Seismicity and Crustal Structure in southeastern Tennessee, Abstract, EOS Transactions, AGU, Vol. 67, No. 16, p. 314.

Long, L.T., K.-H. Zelt, J.-S Liow, R.P. Propes, J. Shand, D. Reinbold and B. Schechter, July-September 1986. The North Georgia Earthquake of October 9, 1984, Earthquake Notes, Vol. 57, No. 3. ESSA, pp. 77-82.

Long, L.T., 1988. A Mechanism for Major Intraplate Earthquakes, Abstract, EOS, Transactions, AGU, Vol. 69, No. 16, p. 402.

Mareschal, J.C. and Jian Kuang, 1986. Intraplate Stresses and Seismicity: The role of topography and density heterogeneities, Tectonophysics, Vol. 132, pp. 153-162.

McKeown, F.A., 1978. Hypothesis: Many earthquakes in the central and southeastern United States are casually related to mafic intrusive bodies, Jour. Research U.S. Geol. Survey, Vol. 6, No. 1, pp. 41-50.

Propes, R.L., 1985. Crustal Velocity variation in the Southern Appalachians, Thesis, Master of science, School of Geophysical Sciences, Georgia Institute of Technology, Atlanta, GA 30332.

Reinhold, D. and J. Cornwell, March 1983. The Greenback, Tennessee Earthquakes of 24 September 1982 and their tectonic associations, TEIC Special Report No. 9, Tennessee Earthquake Information Center, Memphis State University.

Sachs, L., 1982. Applied Statistics, A Handbook of Techniques, Springer Verlag, pp. 139-141.

Snoke, J.A., J.W. Munsey, A.G. Teague and G.A. Bollinger, 1984. A Program for Focal Mechanism Determination by Combined use of Polarity and SV/P Amplitude Ratio Data, Abstract, Earthquake Notes, Vol. 55, No. 3, p. 15.

Teague, A.G., December 1984. Focal Mechanisms for Eastern Tennessee Earthquakes, 1981-1983, Master's Thesis, Virginia Polytechnic Institute and State University, Dept. of Geological Sciences, pp. 161.

Teague, A.G., G.A. Bollinger and A.C. Johnston, February 1986. Focal Mechanism Analyses for Eastern tennessee Earthquakes (1981-1983), BSSA, Vol. 76, No. 1, pp. 95-109.

Tie, An, J.-S, Liow and L.T. Long, 1986. Study of traveltime residuals at seismic stations in the southeastern Tennessee area, SEUSSN Report No. 18, pp. 73-77.

Tzeng, W.S., 1982. Investigation of SV to P Wave Amplitude Ratio for Determining Focal Mechanism, Thesis, Master of Science, School of Geophysical Sciences, Georgia Institute of Technology, Atlanta, GA 30332.

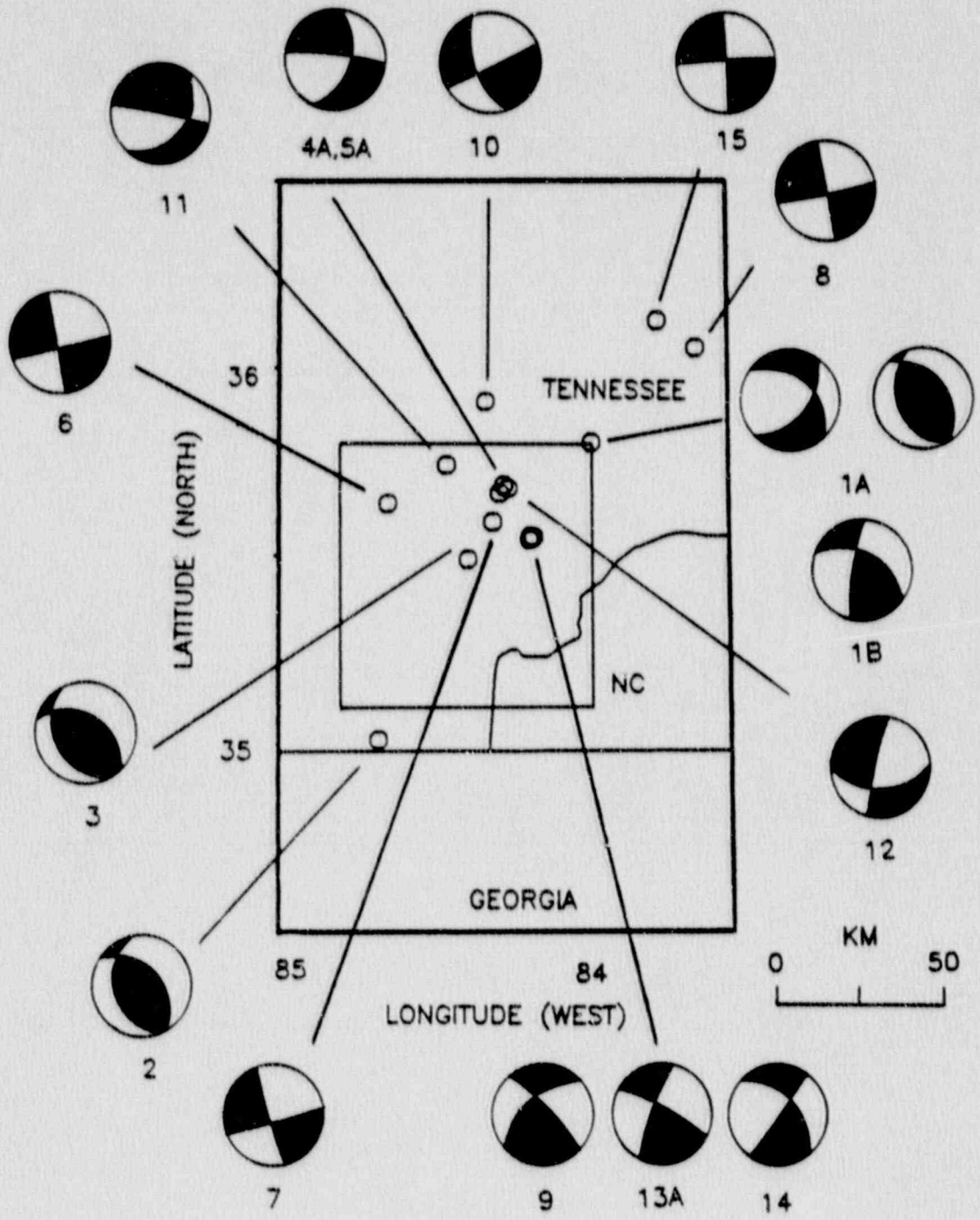

Figure 1. Published focal mechanism solutions for southeastern Tennessee (see Table I for reference numbers).

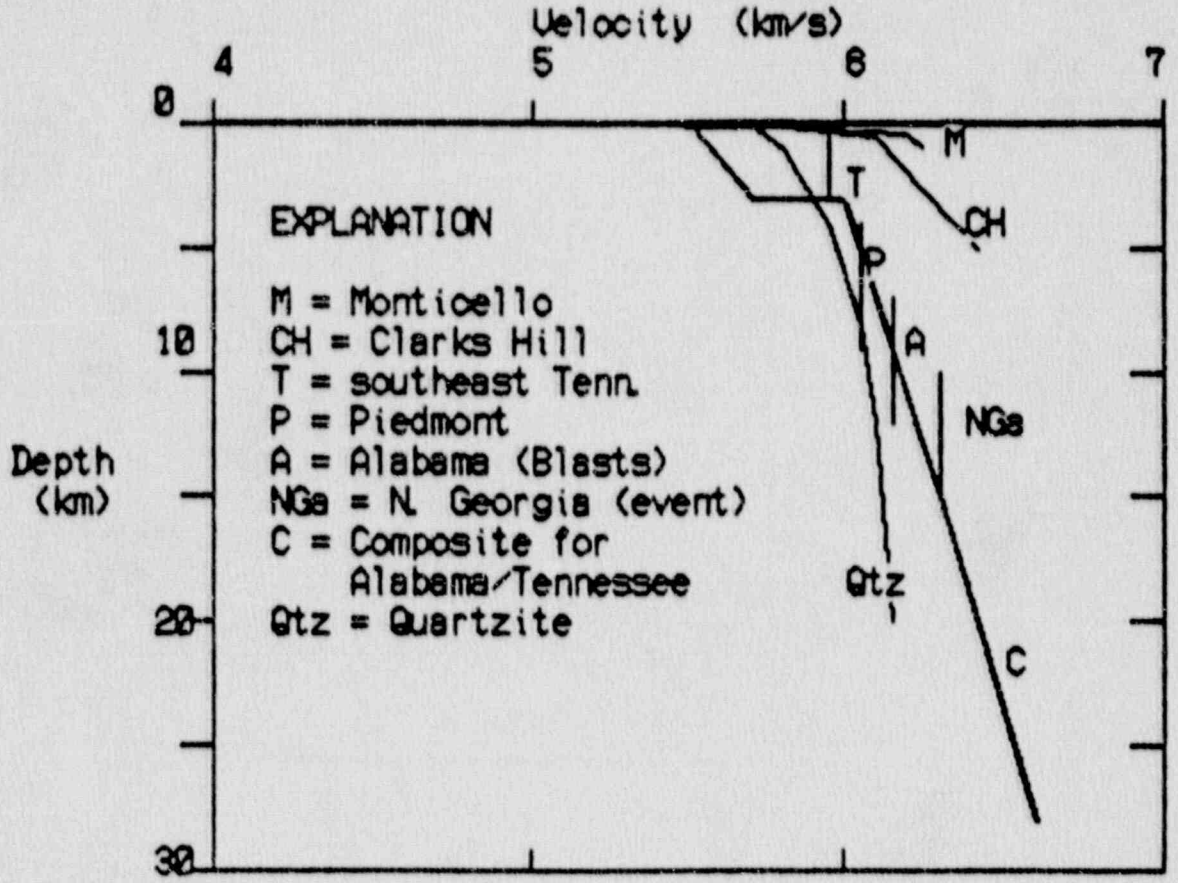

Figure 2. Composite plot of seismic refraction velocities in the southeastern United States showing the relation of velocity with depth.

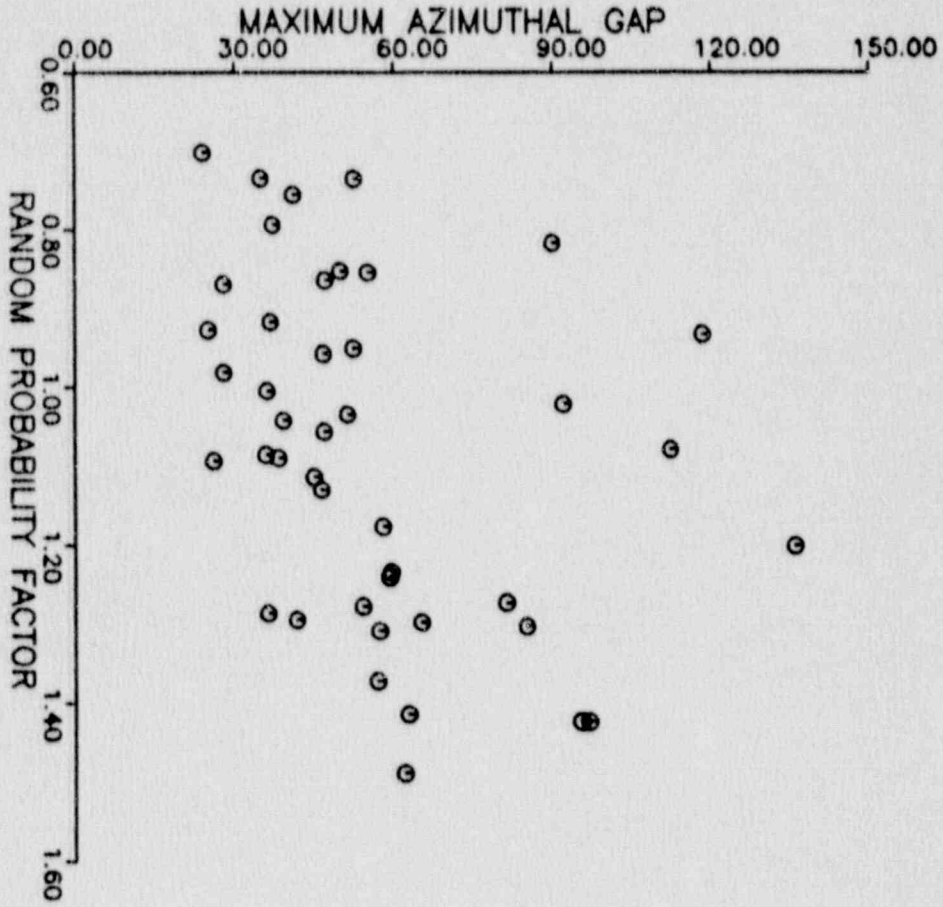

Figure 3. Relation between random probability factor and maximum azimuthal gap.

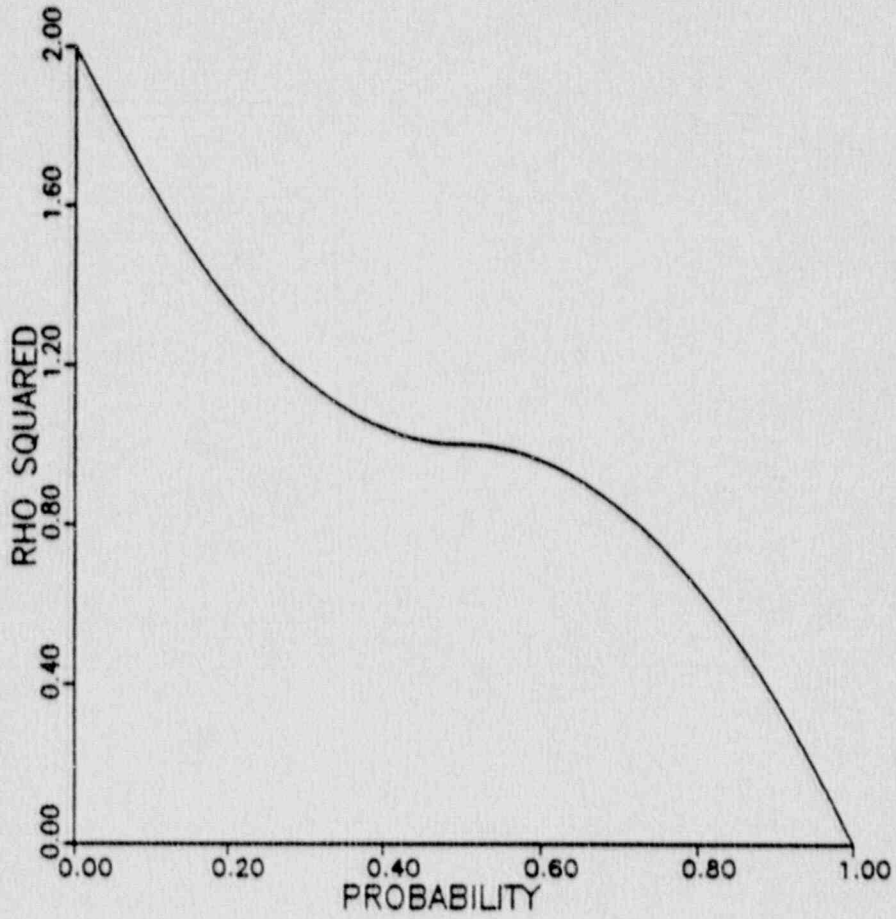

Figure 4. Relation between variance of polarity observations and probabilities of a correct reading.

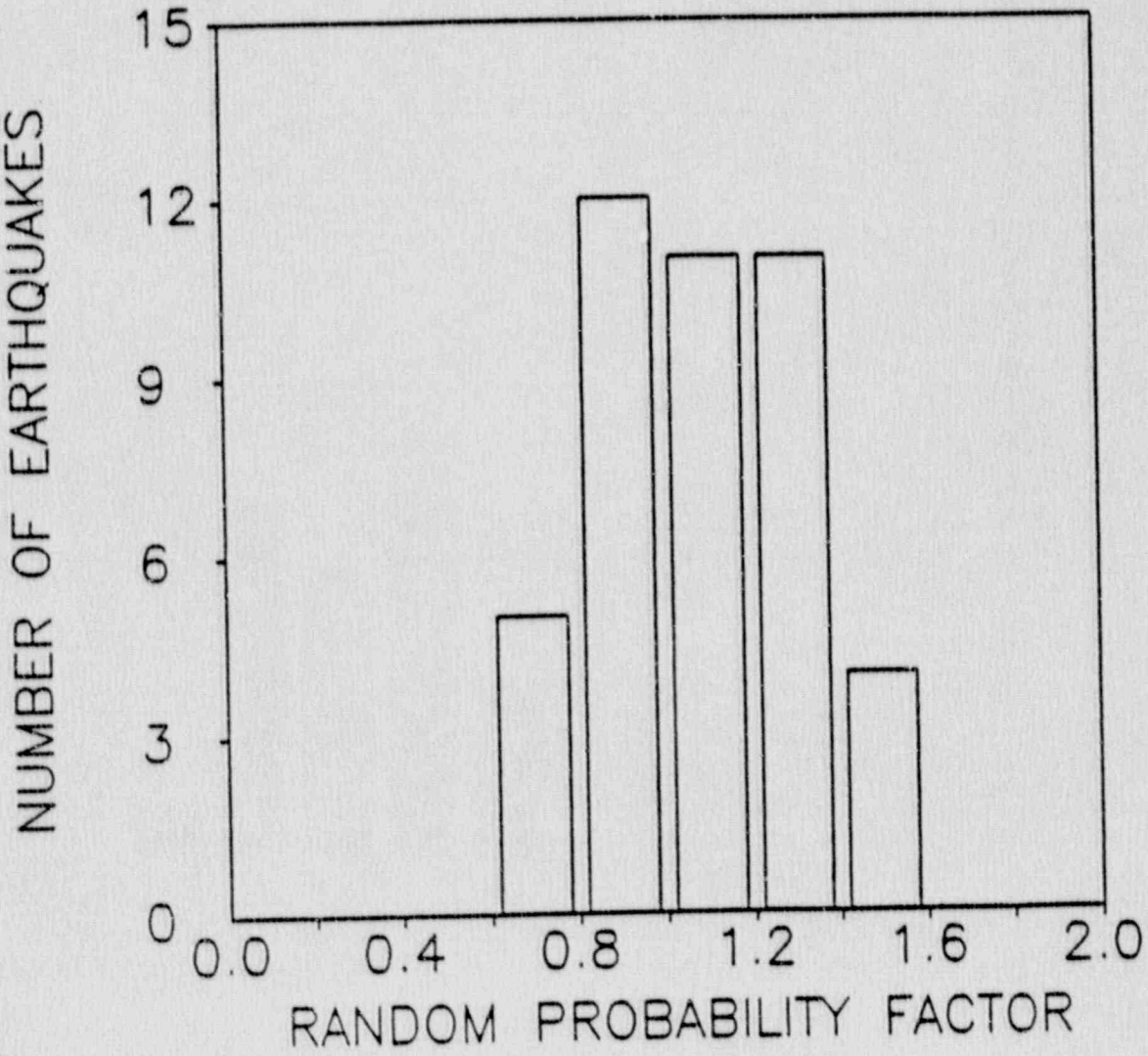

Figure 5. Distribution of the random probability factor for all earthquakes.

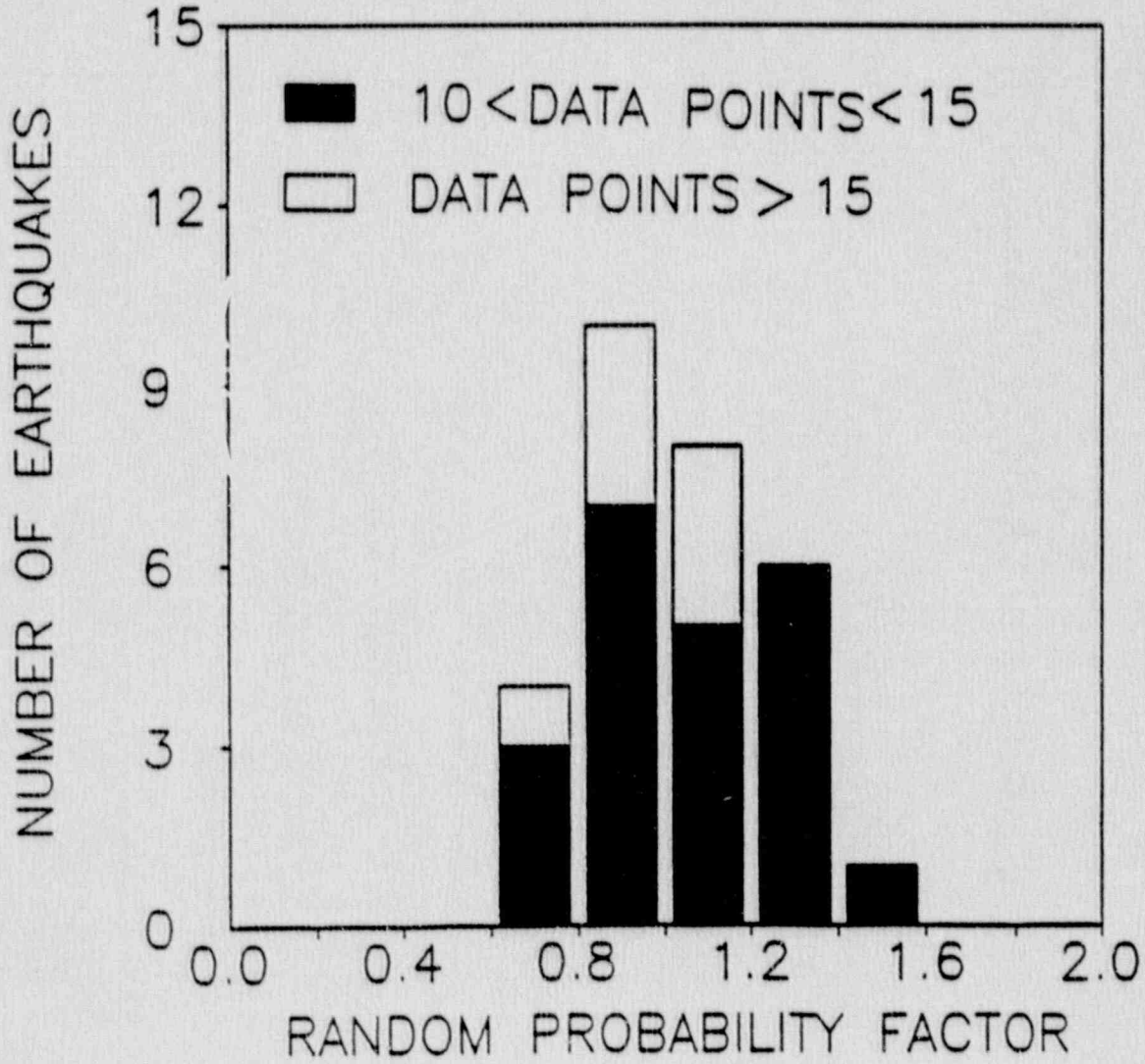

Figure 6. Relation between random probability factor for small and large numbers of stations.

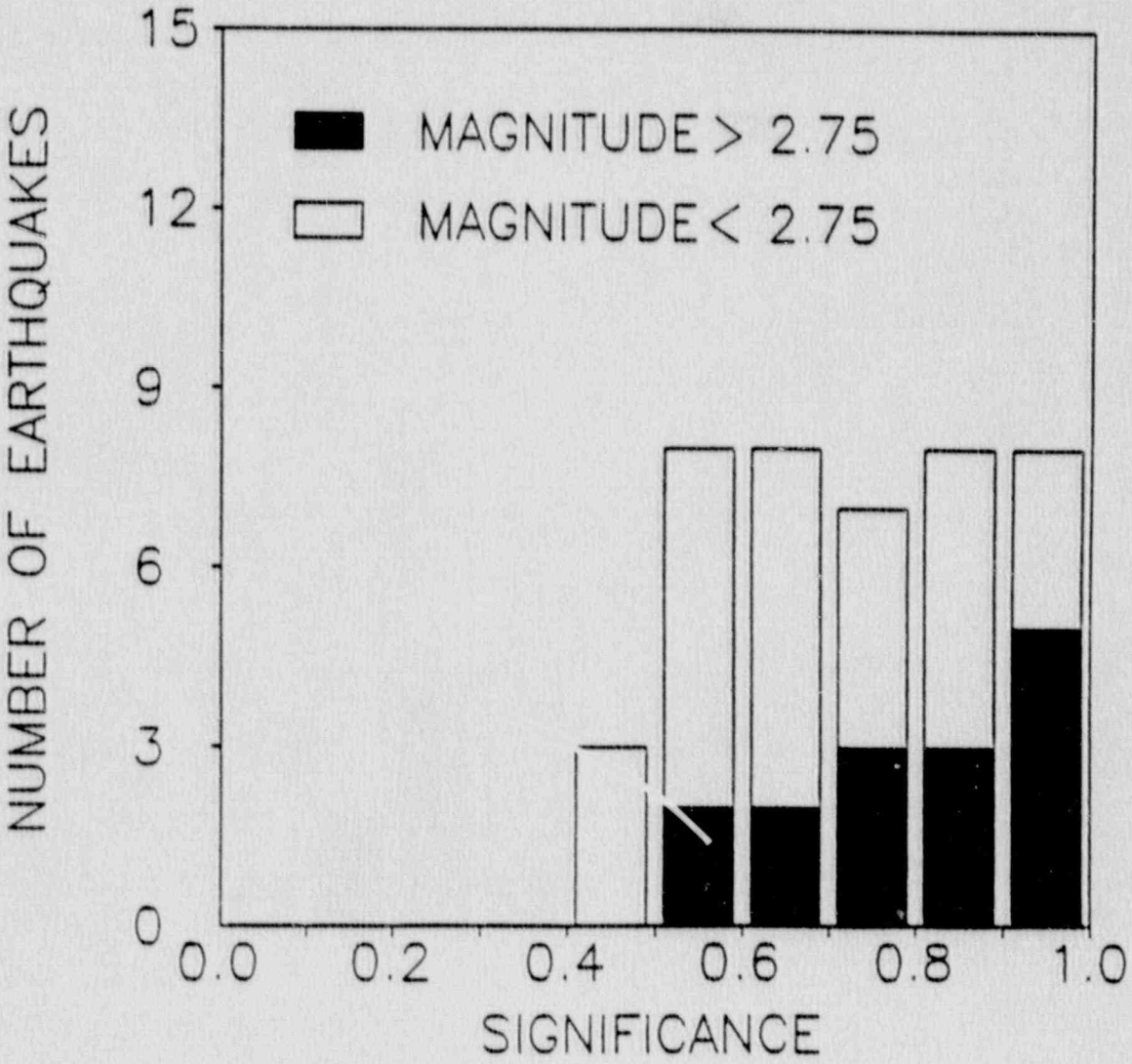

Figure 7a. Significance for all events for polarity data.

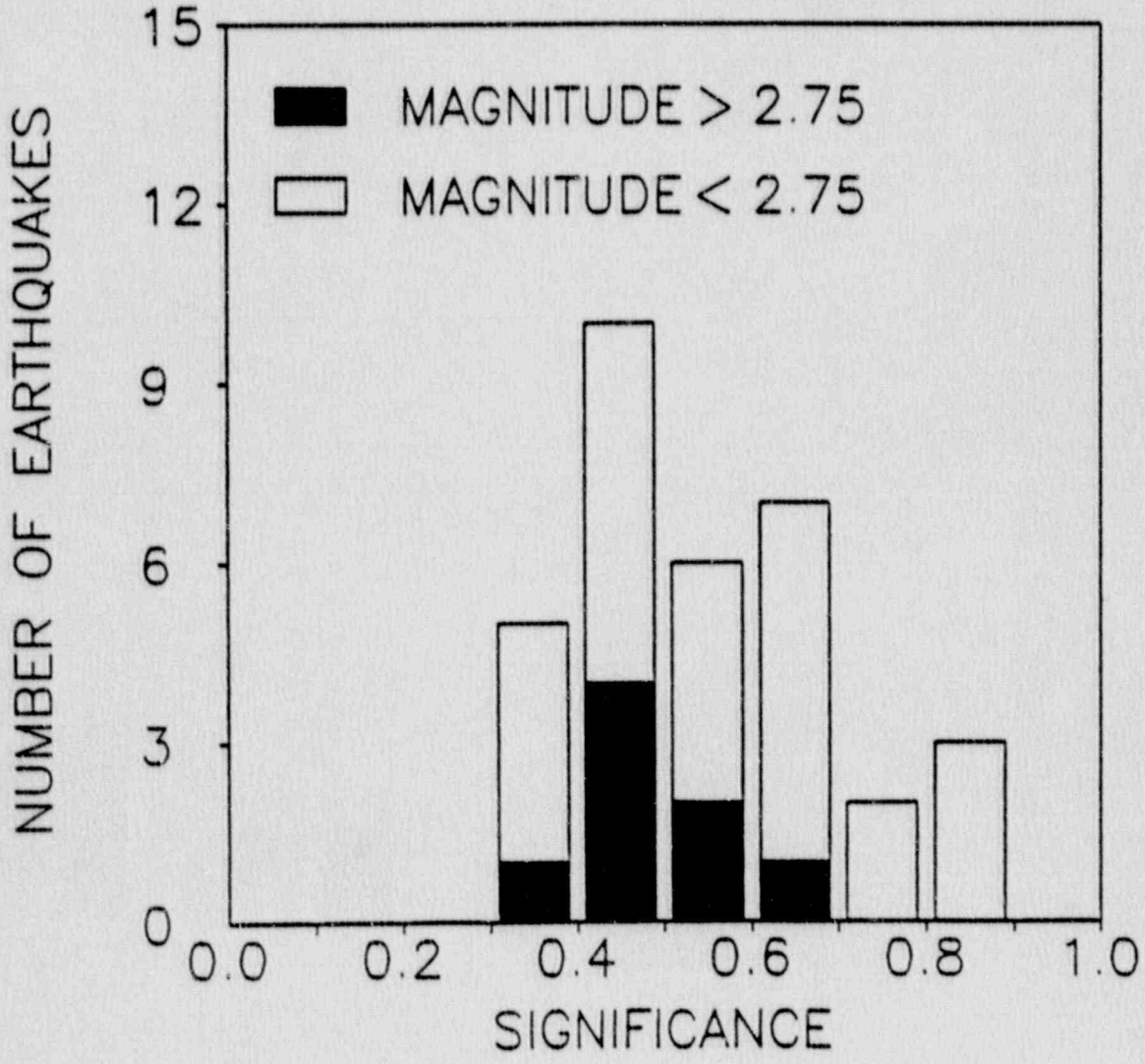

Figure 7b. Significance for all events for SV/P amplitude ratios.

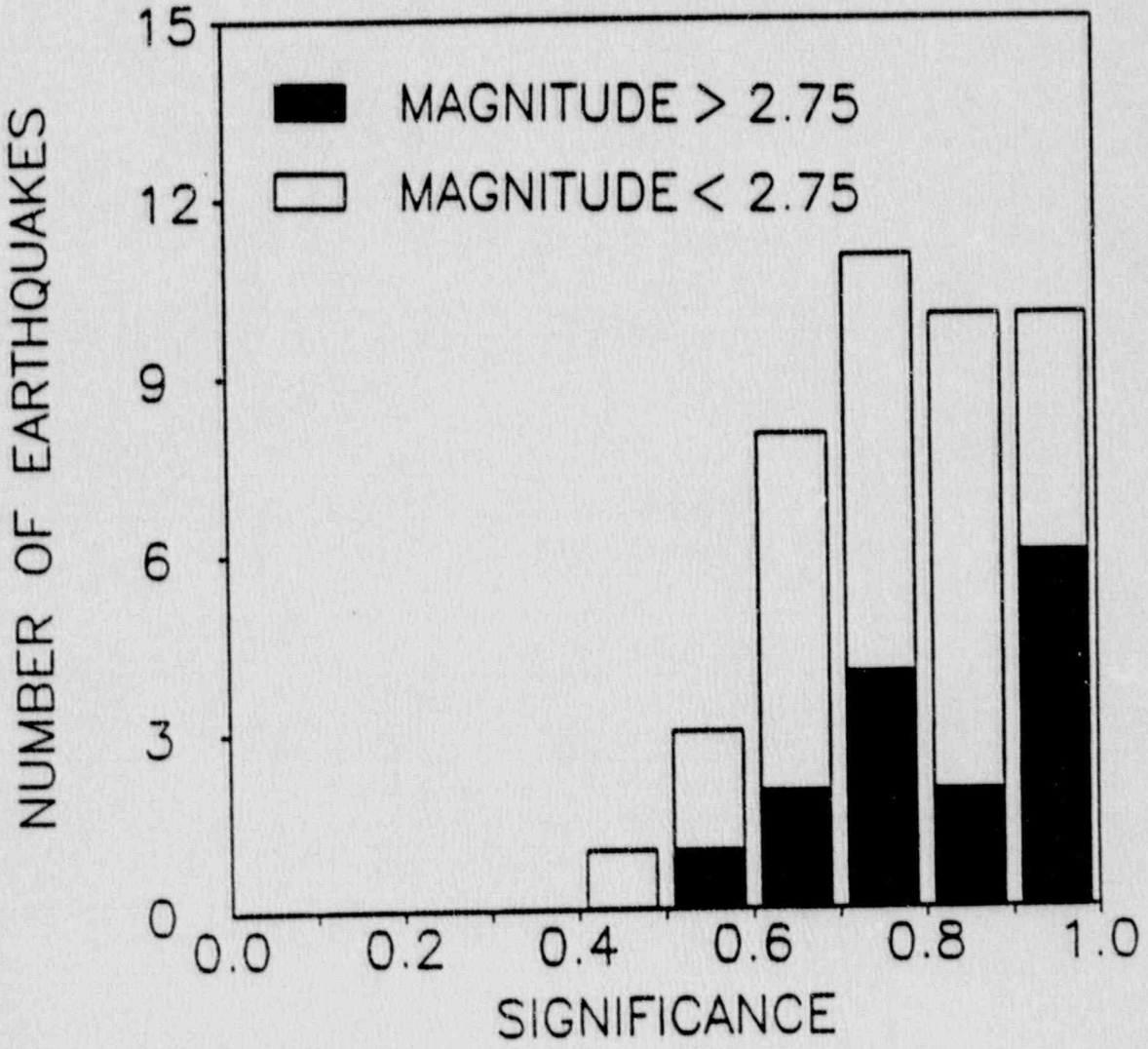

Figure 7c. Significance for polarity and SV/P amplitude ratios.

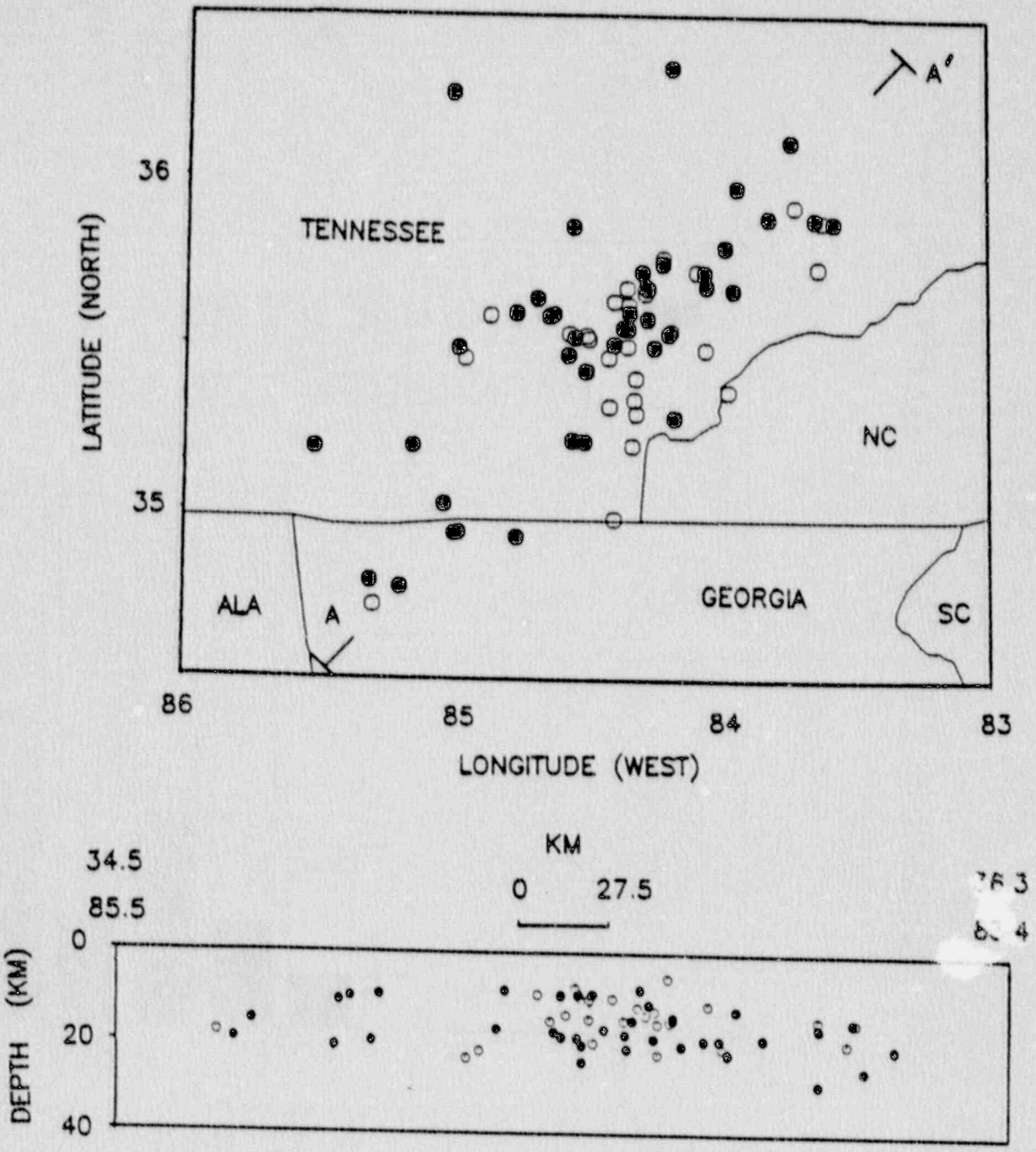

Figure 8. Location of earthquakes in southeastern Tennessee. Solid dots are events which have focal mechanism solutions.

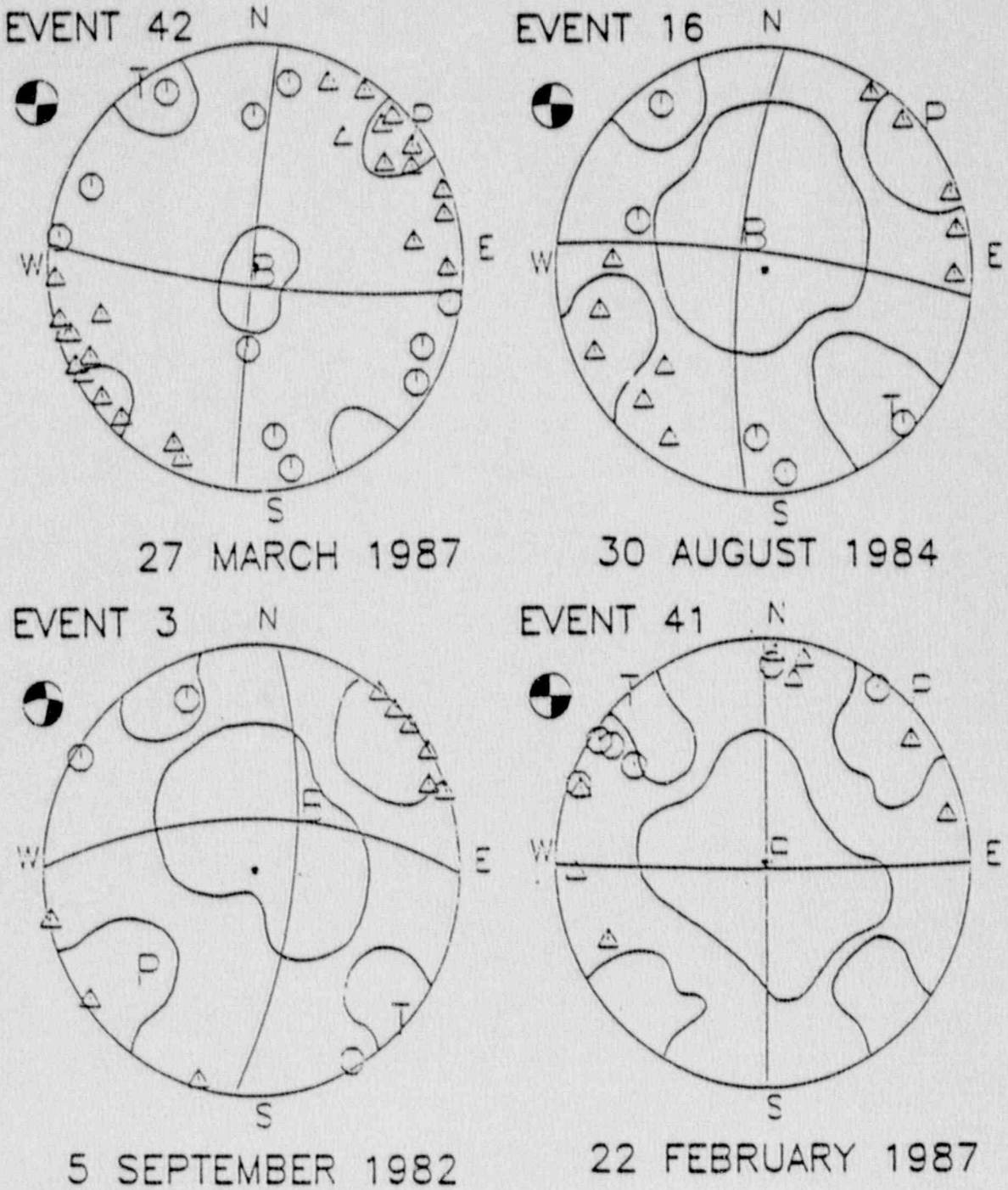

Figures 9a-d. Focal mechanism solutions.

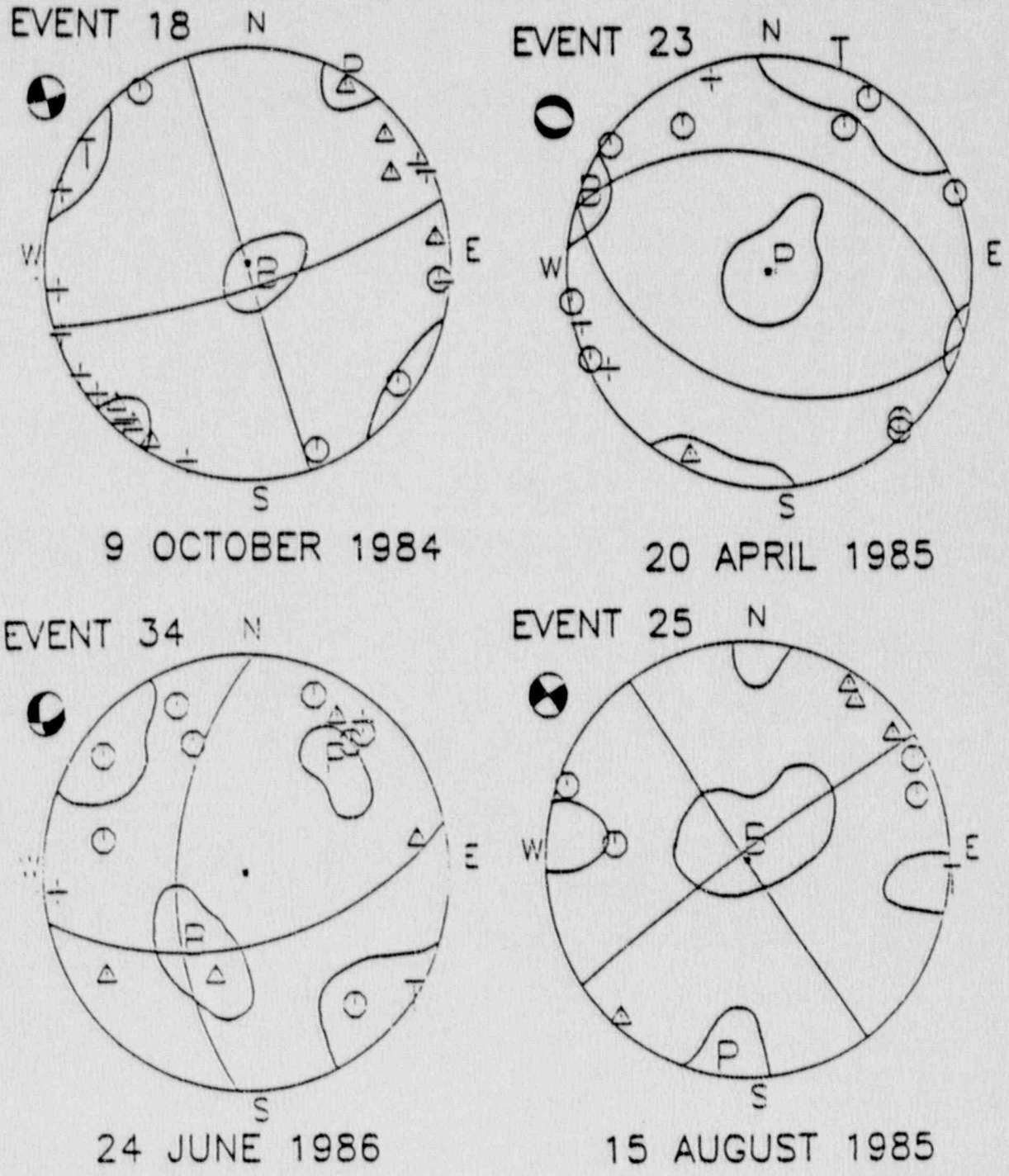

Figures 9e-h. Focal mechanism solutions.

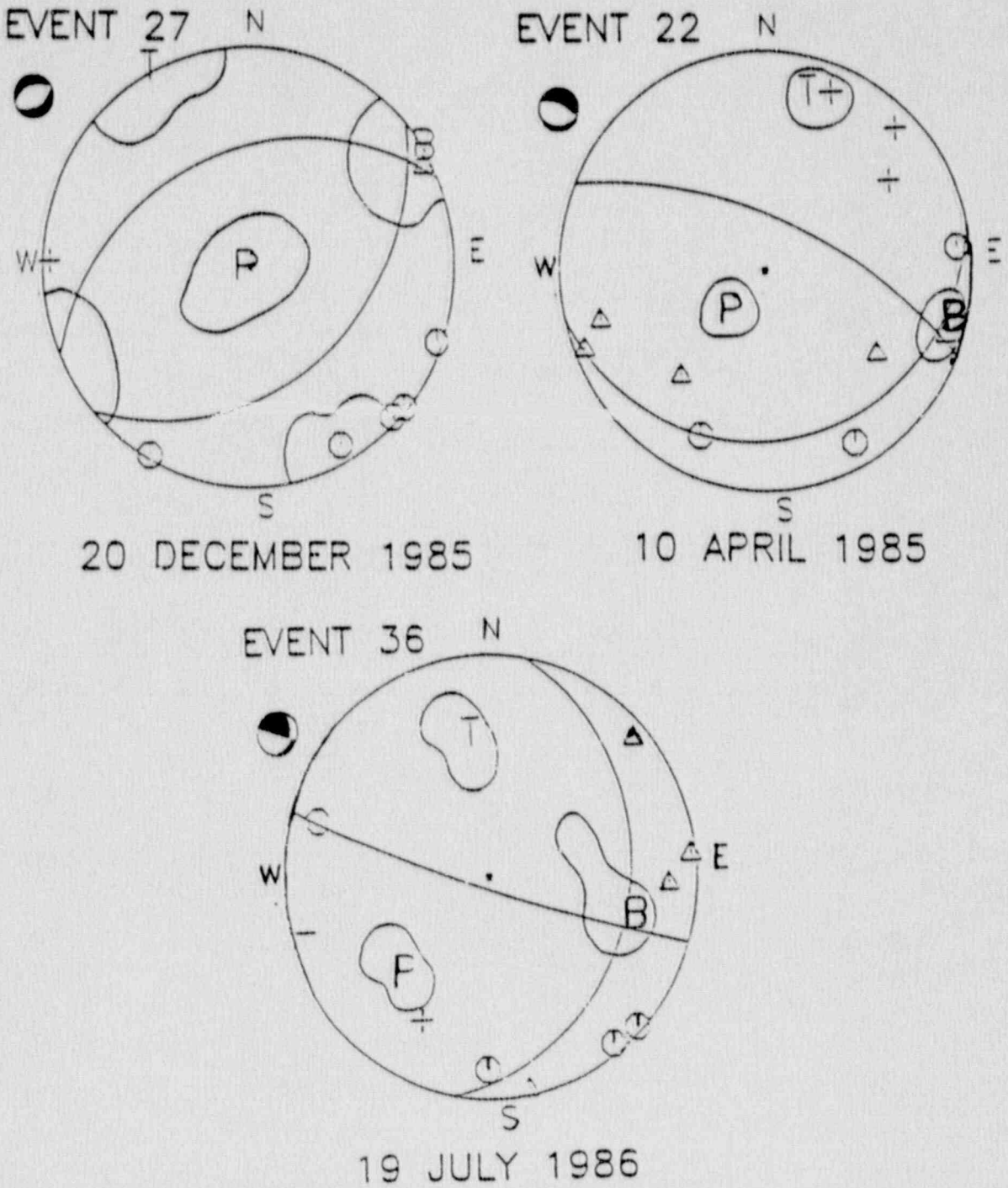

Figures 9i-k. Focal mechanism solutions.

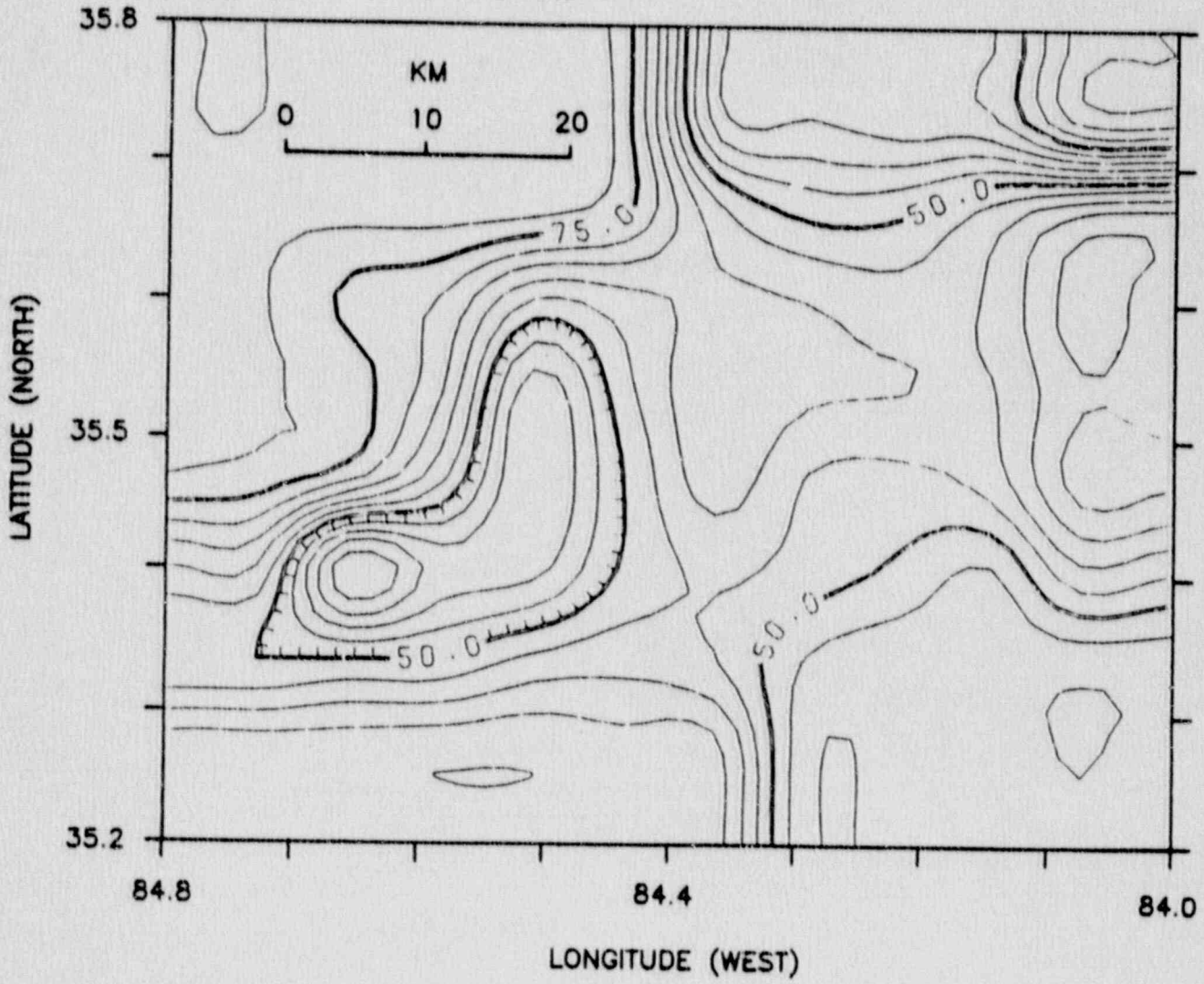

Figure 10. Dip of the null-axis in the central zone. This is a measure of strike-slip motions.

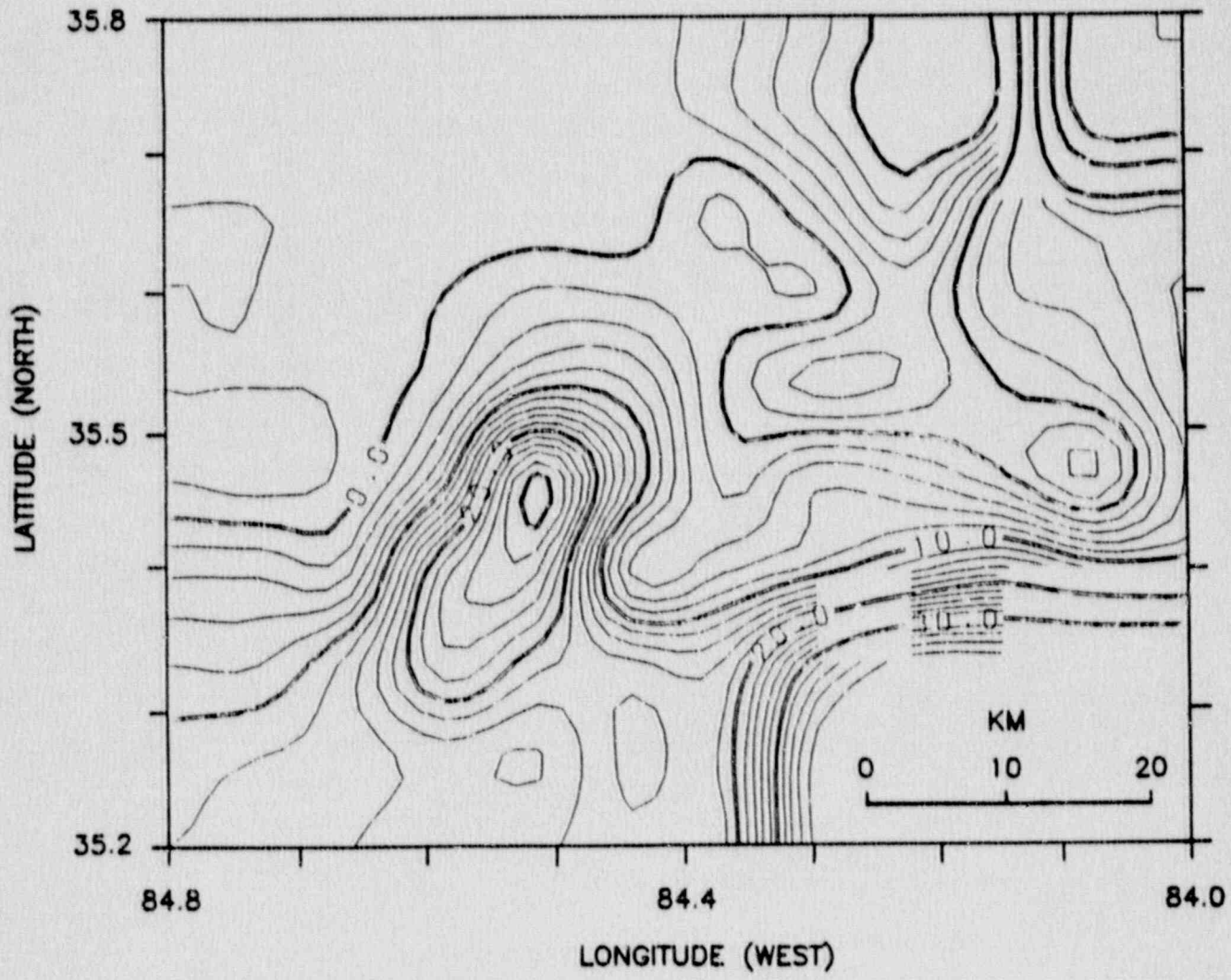

Figure 11. Difference between the dip of the tension axis and pressure axis. A value of -90 corresponds to a pure reverse fault. A value of +90 corresponds to a pure normal fault.

TABLE I.

No.	REFERENCE	DATE	M_D	DEPTH (KM)	EPICENTER
1a	Bollinger et al. (1976)	731130	4.6	3.0	35.799N, 83.962W
1b	Herrmann (1979)	731130	4.6	13.0	35.8N, 84.0W
1c	Guinn (1980)	731130	4.6	3.0	35.799N, 83.962W
2		760204	3.1	4.0	35.01N, 84.67W
3		770727	3.5	4.5	35.49N, 84.37W
4a	Reinbold and Cornwell (1983	820924	3.2	14.0	35.678N, 84.236W
5a			3.5	10.0	35.686N, 84.250W
6	Teague 1984 and Teague et al. (1986)	811125	2.9	12.67	35.639N, 84.638W
4b		820924	3.2	10.0	35.678N, 84.236W
5b			3.5	14.0	35.686N, 84.250W
7		830118	2.3	8.22	35.589N, 84.287W
8		830127	3.1	18.29	36.052N, 83.608W
9		830405	2.0	12.89	35.542N, 84.166W
10		830516	1.9	16.36	35.916N, 84.311W
11		830525	1.6	17.8	35.741N, 84.441W
12		830526	2.5	3.3	35.666N, 84.264W
13a		830708	3.4	9.25	35.545N, 84.156W
14		830715	2.7	15.8	35.550N, 84.162W
4c	Johnston et al. (1985)	820924	3.4	14.0	35.678N, 84.236W
5c			3.5	10.0	35.686N, 84.250W
13b		830708	3.4	9.7	35.548N, 84.153W
15		840214	3.8	9.8	36.125N, 83.737W

TABLE II.

DATA TYPE	CONFIDENCE VALUE
Polarities:	
Incident, digital and develocorder	1.00
Incident, analog	0.85
Emergent, but readable	0.70
Emergent and random (not usable)	0.50
SV/P amplitude ratios:	
Incident, non-clipped	1.00
Emergent, non-clipped	0.70
Clipped and random (not usable)	0.50

TABLE III. Earthquake locations and focal mechanisms.

Date YrMoDa	Origin Time	Lat. North	Long. West	Dur. Mag.	Depth km	# of pts.	Sig.	Tension az.	Tension dip	Presure az.	Presure dip	Null az.	Null dip	P-T
820130	12:39	35.80	83.94	2.8	18.8	9	0.76	38	47	221	43	130	1	-4
820224	12:10	35.72	84.29	1.3	20.4	8	0.69	189	7	283	27	86	62	20
820905	10:11	35.21	84.51	3.2	8.4	12	0.86	138	2	229	24	44	66	22
820924	21:57	35.68	84.24	3.2	14.0	12	0.78	161	25	257	14	14	61	-11
821214	06:35	35.29	84.17	2.4	9.1	11	0.81	312	8	51	47	215	42	39
821215	02:27	35.75	84.22	2.1	19.2	9	0.65	252	57	13	18	112	26	-39
830118	05:09	35.58	84.27	2.3	11.2	11	0.71	335	49	71	6	166	40	-43
830129	18:08	36.12	83.74	2.1	20.7	10	0.91	322	31	220	20	102	52	-11
830304	14:03	35.60	84.34	2.3	8.0	7	0.71	53	20	150	17	277	63	-3
830316	09:13	35.22	84.55	2.6	16.9	6	0.71	327	8	234	16	83	72	8
830405	03:17	35.54	84.19	2.1	18.8	7	0.96	176	16	266	3	6	74	-13
830526	12:30	35.67	84.27	2.5	14.6	12	0.88	146	4	54	19	247	71	15
831016	22:02	35.86	84.55	2.5	19.8	12	0.84	348	24	82	9	191	64	-15
840207	06:32	35.65	84.64	1.8	20.4	7	0.71	19	2	289	1	172	88	-1
840525	10:15	35.60	84.62	2.0	24.1	11	0.87	319	34	110	53	219	14	19
840830	16:26	35.55	84.35	3.1	21.1	16	0.96	142	12	59	3	315	78	-9
840830	16:41	35.55	84.35	2.4	18.0	7	0.99	331	7	239	16	84	72	9
841009	11:54	34.77	85.19	3.5	15.0	22	0.78	298	6	29	7	168	81	1
841107	09:31	35.59	84.64	2.0	18.7	14	0.71	308	40	199	21	88	43	-19
850309	14:29	35.03	85.03	2.5	9.7	12	0.68	8	6	277	8	134	80	2
850312	13:04	35.87	83.57	2.0	25.6	12	0.82	311	7	218	16	64	72	9
850410	10:53	35.72	84.06	2.3	22.0	11	0.53	14	24	226	62	110	13	38
850420	04:21	35.48	84.56	2.5	9.4	13	0.78	20	1	151	89	290	1	88
850712	18:20	35.20	85.15	3.0	19.6	10	0.60	123	17	216	9	333	71	-8
850815	17:31	35.67	83.95	1.8	12.5	8	0.78	100	3	190	2	314	86	-1
850924	00:01	35.68	84.05	1.7	19.1	9	0.88	140	10	233	16	19	71	6
851220	15:15	34.93	84.76	2.9	9.3	7	0.68	329	0	236	81	59	9	81
860107	01:26	35.60	84.76	3.1	17.5	24	0.95	107	11	198	4	308	78	-7
860127	06:44	35.88	83.65	2.6	15.0	11	0.83	289	8	21	17	175	71	9
860419	07:40	35.19	85.51	3.0	21.0	27	0.91	183	9	280	35	81	53	26
860423	07:18	34.79	85.30	1.8	19.1	8	0.60	120	2	24	70	211	20	68
860519	23:46	35.53	84.54	2.6	9.7	14	0.67	284	11	16	15	159	71	4
860602	07:46	35.43	84.50	2.5	18.6	14	0.87	132	32	31	17	277	53	-15
860624	19:22	35.98	83.94	2.8	28.8	14	0.67	131	1	40	41	222	49	40
860711	14:26	34.93	84.99	3.8	20.7	30	0.98	329	18	60	3	159	72	-15
860719	12:31	34.94	84.97	1.9	10.6	10	0.66	349	40	226	32	112	33	-8
860807	12:36	35.49	84.54	2.5	14.9	11	0.49	285	15	25	32	174	54	17
860819	20:51	36.26	85.01	2.9	20.0	13	0.73	112	20	244	62	15	19	42
861115	12:08	35.88	83.82	2.0	16.4	9	0.70	172	2	81	7	278	83	5
870112	18:56	35.50	84.25	2.1	14.8	9	0.85	320	23	121	65	227	7	42
870222	10:35	36.39	84.21	2.8	19.0	14	0.81	314	2	44	1	161	88	-1
870327	01:26	35.60	84.76	3.9	17.5	35	0.99	323	4	53	6	199	83	2
870901	23:02	35.51	84.40	3.2	16.9	17	0.99	304	20	41	18	170	63	-2

The significance measure is based on the number of points, the distribution of data points, quality of first motions and SV/P ratios, and a Chi-square estimate of goodness of-fit.

TABLE IV.

CATEGORY	FOCAL MECHANISM SOLUTION	LIMITS OF P- AND T- AXES (DEGREES)
1	Strike-slip	Dip < 25 Degrees
	Strike-slip with normal or reverse component	25 ≤ Dip ≤ 45
2	Normal	Dip of P-axis > 60
	Normal with strike-slip component	45 ≤ Dip of P-axis ≤ 60
3	Reverse	Dip of T-axis > 60
	Reverse with strike-slip component	45 ≤ Dip of T-axis ≤ 60

TABLE V.

SIGNIFICANCE	Q	R	Q	NO. OF POINTS	Q
≥ 0.9	S1	0.8 ≤ R ≤ 1.2	R1	P ≥ 15	P1
.8 ≤ S < .9	S2	0.8 > R > 1.2	R2	15 > P ≥ 10	P2
.7 ≤ S < .8	S3	0.6 > R > 1.4	R3	10 > P ≥ 5	P3
< 0.7	S4	0.4 > R > 1.6	R4	P < 5	P4

APPENDIX B

A Technique for the Inversion of Coda Q

APPENDIX B

A TECHNIQUE FOR THE INVERSION OF CODA Q

Leland T. Long Jeih-San Liow and Frank B. Jones

ABSTRACT: Digital data from station CBT in southeastern Tennessee provide estimates of coda Q with variations which depend on the direction to the earthquake. We interpreted this azimuthal variation to indicate a spatial variation of the properties of the crust that determine coda Q. Coda Q is a phenomenological parameter characterizing coda decay and it is determined by the integrated effects of crustal parameters in the ellipsoidal volume of crust with the recording station and hypocenter as foci. Zones of anomalous crust will influence the computation of coda Q differently for different station and hypocenter pairs. Through a sequence of approximations, we have linearized the relation between the measured apparent coda Q and an assumed constant coda Q for discrete zones of crust. Inversion of coda Q data from regional stations in the southeastern United States suggests a reduction in coda Q as one nears the coastal plane. Inversion of coda Q data near station CBT suggests an anomalously low coda Q region (Q=38) in a 300 square kilometer region northeast of station CBT.

INTRODUCTION

The wavelets that make up a seismic coda are affected by the size, shape, and distribution of scatterers and by intrinsic attenuation. In a coda, the combined influence of intrinsic attenuation and scattering are difficult to separate. Hence, coda Q, as measured from the rate of decay of the coda, should with objectivity be treated as a phenomenological parameter characterizing coda decay.

We have observed significant variations in the shape of the shear wave coda in records from our station CBT in southeastern Tennessee. Figure 1 shows some of these records and the epicenters for these events. In particular, note the rapid decay for events northeast of CBT and the slow decay of the coda for events to the northwest.

We use coda Q in this study only as a phenomenological parameter to characterize this variation in coda decay. The assumptions invoked in the derivation of equations used to give numerical values to coda Q will change the values of coda Q, although relative differences in coda Q will generally remain the same. We leave the interpretation of Q for later studies.

Coda Q is of particular interest because low Q values have been associated with greater rates of occurrence of large events in China and in the western US. In those studies, the spatial variation of coda Q was inferred from estimates of Q for a distribution of single station average values. Alternately, for single events the coda Q could be assigned to the midpoint of the line connecting the epicenter and station. In this analysis we consider the possibility of using coda Q as measured at an array of stations for an array of epicenters to determine the spatial variation of coda Q in the crust. Hence, we are attempting to attain a higher resolution of coda Q than is currently possible with single station techniques.

THEORY

One can not do justice to the multiplicity of mechanisms in scattering and attenuation with this abbreviated derivation. For a single arrival that traverses media of varying Q, the cumulative attenuation (1/Q) is the sum of the effects of attenuation in each segment. The resulting equations are intuitively correct for one dimension. The extension to three dimensional scattering and attenuation is not straight forward, but the relation can be shown to be approximately correct.

Fundamental to showing this result is the assumption that coda Q calculated from increasingly longer lengths of the coda are representative of increasingly larger "ellipsoidal" volumes of the crust. It would be natural to generalize the analysis to a crust divided into many segments, but in this presentation we consider only acknowledged regional provinces or a single anomalous zone.

First we assume that the amplitude in the coda is given by,

$$A(t) = A_o(t) \exp[-\pi ft/Q] \tag{1}$$

where f = frequency, t = time form origin, A(t) = amplitude in the coda at time t, $A_o(t)$ = geometrical attenuation of the original amplitude and Q = attenuation coefficient that describes the decay with time.

We next consider the energy density for the path to the jth scatterer in a single scattering model for individual scatterers to be,

$$dn_j \exp[-2\pi ft/Q]$$

and the attenuation is expressed as an integral over the path,

$$t/Q = \int (1/Q)\, dt.$$

The integral is converted to a discrete summation by approximating the crust as discrete zones of constant coda Q. Combining the two expressions above gives,

$$\sum_j dn_j \exp[-2\pi f \sum_i T_{ij}/Q_i] \tag{2}$$

where T_{ij} = the fraction of time within the zone of Q_i along the path to the jth scatterer. The next step is to expand exponent in Taylor series and interchange order of summation. This requires one assume a uniform distribution of scatters. From geometrical arguments, we note that only a fraction (P_i) of the arrivals will pass through the ith crustal block. This allows in a first approximation, that the P_i are the percent of the energy at time t,

$$\sum dn_j + \sum_i -\pi f/Q_i \sum_j dn_j T_{ij}$$

$$\sum dn_j\, T_{ij} \approx [A_o(t)]^2\, P_i \tag{3}$$

The expansions are undone in a similar reverse procedure to show that $1/Q$ is approximately the sum of P_i/Q_i, or that,

$$1/Q \approx \Sigma P_i/Q_i \qquad (4)$$

Equation (4) is a linear relation between observed coda Q and the percent of area "volume" that is assigned an unknown value Q_i.

RESULTS

We can present results for two inversions for Q. The first a study of regional events in the southeastern United States; the second a study of an anomalous area in southeastern Tennessee.

In the regional southeastern United States study, we utilized physiographic provinces: Atlantic Coastal Plane, Piedmont, Folded Appalachians, Interior Lowland Plateau and the Gulf Coastal Plane. The events ranged in location from South Carolina to New Madrid, MO. The data used were recorded on stations equivalent to WWSSN short period records. Q for the interior Lowland Plateau exceeded 700. The Gulf Coastal Plane gave values of 250. In-between values were obtained for the Folded Appalachians and the Piedmont, about 425. The Atlantic Coastal Plane Q of 388 was slightly less than average.

In the study for southeastern Tennessee we used data from four stations and about 50 records of earthquakes. Figure 2b shows the epicenters and stations used. The area considered for computation of anomalous Q is shown shaded in Figure 2a and was based on seismicity and travel time residuals. This area was then used to define the area or volume of the ellipse that optimized the influence of the anomalous zone and, hence, the length of coda for computation of coda Q. Figure 2a shows a set of ellipses for station CBT. Note the variation in area of influence that allows use of such data in a linear inversion technique. The inversion in this case gave a coda Q in excesses of 1000 for the surrounding area, and a value of 4000 was assigned to the regional area based on measurements of extended lengths of coda. A least squares estimate of Q for the anomalous zone gives Q = 38 with a range from 10 to 100 at one standard deviation.

Figure 3 shows the fit of the data to theoretical curves for various values of anomalous Q, with a fixed regional Q of 4000. The scatter may be related to a number of factors:

1) inappropriate choice for boundaries of anomalous zone,
2) expected uncertainty in measurement of coda decay,
3) choice of 2 or 3 dimensional models for scattering,
4) existence of other anomalous zones , and 5) multiple versus single scattering contributions.

ny case, a definite trend exists in this data and that trend is consis- with a zone of anomalous crust in southeastern Tennessee. This tech- ue, with appropriate refinements and tests, will be capable of defining da Q in relatively small areas of the crust.

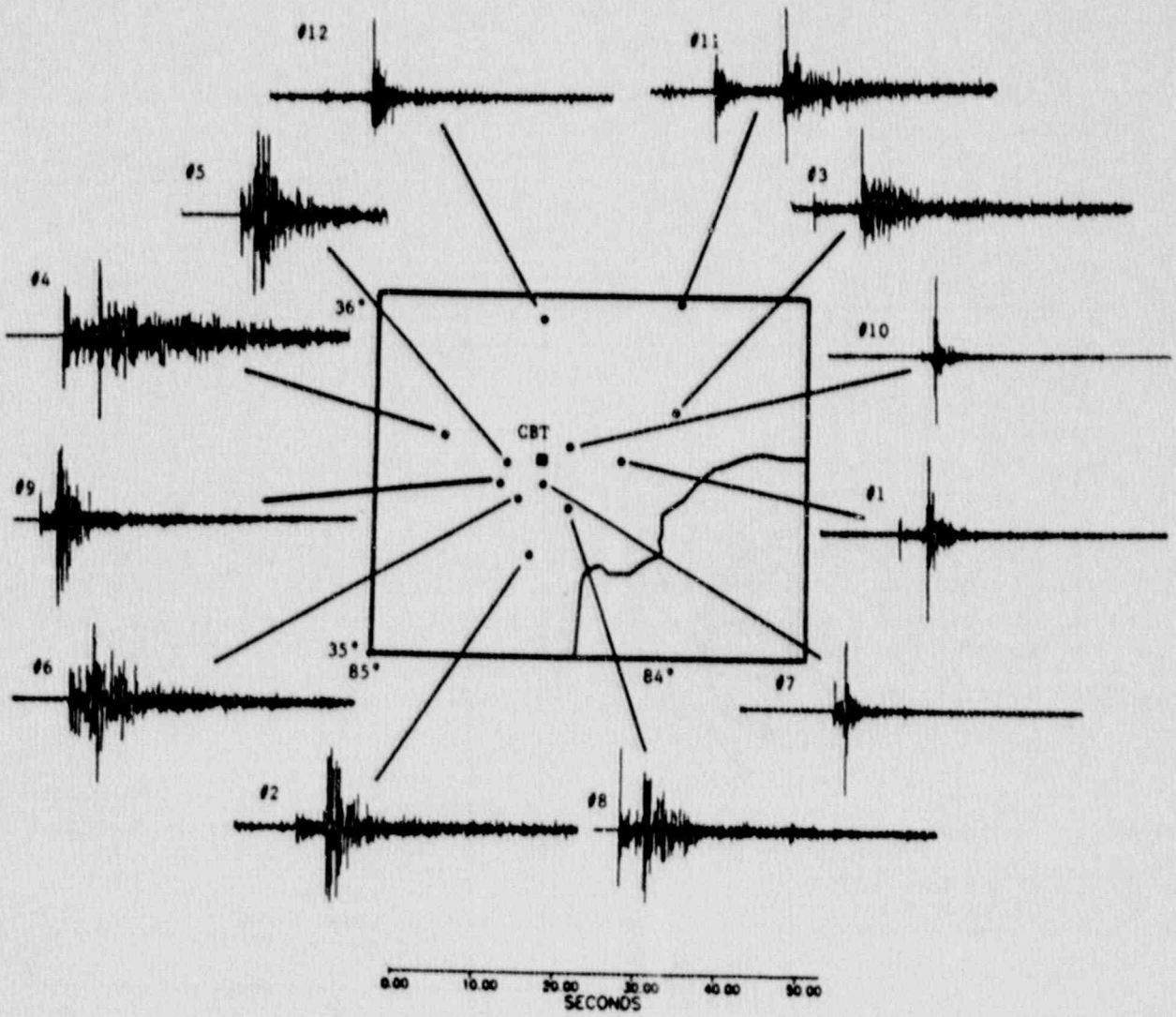

Figure 1. Seismograms recorded at station CBT showing variation in character of coda decay and their location relative to CBT.

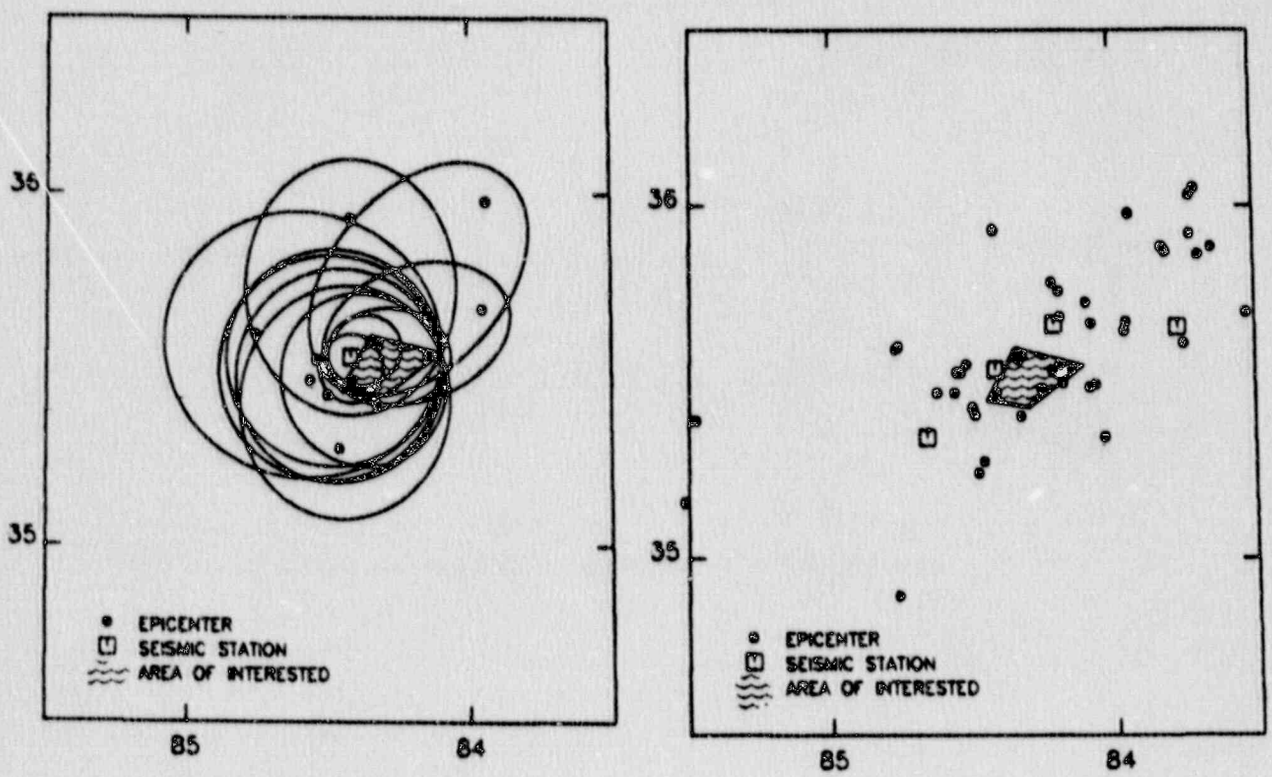

Figure 2. Data for preliminary analysis. (a) Comparison of anomalous area and ellipses of influence, and (b) locations of stations and events used.

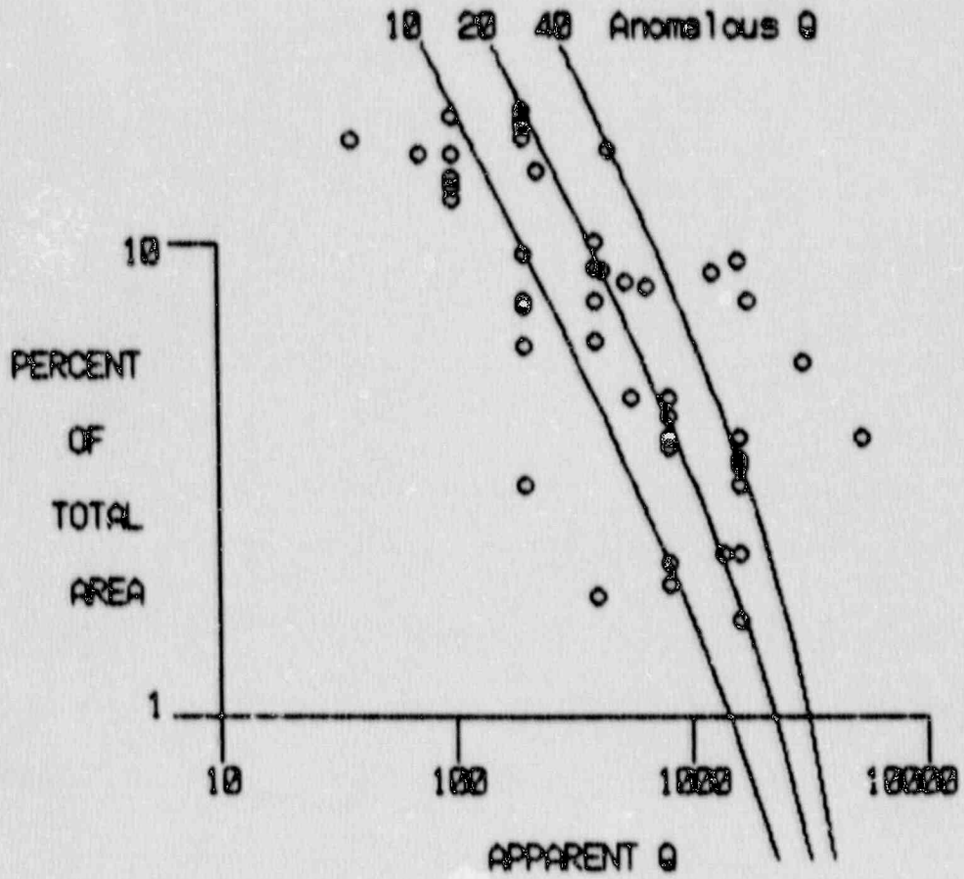

Figure 3. Apparent Coda Q versus percent contribution of anomalous area in the ellipse of influence.

APPENDIX C

Fracture Intensity and Reservoir Induced Seismicity

APPENDIX C

FRACTURE INTENSITY AND RESERVOIR INDUCED SEISMICITY

Leland T. Long, Christopher C. Sorlien and Thomas J. Schmitt

ABSTRACT: Detailed field measurements of fractures and joints were taken near the epicentral zone of the August 2, 1974, magnitude 4.3 earthquake in the Clarks Hill Reservoir (now Lake Strom Thurmond). Zones of anomalous fracture intensity are consistent over distances of a kilometer and an observation spacing of 0.5 to 1.0 km will allow contouring of fracture intensity. The joint intensity varied systematically in the study area. The area of induced earthquakes was concentrated along the edge of a zone of low fracture intensity and high rock quality. Hypocentral depths of earthquakes which are attributed to movement on shallow joints are typically less than 1 km, and within this depth range the fracture intensity does not significantly decrease or vary. Quantitative surface measurements of rock quality (which includes fracture intensity) can be extrapolated to the depths of nucleation of these induced earthquakes. In contrast, stress may be released through creep on (foliated) schists and altered mafic rocks, explaining the lack of seismicity in zones of high fracture intensity and low rock quality. The association of granite gneiss and high rock quality measurements can be used to predict susceptibility to induced or natural shallow seismicity.

INTRODUCTION

Earthquakes in the Piedmont Province of Georgia and South Carolina have unique properties that distinguish them from events in many other seismic areas of the continental interior. These properties are their near surface to 2.0 km depth of focus (Dunbar, 1977; Fogle et al., 1976; Talwani, 1977;), their swarm-type occurrence and associated high b values (Long, 1974; Talwani et al., 1979; Johnson, 1984), their cubic high-frequency spectral decay (Marion and Long, 1980), their association with reservoirs and water loading (Talwani, 1976; Costain et al, 1987; Jones et al, 1986), and the similarity between joint directions and focal mechanism solutions (Guinn, 1980). Taken singly or in concert, these properties of Piedmont earthquakes have been interpreted as supporting an association between Piedmont seismicity and shallow joints or fractures.

In a study of the geology of the area of induced seismicity around Monticello Reservoir, Secor, et al. (1982) observed numerous diversely oriented small fractures and lithological inhomogeneities in the Winnsboro complex, and speculated that these control the diffuse induced seismicity. Although the association between seismicity and jointing or small fractures has been established on the basis of depths of focus, source spectral properties, and a comparison of focal mechanisms with joint plane patterns in the Southern Piedmont, the details of the style of jointing and its correlation with seismicity have not previously been investigated. This study was undertaken to discover how joints and fractures are related to induced seismicity and, hopefully, to suggest ways in which rock quality may be used to asses a potential for induced seismicity. The objective of this paper is to present our systematic examination of joints and fractures in an area of induced seismicity.

THE STUDY AREA

The study area is a rectangle of 6 by 12 km which covers the epicentral zone of the August 2, 1974, M_L 4.3 earthquake (Fogle et al, 1974). Portable seismographs were deployed immediately following the 1974 event (Talwani et al., 1975) in an aftershock survey. Additional intermittent monitoring in the aftershock zone (Bridges, 1975; Guinn, 1977) and continuous monitoring by a regional network (Long et al., 1976) has defined the distribution of epicenters. The aftershocks and study area are located in the upper reaches of the Storm Thurmond Reservoir (figure 1). The aftershocks were not restricted to a single fault plane, but instead were scattered over 7 km^2 area centered 1.5 km northeast of the Savannah River channel. The depth-of-focus of aftershocks to the 1974 earthquake were computed by Talwani (1976) to range from 0.5 to 2.5 km. A relocation using a revised velocity model on an independent set of 81 aftershocks showed that most are above 1 km (Dunbar, 1977). The relocated events had a hypocentral precision of better than 200 meters both horizontally and vertically. The 1974 event and its aftershock sequence was not the first occurrence of seismicity in the Strom Thurmond Reservoir area, with notable events in 1969 (Long 1971) and an intensity VI earthquake felt near Lincolnton, Georgia, in 1875 (Long, 1984).

The geology of the study area is complex, (Griffin, 1973; Hatcher, 1987) consisting of metamorphic lithologies which have been migmatized and intruded by granite. The major contacts strike northeast parallel to the Charlotte belt structures in which they reside. An advantage of the study area is the availability of rock exposures along the shoreline of the Strom Thurmond Reservoir and in adjacent streams. The rocks in these exposures were sufficiently intact to allow joint spacing measurements and most were easily accessible from the reservoir or roads.

ANALYSIS AND FIELD METHODS

Well defined cracks or fractures pervade the near-surface crystalline rocks of the Piedmont province. We refer to these cracks or fractures as joints if the slippage of one block against the other can not be determined or is very slight. The average separation of joints in a joint set may be difficult to quantify because the joint spacing and distribution may display great variety which (among other factors) depends on rock type. The trimean joint intensity was proposed (Wheeler and Dixen, 1980) as a means of quantifying rock strength properties based on field measurements and as a means of minimizing the effects of extreme values of joint spacing. The intensity of a joint set has the dimensions of surface area of joints per cubic meter with units of inverse meters. The trimean estimator of joint spacing was used in this study to compute the trimean intensity, and effectively minimize the effects of extreme values in the separation of joints. The trimean spacing is calculated for each joint set by adding the first and third quartiles to twice the median spacing and dividing by 4 (Wheeler and Dixon, 1980). Trimean intensity then uses trimean spacing in the same way as average spacing is used in average intensity calculations, and is considered a statistically robust estimator of joint intensity.

A proper choice of statistical measures for joint spacing is not well established. The use of average spacing or trimean spacing assumes a distri-

bution of spacings about some mean or median value. In field observations, the distribution of joint spacings can be highly irregular, with variations from almost uniformly spaced joints to highly bunched joints with many small spacings and a few large spacings.

An alternate statistical technique for quantifying joints is to find their fractal dimension. Many related natural systems, such as rock permeability (Wong, 1988) or the roughness of joint and fault surfaces (Scholz and Aviles, 1986), satisfy self similar (fractal) models. In this evaluation we considered that the distribution of joint spacings would satisfy the relation,

$$N = A\left[\frac{L}{r}\right]^{dr} \qquad (1)$$

where N is the number of joints spacings of length greater than or equal to r in a total length (outcrop length) L. The A is a constant of approximate value one that represents the difference between the measured L and its statistical estimate. The fractal dimension is dr and is computed from a least squares estimate of the slope of Log(N) versus Log(L)-Log(r). For those sites that satisfied a self similar distribution, the fractal dimension has the advantage of being the most robust statistical parameter. A disadvantage is that the relation between fractal dimension and rock quality is unknown.

Fracture intensity and fractal dimension determinations require measurements of the attitudes of joint sets and spacings between individual joints. A study of the spatial variation of joint intensity requires a relatively uniform distribution of rock exposures. The shoreline and tributaries of the reservoir provided nearly continuous rock exposure except where limited by the area covered by the lake and by deeply weathered saprolite in the higher elevations northeast of the epicentral zone. Where possible in the study area, rock outcrops were examined at a separation of no more than 2 km. More dense observations were taken along the shore line and where possible in the epicentral zone. Along the lake shore, a minimum of 1 km spacing was maintained, and for 20 stations in the epicentral area, separations of 100 to 500 m were achieved. In the northeast sector, saprolite and rock exposures were limited to stream beds where the saprolite was fresh enough to preserve exposed joint surfaces. The shores of the reservoir provide nearly continuous saprolite or unweathered rock outcrops. Most stream outcrops were from 1 to 5 square meters, and had to be reached on foot. The precision of map coordinate measurement was 0.01 minute or approximately 20 m. Hence, stations located on distinct physiographic features such as points of land by the lake were located to within 20 meters. Those few stations on streams or unmapped roads, which were devoid of easily identified landmarks, allowed a precision that was about 50 meters. No corrections were made for magnetic deviation in location or in fracture attitude measurements, since the magnetic deviation of the study area was less than 1 degree, which is less than the precision of the measurements.

The primary goal of the field study was to obtain fracture spacing measurements distributed uniformly over the study area for the major joint sets. The criteria for the degree of variation of attitude within one set was

dependent on ability to accurately measure the perpendicular spacing measurement. Joints that intersect might be separated into two sets, while the same range of attitudes might fit in one set if attitudes vary smoothly across an outcrop. Usually a variation of 20 degrees about a mean is permitted within one set for both strike and dip, unless there are two distinct sets of parallel joints within that range. The average strike and dip of each joint set was divided into six groups based on azimuth and dip. The classification allowed independent examination of distinct joint sets and a comparison of them with rock quality, average intensity, trimean intensity, and fractil dimension.

Where attitude measurements were limited, usually a few attitudes could be measured to allow correction of joint spacings to the perpendicular. For 75 percent of the measuring locations, the outcrop allowed spacing to be measured perpendicular to the joint surface for each joint set. The resulting data set includes over 4000 spacing measurements. In vertical outcrops, usually only a few spacings of horizontal joints could be measured. Few subhorizontal joints could be found in the horizontal outcrops.

FRACTURE AND ROCK QUALITY MEASUREMENTS

The fracture or joint intensity for a rock volume was determined by adding the intensities of each joint set. To minimize the effects of extreme values, the trimean measure of intensity was adopted. Trimean fracture intensity was computed directly from the inverse of the trimean spacing, where trimean spacing is the weighted average of the first quartile, the third quartile, and the median (Wheeler and Dixon, 1980) according to the equation:

$$I = \sum_{i=1}^{n} I(i)$$

where $I(i) = 4/(S_1+S_3 2S_2)$

for the ith joint set and,

S_1 = first quartile,
S_2 = median spacing
and S_3 = third quartile.

Fracture intensity can be used directly in the calculation of rock quality by using the system described by Barton et al. (1974). This system uses six parameters to describe the rock mass quality, Q. The parameters used in this study include; the number of joint sets (Jsn), the roughness, flatness, and continuity of the joint surface (Jrn), alterations of the joint surface (Jan), and the rock quality designation (RQD) computed from the fracture intensity. The ratio of the joint water reduction factor to the stress reduction factor in this study was taken as one to be compatible with near-surface conditions. Hence, in this study, rock mass quality Q was computed from,

$$Q = (RQD/Jsn)(Jrn/Jan)$$

where RQD = 115 -3.3I, and where Jsn, Jrn, and Jan were estimated according to the scales presented in Barton et al. (1974). In this study, all subplanar open cracks were measured. Because Barton et al. (1974) considers only systematic through-going joints, the data needed to be adjusted. This was accomplished by use of high (1.5 to 2.5) joint roughness numbers for discontinuous, uneven, or extremely fine cracks. Since the surface rocks measured in this study varied from fine, discontinuous cracks to open, mineralized systematic joints, these four parameters serve as a correction for the variability in importance of the fractures in different types of rock. In this study of the variation in rock quality, Q should be a better measure of rock strength than fracture intensity.

Because the size and quality of the outcrops varied widely, a supplemental weighting for the data based on outcrop size and degree of weathering was developed. Although most features were evident in the unweighted data (Figure 4), the weighting of the data helped identify the erratic data of poor quality.

Rock types within five kilometers of inlet A (Figure 2) were in order of predominance, coarse grain granite, coarse and fine grain gray granite gneiss, layered and folded or contorted gneiss, and red clay saprolite derived from mica schist. Mafic dikes with an average thickness of one meter intrude these rocks. Ten stations had more than 25 percent of the measurements in pegmatite dikes or quartz veins, and two stations were entirely in quartzite. Three stations and three stream substations were in unweathered rock. Generally, joints would cut across granite, granite-gneiss, and gneiss equally when present in the same outcrop, but weathering of the gneiss or very coarse grain granite can form a surface crust that obscures fine fractures. These rocks dominate the immediate epicentral region, as well as the area across the lake to the southwest. Therefore, in this study area variations in joint intensity should be determined by factors other than rock type. Outcrops of highly decomposed mica schist that might be expected to fracture with a different intensity under identical conditions are found outside the study area. At stations where mica schist was found in the study area, systematic joints cross both rock types, but are much less noticeable in the mica schist. Stations where a red clay saprolite was found were not used in the trimean data and are given very low weights. The preferential appearance of unfractured rock in outcrops due to its resistance to weathering was considered as a potential source of bias. Although this could influence isolated outcrops, the continuous exposure of rocks along the reservoir shoreline provided data independent of rock hardness. In contrast, thin quartz veins or pegmatite dikes have either more fracturing or more easily recognizable fracturing than the country rock. Outcrops with thin quartz veins or pegmatite dikes generally have lower joint intensities. Although no adjustment for rock type was made, the spatial weighting of the large numbers of stations tend to smooth out local effects.

OBSERVATIONS OF JOINT SETS

The SE and NE striking near-vertical joints occur systematically throughout the Clarks Hill study area (Figure 2). Stream courses near inlet A are controlled by the SE and NE joint sets. The most planar and paralleljoint set strikes SE between 110 and 140 degrees azimuth and the less important

strikes NE between 40 and 60 degrees azimuth (Figure 3). Bell (1973) has also shown NE and SE lineaments in the topography in the southern part of the study area, and the same trends in joint orientations. Bevis and Gilbert (1984) describe pervasive NE and SE striking conjugate joint sets in the southeastern United States. The regional nature of the major joint sets make it improbable that they are purely a near surface phenomena. The SE joint set is probably the oldest, as other sets abut against them and dikes are intruded parallel to the SE set in some outcrops. Generally, the SE set terminates against the NE set. The SE striking set is easily recognized because the joints that make up the set are very continuous, planar, and parallel. At CH37 this set has a 5 mm mineral coating, implying that they were more under tension than other orientations at the time of mineralization. In some cases subhorizontal microfaults offset vertical joints, while in others the subhorizontal surfaces of joincs terminate against other joints. In both cases the subhorizontal joint surfaces are more recent, and may be related to unloading. Observations immediately after the 1974 event in this area revealed flaking or chipping of a crust that forms during weathering of some granitoid outcrops. This effect was not noticed during the 1987 study. Chipping is taken to represent surface movement on joints during the 1974-1975 activity.

RESULTS

For purposes of contouring the data, the value at each point in an evenly spaced distribution of points was estimated by a normalized weighted average determined from the product of the size and quality weight with the inverse of the square of the distance from measured outcrops. A 0.5 km spacing was used in this study and only outcrops within a radius of 1 km were considered in the weighted average. The weighted average smooths the local variations in fracturing and suppresses spurious values associated with smaller outcrops and lower quality rocks.

The raw data show scatter (Figure 4) and to evaluate the appropriateness of the data for contouring we computed its autocorrelation function (Figure 5). The variance of the trimean intensities is 18, but the non-random or correlated portion of this is about 12 suggesting an uncertainty of ±2.3 and a spatial variance of 3.4. The autocorrelation distance is about 1.5 km. An autocorrelation distance of 1.5 km suggests that a data separation of 0.5 to 1.0 km would be sufficient to define the anomalies in this study area. The uncertainty of 2.3 suggests that a contour interval of 5 would be appropriate for this data. The gridded data have the same spatial variance of 12; however, the process of gridding has extended the autocorrelation distance to 2.0 to 2.5 km. The extension of the autocorrelation distance was influenced by the smoothing effects of areas of sparse data on the fringes of the study area, whereas the gridding process would retain the details of the densely sampled central area.

The trimean fracture intensity (Figure 6) shows areas of high and low intensity which generally follow the reservoir. Some of the low fracture intensities adjacent to high fracture intensity are related to the condition or size of the outcrops. The assigned weights for these stations were effective in suppressing the influence of the low quality and smaller outcrops in generating the concurred versions of the data. Some of the variability on a scale of less than 500 m is real and related to lithology or small scale

fracture zones or areas where different fracture sets cross. Examination of the data in its gridded format assumes that the variations on a scale of 10's of meters are not as important to the stress level that can be supported by the rock as are the variations on a scale of kilometers. We consider bulk strength on a scale of kilometers more important than local rock strength.

The contoured values of rock quality (Figure 7) show a large area to the east of the aftershock zone where fracture intensity is very low and rock quality high. A belt of more highly fractured rock extends to the west-northwest. The aftershocks of the August 2, 1974, earthquake occurred along the steep gradient in joint intensity separating the low intensity zone from the high-intensity zone. Low fracture intensities are also found to the southeast, but are based on sparse (two) data points with low weights. These two sites were also more highly weathered and the crusted boulders could have obscured some fractures. Outcrop condition was not a problem in half of the 14 outcrops that showed low fracture intensity near the epicentral zone. The contours of high fracture intensity tended to be elongated parallel to the SE striking fracture set. With the rock quality, (figure 7) a SE striking zone of low rock quality determination values follows the channel of the Savannah River in the reservoir. Rock quality, which uses average intensity, has slightly different contours than the trimean intensity. Where outcrops permit evaluation of Jrn and Jan, and if these evaluations are consistent, rock quality is a better indicator of rock strength. An example of the effect on rock quality occurs at stations CH47 and CH65, where intense but fine and sometimes discontinuous joints were measured. A Jrn of 2.0 caused the rock quality to be double what it would have been if the joints had been open, through, and systematic.

The trimean data (Figure 6) excluded the near-horizontal joint systems, because they are difficult to measure in many of the horizontal and flat outcrops. Since the data requirements were more severe for the trimean computation, these measures should be less dependent of outcrop quality. Generally, trimean intensities were about 25 percent higher than average intensities. This is explained by the suppression of a few large joint spacings by the trimean computation method. Station 4.1 was an example of the influence of widely varying joint spacing on joint intensity estimates. The trimean joint intensity will emphasize the weakest zones of the rock.

DISCUSSION

A key element in associating joint patterns with induced seismicity is verifying that the surface expression of joints extends to the focal depth of the earthquakes. Seeberger and Zoback (1982) showed that in 8 wells near the San Andreas fault in California, the fracture intensity is not dependent on depth in the upper 250 meters. Zoback and Hickman (1982) showed that intensity is only slightly dependent on depth for the upper 1100 meters near Monticello reservoir in the Piedmont of South Carolina. The geology of the Monticello area and the Strom Thurmond Reservoir area are similar and hence the joint intensity likewise in the study area would not be expected to vary significantly with depth. In contrast, the joint intensity of the subhorizontal joints may vary significantly with depth since the subhorizontal joints may have formed relatively recently in a compressive near-surface stress field. Schaeffer (1988) has reviewed evidence for joint intensity variations

with depth in the vicinity of the Bad Creek project, South Carolina, and found little variations in intensity to the 1000 m depths comparable to the hypocentral depths of the induced seismicity.

Although the lithology is variable in the study area, the discontinuities tend to strike NE and dip steeply, and much of the variation is between granitoid rocks of assumed similar rheology. The fact that the major trend in rock quality contours (Figure 7) trends SE, while the strike of most lithologic units is NE, suggests that regional fracture sets, and not lithology, most affects fracturing.

STATE OF STRESS

Focal mechanisms of the aftershocks of the McCormick earthquake were not consistent, with individual aftershocks often showing focal mechanisms that differed from previous events (Guinn, 1980). These include a low angle thrust for the main quake; EW striking sinistral faults, SE striking normal and dextral faulting, and low angle thrusting for aftershocks. A mixture of focal mechanism solutions and stress directions have been observed at other reservoirs in the S. Carolina Piedmont (Zoback and Hickman, 1982; Haimson and Zoback, 1984). Talwani (1977) reports that focal mechanism solutions favor a maximum horizontal compressive stress axis oriented NW at Lake Jocassee, while nearby hydraulic fracturing (Haimson, 1975) show it to be NE. The horizontal stress levels are typically high in the crystalline Piedmont rocks. Stress inferred in wells in Virginia (Rundle et al, 1985), and at Monticello Reservoir in South Carolina (Zoback and Hickman, 1982), show that the rock is near failure.

Reservoir induced seismicity is generally hypothesized to be related to the release of elastic stress due to loading, and to the increase in pore pressure reducing effective stress (Simpson and Narasimhan, 1986). Marion and Long (1978) suggest a process of pressure solution and mineral alteration weakening joints until failure occurs. Near the surface, the residual stress may be related to the formation of tension joints. These release residual horizontal stress (Price, 1966). The release of horizontal stress would contribute to a variable stress field related to fracture intensity. Highly fractured areas would be under a lower stress field, one more favorable to normal faulting than adjacent unfractured regions of low intensity or high rock quality. Hence, as suggested in this paper, rock quality may control the availability of stress for reservoir induced earthquake.

CONCLUSIONS

Aftershocks of the 1974 McCormick South Carolina earthquake near Clarks Hill Reservoir are spatially related to the border between relatively unfractured rock to the southeast and intensely fractured rock to the northwest. Seismicity occurred in areas of gneiss and granite, and not in mica schist, which is assumed not rigid enough to accumulate high stresses. The region of lightly fractured high quality rock will not deform at the same rate as intensely fractured rock, and so higher than average stresses were concentrated along the margin. Rock strength is lower in highly fractured areas, and so with a homogeneous stress field failure will occur there. Thus the largest shallow earthquakes should take place on pre-existing fractures in otherwise high quality rock.

Pressure solution along joints, or alteration of feldspars will weaken the strength of a fracture and accelerate the time of failure. Major throughgoing faults are not required in this model, although ancient faulting may influence fracture intensity. The dominant orthogonal joints are continuous enough to form fracture zones that could transmit hydraulic pressure pulses or be permeable, especially if in an orientation under tension in the current stress field, or if they were rebroken in the main quake. A combination of long term alteration in joints, yearly spring rises in lake level, rapid rise after heavy rainfall, and possibly infiltration of rain directly into joints could affect the timing of aftershocks here. The low recent level of seismicity means that most of the excess stress along the unfractured rock margin was released.

We conclude that induced earthquakes are unlikely to occur in unfractured crystalline rock, and unlikely to occur in the middle of a large area of low rock quality or otherwise weak rock. Therefore areas of intense fracturing in rigid rock adjacent to unfractured rock should be avoided in the siting of facilities that might be damaged by shallow focus local magnitude 4 to 5 earthquakes.

REFERENCES

Angelier, J. and P. Mechler, 1977. Sur une methode graphique de recherche des contraintes principales egalement utilisable en tectonique et en seismologie: la methode des diedres droits, Bull. Soc. Geol. France, No. 6, 1309-1318.

Angelier, J., 1979. Determination of the mean principal stresses for a given fault population, Tectonophysics, 56, T17-T26.

Barton, N., Lien, R. and J. Lunde, 1974. Engineering classification of rock masses for the design of tunnel support, Rock Mechanics, 6, p. 189-236.

Bell, H., III, 1973. Some results of geochemical sampling in McCormick county, South Carolina, Geological Survey Bulletin 1376.

Costain, J.K., G.A. Bollinger and J.A. Speer, 1986. Hydroseismicity: A hypothesis for intraplate seismicity near passive rifted margins, Earthquake Notes, 57, 13.

Costain, J.K., G.A. Bollinger and J.A. Speer, 1987. Hydroseismicity: a hypothesis for the role of water in the generation of intraplate seismicity, Seism. Res. Lett., 58, 41-64.

Costain, J.K., G.A. Bollinger and J.A. Speer, 1987. Hydroseismicity: a hypothesis for the role of water in the generation of intraplate seismicity, Geology, 15, 618-621.

Dunbar, D.M., 1977. A seismic velocity model of the Clarks Hill Reservoir area, Master Thesis, Georgia Institute of Technology, Atlanta, GA, 59 pp.

Fogle, G.H., R.M. White, A.F. Benson, L.T. Long and G.F. Sowers, 1976. Reservoir induced seismicity at Lake Jocassee, northwestern South Carolina, Law Engineering Testing Co., Marietta, Georgia.

Griffin, V.S., Jr., 1973. Geology of the Old Pickens Quadrangle, South Carolina, Publication MS-18, div. of Geology, S.C., State Development Board, Columbia, S. C., 54pp.

Guinn, S.A., 1980. Earthquake focal mechanisms in the southeastern United States, Nureg/Cr-1503, 150 p.

Haimson, B.D., 1975. Hydrofracturing stress measurements, Bad Creek Pumped Storage project, Report for Duke Power Company, 19pp.

Haimson, B.C. and M.D. Zoback, 1978. A new look at the hydrofracturing stress measurements near the Monticello Reservoir, S. Carolina, EOS (Am. Geophys. Union Trans.), 65, No. 16, 278.

Hatcher, R.D., Jr., 1987. Tectonics of the southern and central Appalachian internides, Annual Reviews of Earth and Planetary Sciences, v. 15, p. 337-362.

Johnson, A.P., 1984. The Twiggs County earthquake swarm, Master Thesis, Georgia Institute of Technology, Atlanta, GA 125 pp.

Jones, Frank B., L.T. Long, M.C. Chapman and K.-H. Zelt, 1985. Columbus, Georgia, earthquakes of October 31, 1982, Earthquake Notes, 56, No. 2, 55-61.

Long, L.T., 1974. Earthquake sequences and b values in the southeast United States, Bull. Seism. Soc. Am., 64, 267-273.

Long, L.T., 1976. Short-period surface wave attenuation and intensities in the Georgia-South Carolina Piedmont Province, Earthquake Notes, 47, 3-11.

Long, L.T., 1979. The Carolina Slate Belt-Evidence of a continental rift zone, Geology, 7, 180-184.

Long, L.T., 1982. Seismicity of Georgia, in Arden, D.D., Beck, B.F., and Morrow. Petrolium geology of the southeastern Coastal Plain, Americus, Georgia, March 5-6, 1979: Atlanta, Georgia Geologic Survey Information Circular 53, 202-210.

Marion, G.E., and L.T. Long, 1980. Microearthquake spectra in the southeastern United States, Bull. Seism. Soc. Am., 79, 1037-1054.

Price, N.J., 1966. Fault and Joint Development, Pergamon Press, London.

Rundle, T.A., M.M. Singh and C.H. Baker, 1985. In situ stress measurements in the earth's crust in the eastern United States, final report, Engineers International, Inc., prepared for U.S. Nuclear Regulatory Commission, 75 pp.

Scholz, C.H. and C.A. Aviles, 1986. The fractal geometry of faults and faulting, in Earthquake Source Mechanics, (eds. S. Das, J. Boatwright, and C. H. Schloz) Geophysical Monograph 37, American Geophysical Union, Washington, D.C. 147-155.

Secor Jr., D.T., L.S. Peck, D. Pitcher, D. Powell, D. Simpson, W. Smith and A. Snoke, 1982. Geology of the area of induced seismic activity at Monticello Reservoir, South Carolina, J. Geophys. Res., 87, B8, 6945-6957.

Seeberger, D.A., and Zoback, M.D., 1982. The distribution of natural fractures and joints at depth in crystalline rock, J. Geophys. Res., 87, 5517-5534.

Simpson, D.W. and T.N. Narashimhan, 1986. Reservoir-induced earthquakes and the hydraulic properties of the shallow crust, (Abs.) EOS, Trans. Am. Geophys. Un., 67, 242.

Talwani, P., 1976. Earthquakes associated with the Clark Hill reservoir, South Carolina - A case of induced seismicity, Engineering Geology, 10, 239- 253.

Talwani, P., 1977. Stress distribution near Lake Jocassee, South Carolina, Pageoph, 115, 275-281.

Talwani, P., D. Stevenson, D. Amick and J. Chiang, 1979. An earthquake swarm at Lake Keowee, South Carolina, Bull. Seism. Soc. Am., 69, 825-841.

Wheeler, R.L. and J.M. Dixon, 1980. Intensity of systematic joints: Methods and application, Geology, v. 8, 230-233.

Wong, Po-zen, 1988. The statistical physics of sedimentary rock, Physics Today, v 41, no. 12, 24-32.

Zoback, M.D. and S. Hickman, 1982. In situ study of the physical mechanisms controlling induced seismicity at Monticello Reservoir, South Carolina, J. Geophys. Res., 87, B8, 6959-6974.

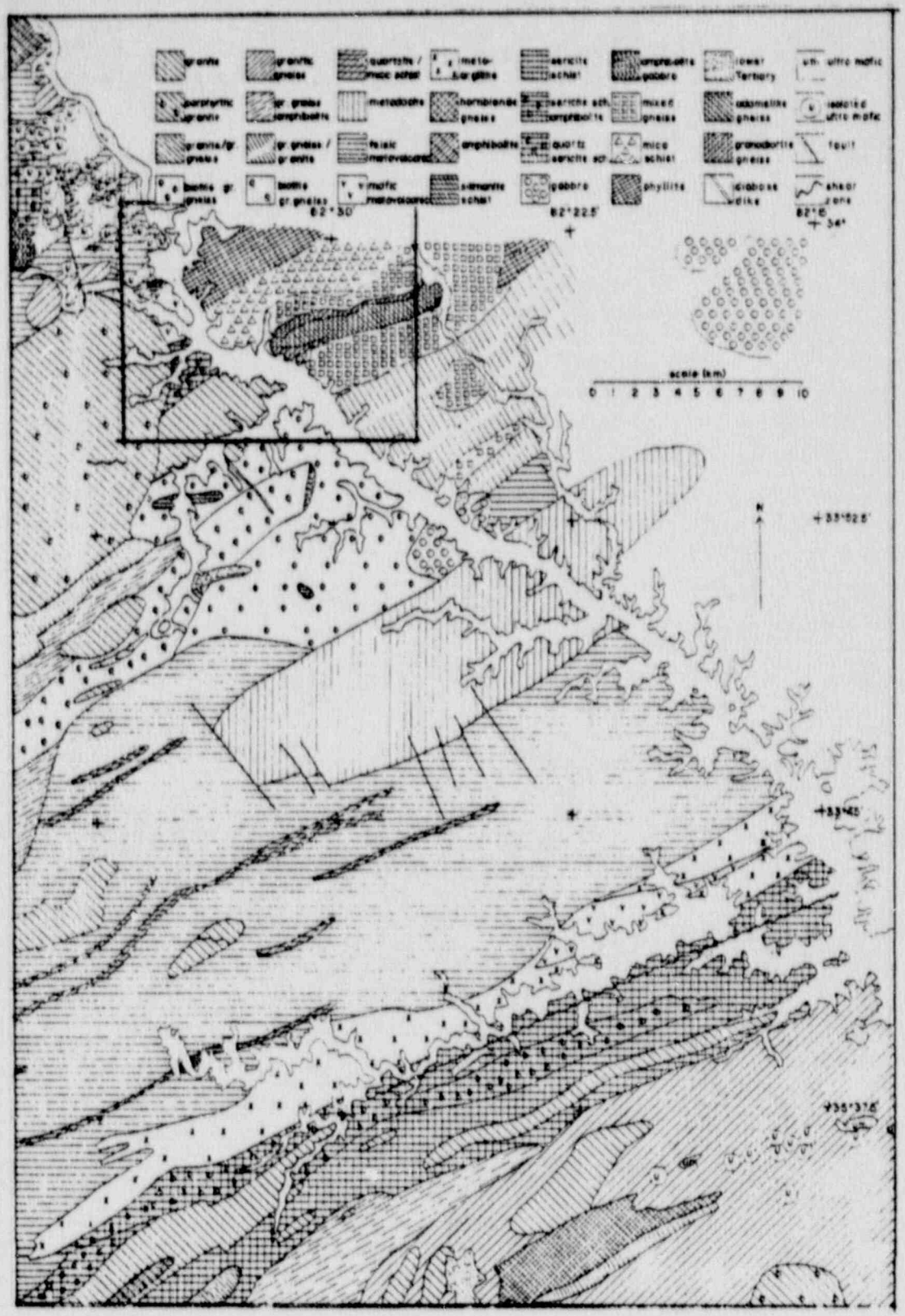

Figure 1. Location map for area of joint measurements in the Clarks Hill Reservoir. Geology abstracted from Griffin (1973).

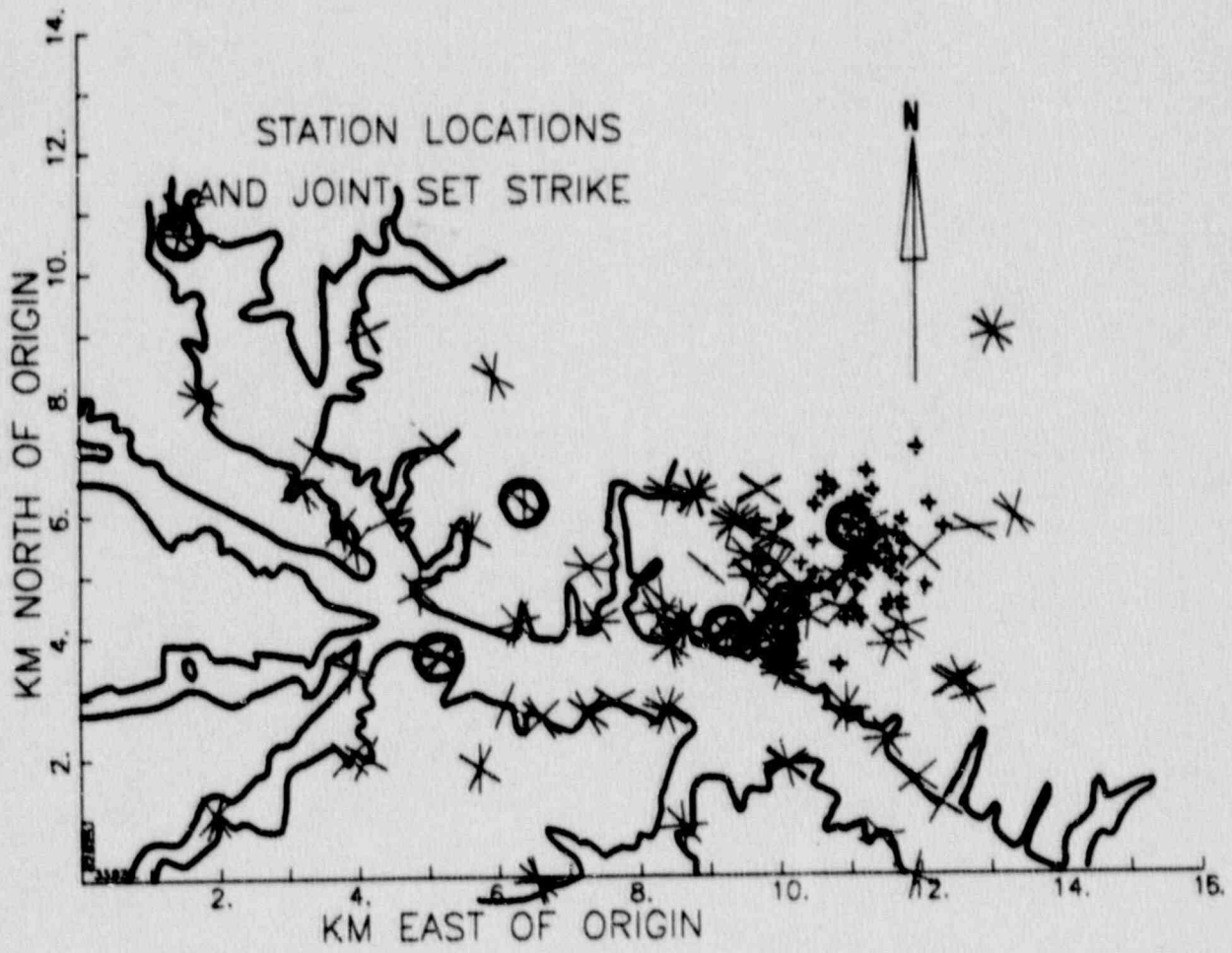

Figure 2. Outline of the study area showing station locations and joint directions. Small crosses are the epicenters of earthquakes from Dunbar (1977). Origin is 33.925 N, 82.625 W.

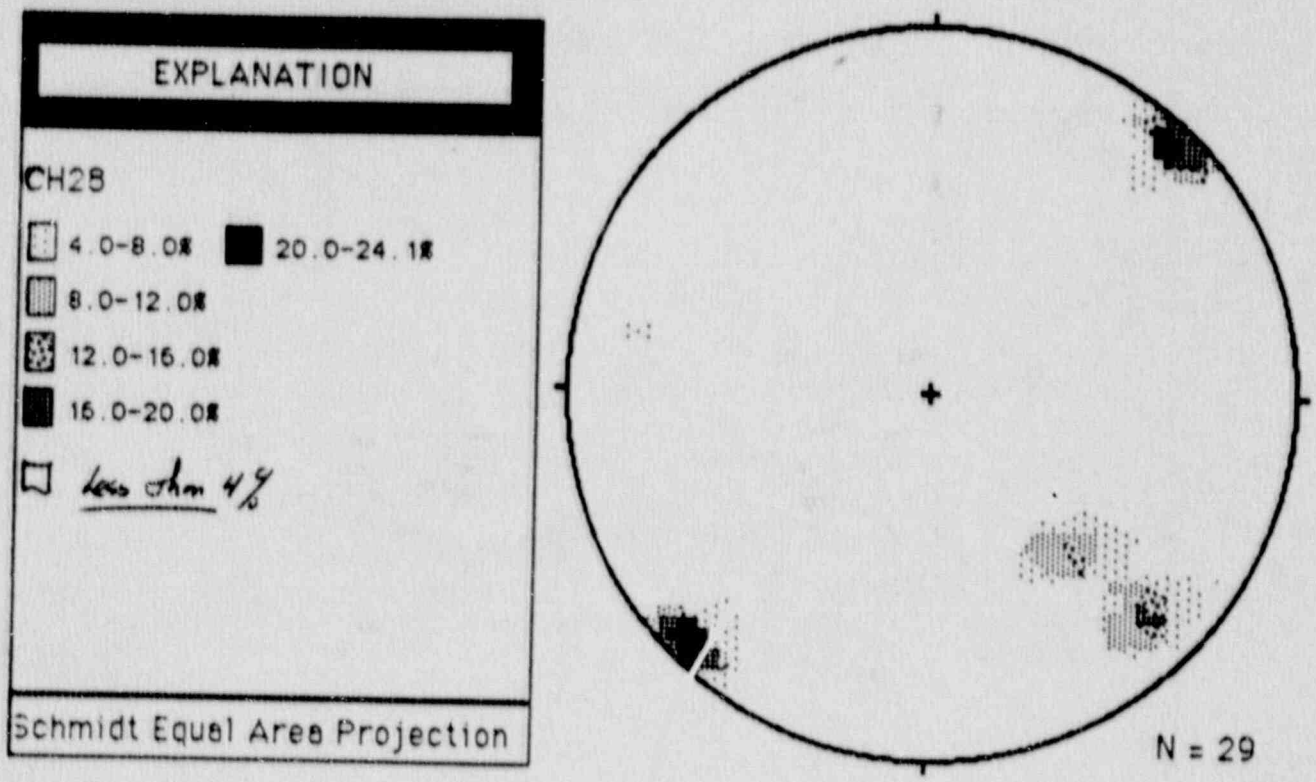

Figure 3. Joint pole plot for station ch28 showing dominant joint set for the Clarks Hill Reservoir.

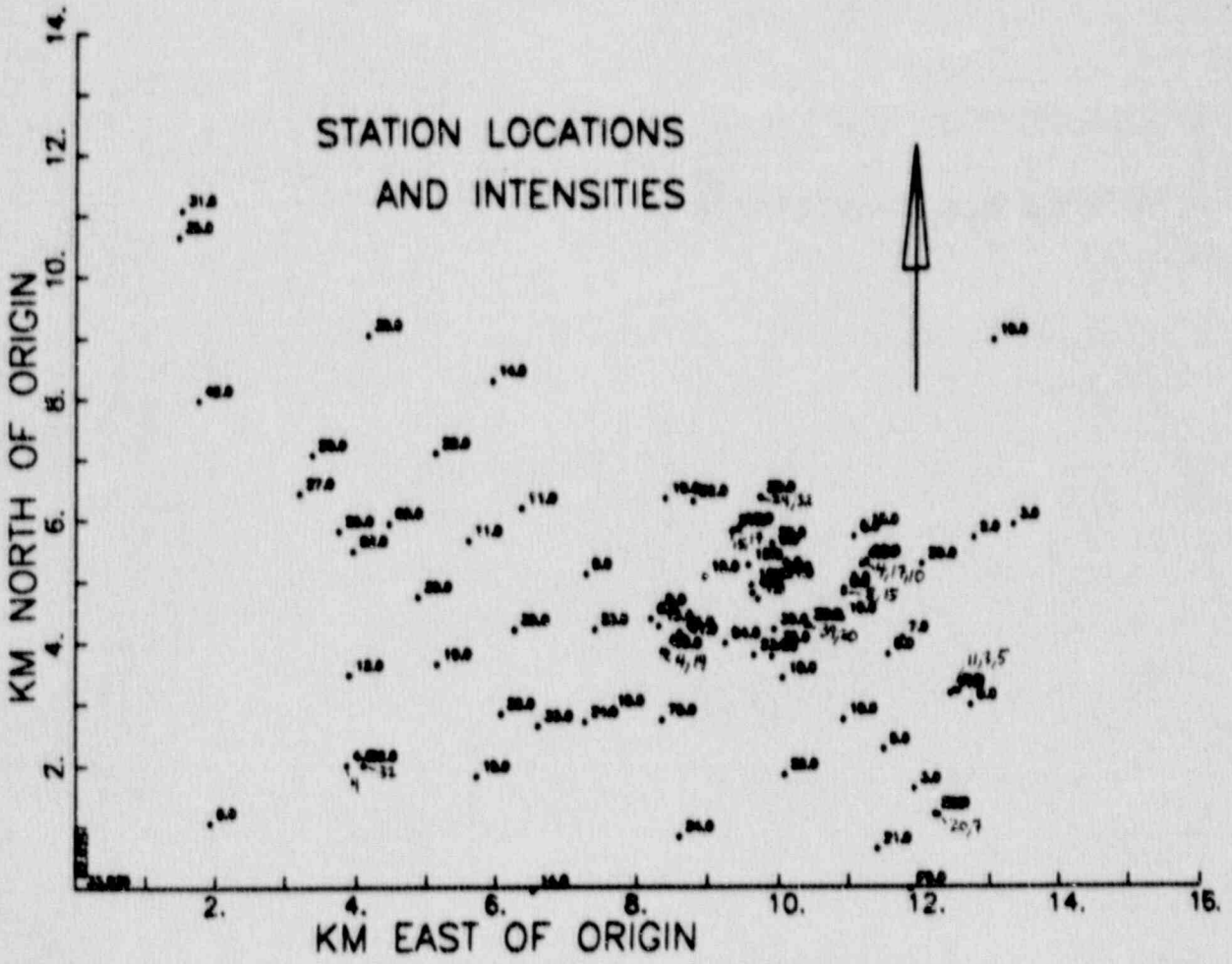

Figure 4. Average fracture intensity plot of observation points.

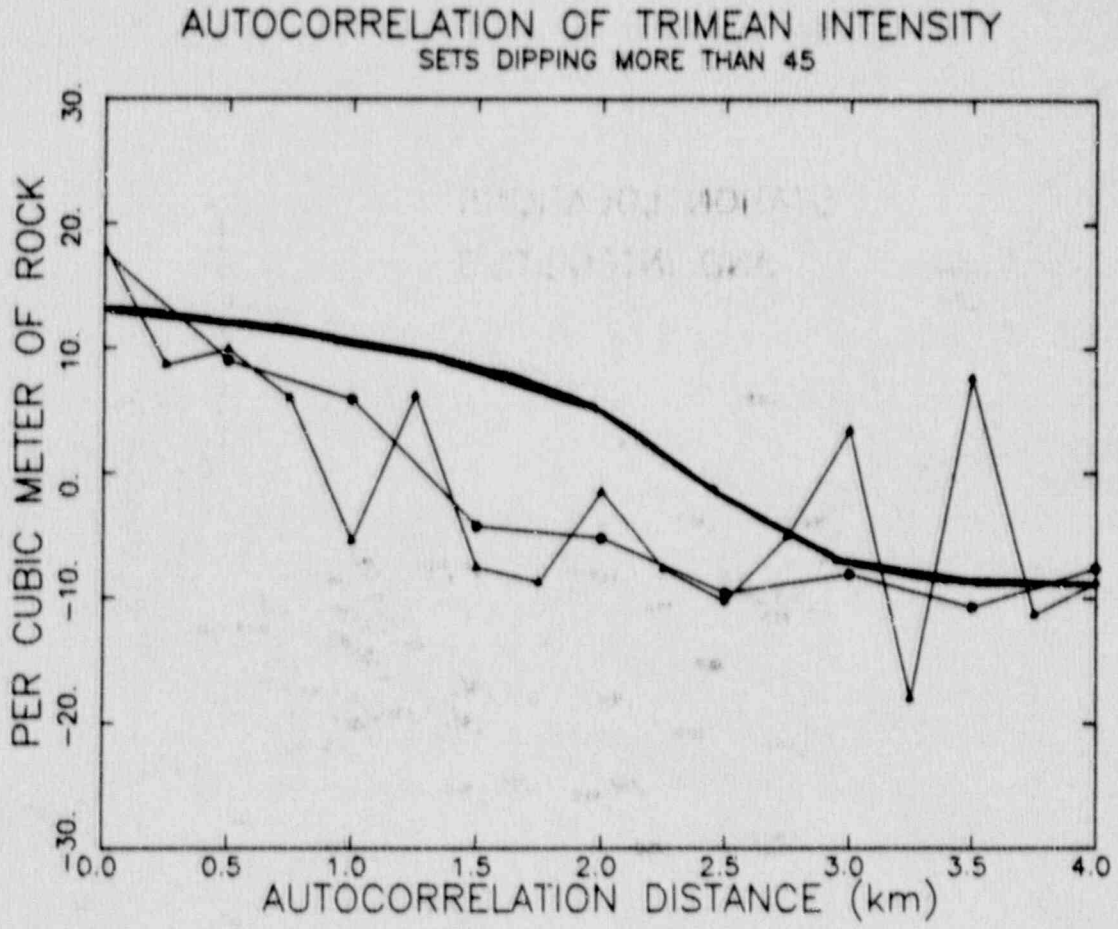

Figure 5. Autocorrelation of the trimean intensity data at separation distances of 0.5 and 0.25 km. Heavy line is autocorrelation function for the gridded data.

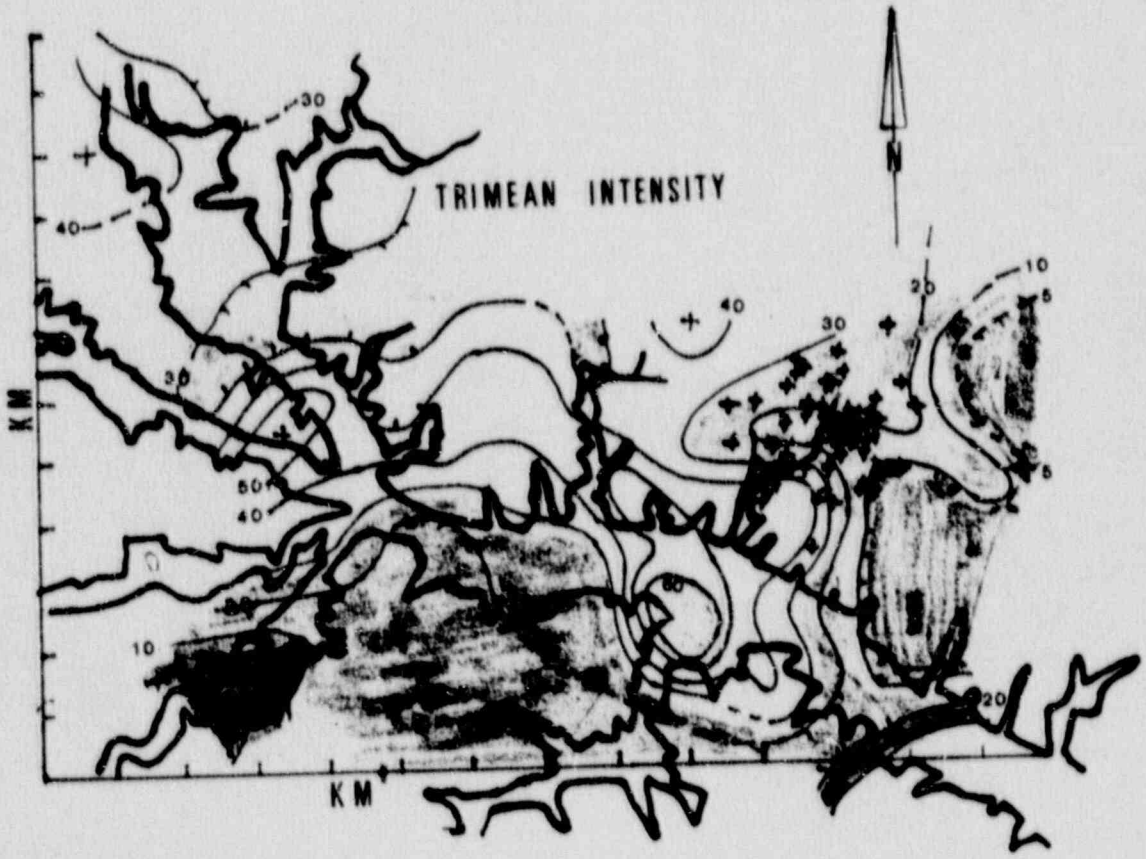

Figure 6. Contoured map of the trimean fracture intensity. The crosses indicate locations of epicenters.

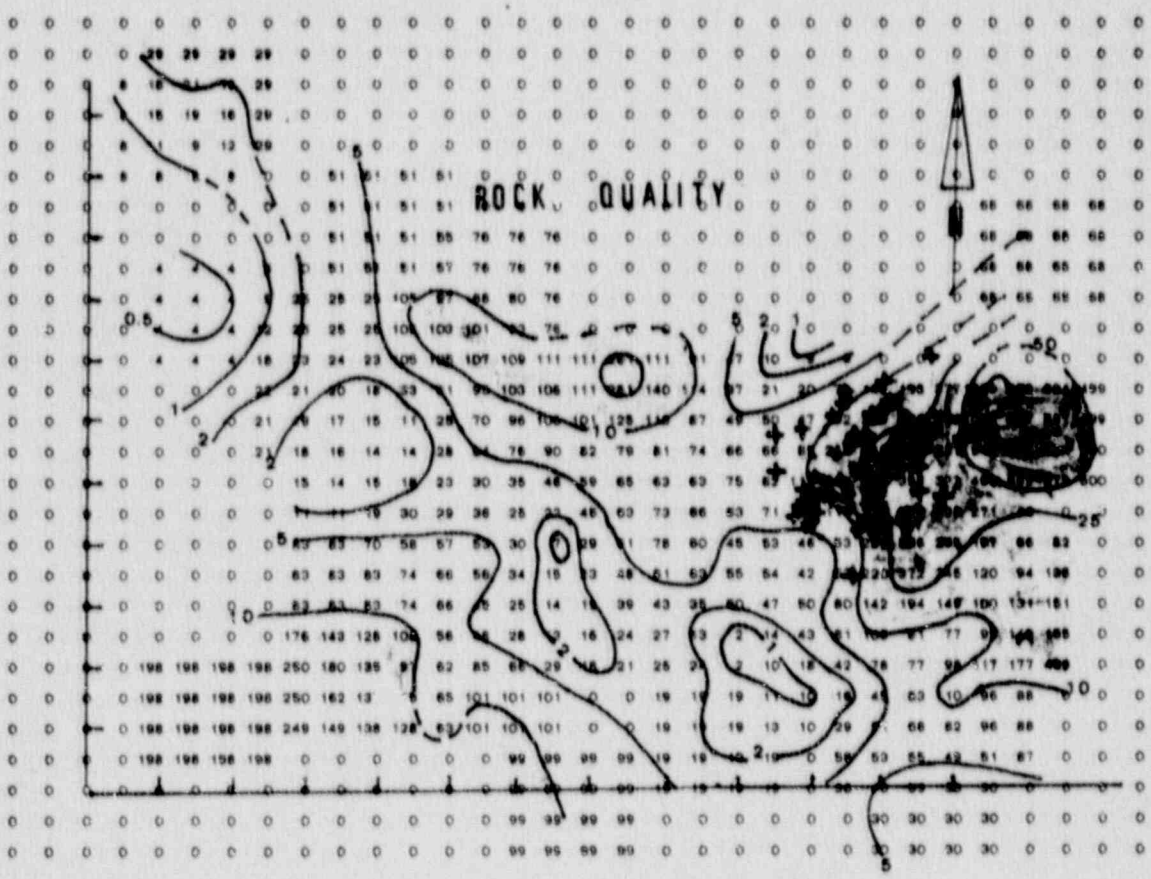

Figure 7. Contoured map of Rock Quality. The crosses indicate locations of epicenters.

APPENDIX D

Relocation of Earthquakes in the Lake Sinclair Reservoir Area

APPENDIX D

RELOCATION OF EARTHQUAKES IN THE LAKE SINCLAIR RESERVOIR AREA

Wilbur Edward Radford, Jr, and Leland T. Long

ABSTRACT: One hundred and eighty-nine earthquakes in the Lake Sinclair and Lake Oconee areas of central Georgia were located. The epicenters were computed with a technique designed to reduce reading error and inconsistency in the data by separating the origin time computation from the epicenter computation. The small separations among stations did not allow computation of focal depths. With respect to previous locations, the epicenters exhibited significant reduction of scatter and defined four distinct clusters of events in the Lake Sinclair area. The area of the average error ellipse for the relocations was 0.10 square kilometers. The clusters are centered on or near the body of Lake Sinclair. The travel-time residuals for the relocated epicenters were increasingly negative for stations greater than 20 km distant from the epicenters. A two-layered velocity model was developed to explain the travel times for stations at distances greater than 20 km. The Model consists of the observed 6.0 km/s surface layer of thickness of 2.37 km above a layer with a P-wave velocity of 6.6 km/s. Shear wave velocities were determined from Poisson's relation. The two-layered model reduced the area of the average error ellipse for the relocations from 0.11 km^2 to 0.10 km^2.

INTRODUCTION

The seismicity of central Georgia is contained within a circle of radius 75 km centered on Milledgeville, Georgia (see Figure 1). The seismicity is moderate and includes historic events as large as 4.9 m_{blg}. The larger historical earthquakes have been documented by Allison (1980). The impoundment of Lake Sinclair in the 1950's and the continued sporadic seismicity in central Georgia, along with occurrences of reservoir-induced seismicity at the Jocassee and Monticello reservoirs in South Carolina, raised the possibility that the Lake Sinclair seismicity is reservoir-induced and increased concern that the new reservoir, Lake Oconee, would induce significant activity. Because of this concern, the seismicity was closely monitored during the impoundment of Lake Oconee by Wallace Dam in 1977.

The impoundment of Lake Oconee by Wallace Dam was followed by only a few small events and significant reservoir-induced seismicity was not triggered. Natural seismicity before the lake was impounded consisted of the historical events and one prefilling event of magnitude 1.4. A post-filling swarm of earthquakes with magnitudes between -0.3 and 0.8 occurred in May 1980. The swarm showed no single outstanding event and did not precede a larger event as in the usual case of earthquake swarms near Lake Sinclair. Most of the events in the Lake Oconee swarm occurred in a tight spatial cluster. The majority of the seismicity in central Georgia occurs in the Lake Sinclair area (LSA). Spatial distribution of the epicenters with respect to Lake Sinclair and the characteristics of LSA swarms suggests possible reservoir-induced seismicity. However, the existence of significant pre-impoundment earthquakes suggests a natural explanation for seismicity.

The epicenters of Lake Sinclair events occur in clusters (Allison, 1980); however, scatter in those clusters does not allow the identification of subclusters or alignments within the clusters. The events were recorded on analog pen-and-ink recorders. A few were recorded on analog tape. The arrivals and phases were picked by different persons. As a result, considerable inconsistency may exist in the P and S arrival times. Such variations in precision could account for much of the scatter in the epicentral distribution. Also, the local velocity model was determined for the Lake Oconee Area (LOA) where the station-to-epicenter distance ranged from ten to twenty kilometers. This velocity model may cause problems with the location of the Lake Sinclair events because the velocity model was not defined for distances greater than twenty kilometers. The object of this study has been to reduce the scatter in the data by relocating the events. The possible inconsistency in the reading has been minimized by reevaluating all phases. Events occurring after Allison's (1980) study have been added to the catalog. Consistency in readings have been further checked by separating the origin time computation from the epicenter computation. A reduction of scatter would reveal clusters or other patterns that might suggest possible causes of the seismicity in this area. The re-evaluation of the velocity model would aid in understanding geologic units in the crust.

WALLACE DAM NETWORK AND SEISMIC RECORDING

Earthquakes for this study occurred in the Lake Sinclair and Lake Oconee areas between longitudes 82.8° and 83.6°W and latitudes 32.9° and 33.5°N (see Figure 2). The earthquakes were recorded by the Wallace Dam Seismic Network (WDN) which became operational in June 1977 under a commission from the Georgia Power Company. Although the network was implemented in order to monitor the Lake Oconee area, the network also provided coverage for Lake Sinclair through the addition of station ETG (see Figure 2) under a commission from the Nuclear Regulatory Commission. The detection threshold for the Lake Sinclair and Lake Oconee areas was magnitude -0.3.

From June 1977 through May 5, 1980, 167 events were recorded by the Wallace Dam Network. Of these, 135 were located in the Lake Sinclair area. These earthquakes made up the data base that was used in the initial report of the monitoring by the Wallace Dam Network (Allison, 1980). The majority of the seismic activity occurred in the Lake Sinclair area. The Lake Sinclair seismicity has two major concentrations of events. The largest of these is centered at 33.24°N, 83.29°W and contains the majority of all recorded events. The uncertainty in the locations makes it impossible to determine clusters on a smaller scale within the two major concentrations of events. One of the goals of this study is to reduce the epicentral uncertainty in order to better define the areas of concentrations of these events.

The arrival times for Allison's (1980) locations came directly from the WDN log books. These books were maintained by different graduate students over a period of four years and the interpretation and recording of the data could vary systematically. This introduces the uncertainty of inconsistent precision in the P- and S-wave arrivals used in the locations. P and S arrivals from a microearthquake can be picked to a precision of ± 0.1 seconds when the event is recorded at 1 mm/s as on ink and paper recorders. Figure 3 shows typical LSA events that were recorded with ink on paper. The traces vary from

having strong, clear P and S arrivals to having barely discernible arrivals. Different individuals may have different interpretations on the latter. To guarantee consistency in this study, all the records were reevaluated and a magnifying lens was used to facilitate a 0.1 s precision. The resulting P and S arrivals for 189 events were used for the relocations in this study. The 189 events include most of Allison's (1980) events and 22 previously unlocated events.

RELOCATION TECHNIQUE

The previous locations were found using an iterative, least-squares error minimization based on the method introduced by Geiger (1910). The

algorithm solves a set of equations of the form:

$$b' = A'dp \qquad (1)$$

where for n observations, A' is the n x 4 matrix of the partial derivatives with respect to T (origin time), x (longitude), y (latitude), and z (depth) of the travel times from a trial hypocenter, b' is the n-length vector of observed minus theoretical travel times for individual phases and dp is the four-dimensional vector representing a correction in time, latitude, longitude and depth of the trial hypocenter. The problem is to find dp = (dT,dx,dy,dz) such that the length of A"dp-b' is minimized (Boyd and Snoke, 1984) in the least-squares sense.

For a closely spaced network such as the WDN, influence of the variation in velocity within various geologic units is assumed to contribute the same uncertainty at each station. However, events that have both P and S phases recorded at the same station would be expected to exhibit a correlation between the residuals and have a correlation between the standard deviations of the residuals. In this study, the correlation of the P- and S-wave residuals is used to develop an alternate method for separating the origin time computation from the hypocenter computation. In this method, the seismograms that have readable P and S arrivals are separated from observations that have only one readable arrival in order to compute the origin time. This origin time is then fixed and we solve for the parameters of the epicenter by using all the observations. With the reading precision of 0.1 seconds, the origin times are typically precise to less than 0.2 seconds. Because the distances were short and velocity anomalies were lacking in the area, origin times in error by more than 0.2 seconds are considered mispicked phases. The assumed mispicked traces were re-examined and origin times were recomputed. This was repeated until the best possible picks were obtained for the P and S arrivals. As a result of this quality control in identifying phases, the standard deviation of the origin time is generally less than 0.2 s.

RELOCATIONS

The initial velocity model used for relocations in this study was the same as that used by Allison (1980). The P-wave velocity of 6.0 km/s and the S-wave velocity of 3.43 km/s were determined in a refraction survey completed for the Lake Oconee area by Allison (1980). Records from smoked-paper seismographs deployed before the implementation of the WDN indicated shallow events

(Allison, 1980). Thus, the depth for each relocation was constrained to 0.5 km.

The distribution of the relocated epicenters suggests five clusters designated A through E in Figure 4. Clusters A, B, and C were the main concern of this study. Scatter has been reduced by relocation most significantly in Cluster A. This reduction allowed part of this cluster to be separated as another cluster (d) centered approximately 6 km southwest. Felt reports from recent events give epicenters between these clusters. Because this data set represents only four years of seismic coverage out of twenty three years of suspected reservoir-induced seismic activity in central Georgia, clusters A and D may be part of a larger cluster. The relocated epicenters of cluster B are more concentrated near the center of the cluster than they were prior to relocation.

The most notable difference generated by relocation is the shifting of certain epicenters from the main cluster to a cluster near the westernmost branch of Lake Sinclair. It was discovered while reexamining the original records that these events were located using only arrivals from station ETG and REG. This fact, along with the geometry of the locations of these stations, allowed solutions for epicenters in cluster A or in cluster C. The travel-time data alone provide insufficient criteria to distinguish the correct epicenters. To establish correct epicenters, all events in this category were relocated again. Because location are determined by a least-squares minimum in residual travel times, certain combinations of stations and locations may possess multiple minima. In the case of cluster A, the location process will find the minimum closest to the initial guess. Therefore, events in this category were relocated using first guesses corresponding to each cluster. Most of these events remained in cluster A. The records of the remaining events were reexamined for evidence for arrivals at stations WDG and GBG. The phases at these two stations were weak compared to events definitely located in clusters A or D. The weakness of the signals was interpreted to mean that the sources of these events were located at a greater distance from the recording station than from both stations ETG and REG. Thus, these events were relocated in cluster on the basis of signal amplitude. The dimensions of cluster C are poorly defined and the cluster is not dense.

VELOCITY ANALYSIS

With the origin time computation removed from the epicenter computation, the errors associated with the epicenters were small. Considering only latitude and longitude, the average error ellipse for events that had P and S phases recorded on three or more stations is 0.11 square kilometers compared to error ellipses of 1.15 square kilometers prior to relocation. The residuals for the P arrivals are plotted versus azimuth in Figures 5 and 6. The mean residuals are consistent with the reading error of 0.1 s for each station. Thus, no obvious corrections would be expected to m-improve the arrival times. It is interesting to note, however, that the averages of the residuals shown in Figure 5 for stations ETG and WDG are slightly positive while the averages of the residuals shown in Figure 6 for stations REG and GBG are slightly negative. Since the majority of the LSA events are located in cluster A, one can consider that stations REG and GBG are greater than 25 km from the cluster while stations ETG and WDG are less than 25 km from the cluster.

This suggests that the crustal velocities used in the relocations may be too large for the close-in stations and too small for the distant stations.

The original velocity survey (Allison, 1980) was obtained for distances of only up to 20 km. The mean P residuals for cluster A events that were recorded on all four station are plotted versus station distance in Figure 7. The residuals become increasingly negative beyond 20 km. Because the residuals were computed with a constant velocity of 6.0 km/s, the increasingly negative residuals for stations beyond 20 km indicate that a velocity of 6.6 km/s would be necessary beyond 20 km to obtain a zero residual. Because the mean P residuals are essentially constant for station ETG and WDG and drop off rapidly for stations REG and GBG, a two-layered model was adopted for this study. The 6.0 km/s velocity of the near-surface layer was defined by Allison's (1980) refraction survey. The slope of the mean P-wave residual arrival times for the three more distant stations define a velocity of 6.6 km/s ± 0.2 and a zero-distance intercept of 0.2 seconds. Figure 8 shows the resulting mean P residuals for a relocation of all events using the two-layered model. This model reduced the area of the average error ellipse from 0.11 square kilometers for the half-space model to 0.10 square kilometers for the two-layer model computed from events of cluster A recorded on 4 stations.

Figure 9 shows a detailed Bouguer map of the LSA (O'Nour, 1982). The positive anomalies exceeding +20 mGals and sharp gradients (near REG and GBG) indicate that shallow, mafic rocks underlie much of the LSA. For a crossover distance of 20 km, the two-layered model gives a high-velocity medium at 2.4 km depth. A velocity of 6.6 km/s as indicated by Figure 7 would be consistent with the hypothesis that the area is underlain by a fragment of high velocity (oceanic ?) crust as shown in Figure 10. The reduced travel-time plot for the two-layered model is also shown in Figure 10. Relocations using a two-layer velocity model are shown in Figure 11. Cluster A is slightly tighter and the Lake Sinclair clusters are shifted 2 to 3 km southward. The improvement in the epicentral distribution is more evident for events of magnitude greater than 0.7. One should note the further separation of cluster D from cluster A and the tightening of cluster D.

DISCUSSION AND CONCLUSIONS

The efforts of this study can be divided into four major results. First, the events of the Lake Sinclair area have been systematically reviewed for accuracy and consistency. Second, the scatter of the epicenters has been reduced relative to those based on the original data. This reduction has allowed the identification of four distinct clusters in the Lake Sinclair area: however, the reduced scatter did not reveal any evidence in the form of linear trends that would suggest an active fault. Third, the epicenters are close to the lake suggesting that fluid penetration, related to the reservoir, is a factor in the triggering of these earthquakes. The historical pre-reservoir events suggest a natural cause. Hence, the cause of this seismicity may be a combination of reservoir-induced seismicity and release of natural stresses. Fourth, the seismic arrival times were used to develop a velocity model for the Lake Sinclair area. The model consists of two layers, a shallow 6.0 km/s layer and a 6.6 km/s half-space below 2.4 km. Gravity data also suggest the presence of dense material at shallow depths under much of the Lake Sinclair and Lake Oconee areas.

REFERENCES

Allison, J.D., 1980. Seismicity of the Central Georgia Seismic Zone, Master's Thesis, Georgia Institute of Technology, Atlanta, GA 30332.

Boyd, T.M. and J.A. Snoke, 1984. Error estimates in some commonly used earthquake location programs, Earthquake Notes, 55, 3-6.

Geiger, L, 1910. Herdbestimmung bei Erdeben aus den Arnkunftszeiten, K. Geseau. Wiss. Gott., 4, 331-349.

Long, L.T., 1982. Seismicity of Georgia, in Arden, D.D, Beck, B.F., and Morrow, E., eds., Proceedings of the second Symposium on the Geology of the southeastern Coastal Plain, Americus, Georgia, March 5-6, 1976: Atlanta, Georgia Geologic Survey Information Circular 53, pp. 202-210.

O'Nour, I.M., 1982. Gravity Anomalies in Central Georgia. Master's Thesis, Georgia Institute of Technology, Atlanta, GA 30332.

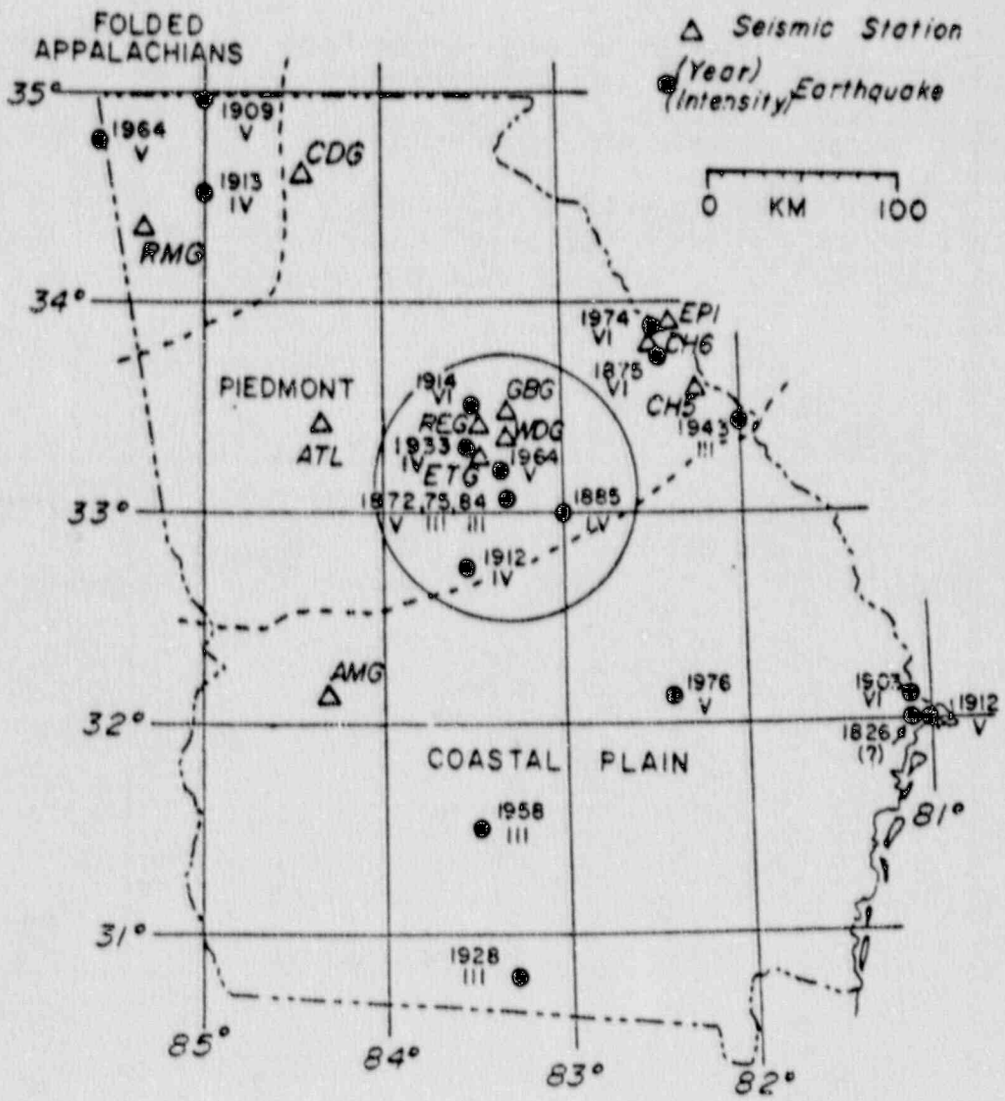

Figure 1. Historical Seismicity of Central Georgia (after Long, 1982).

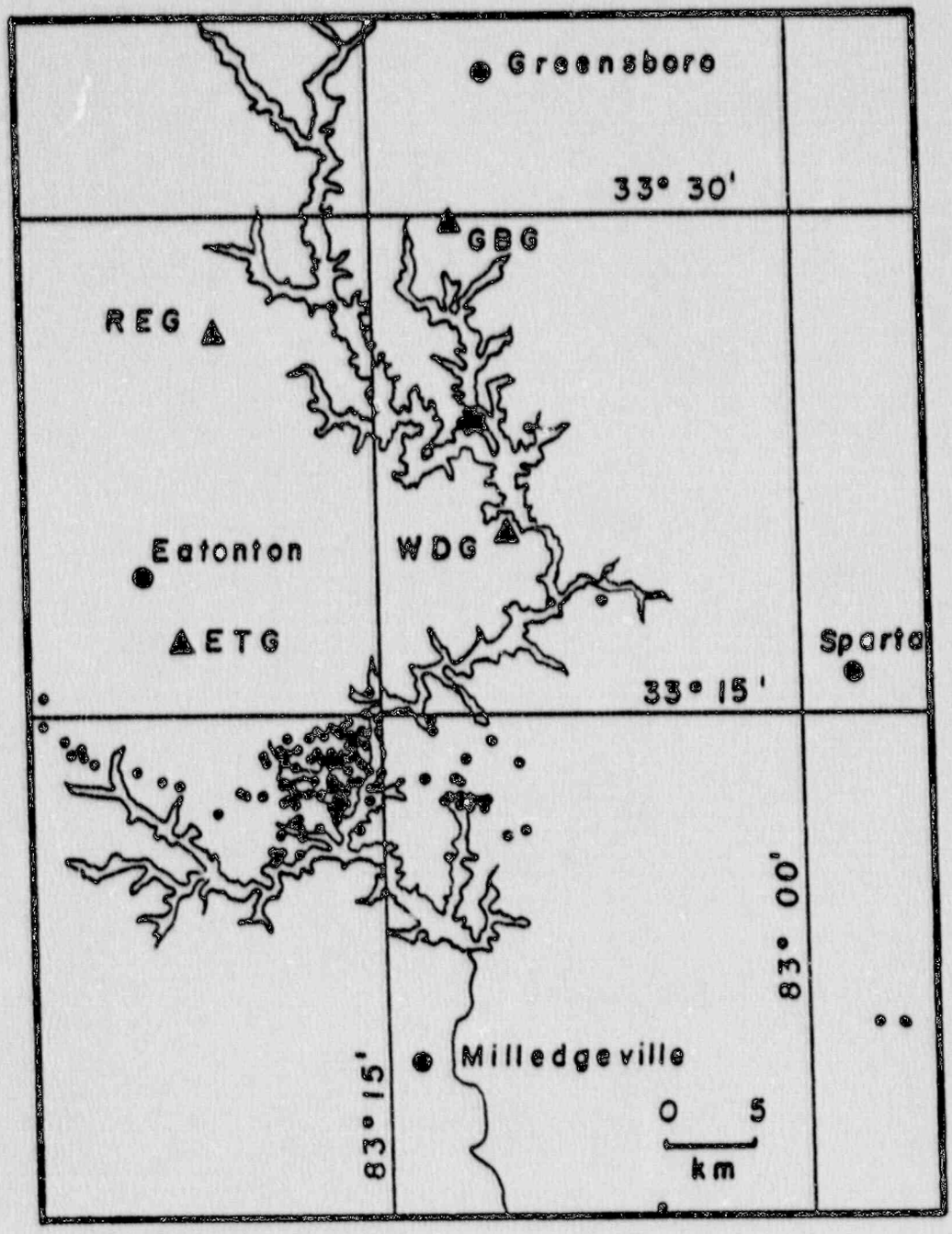

Figure 2. Locations of events in the Lake Sinclair and Lake Oconee Areas (from Allison, 1980).

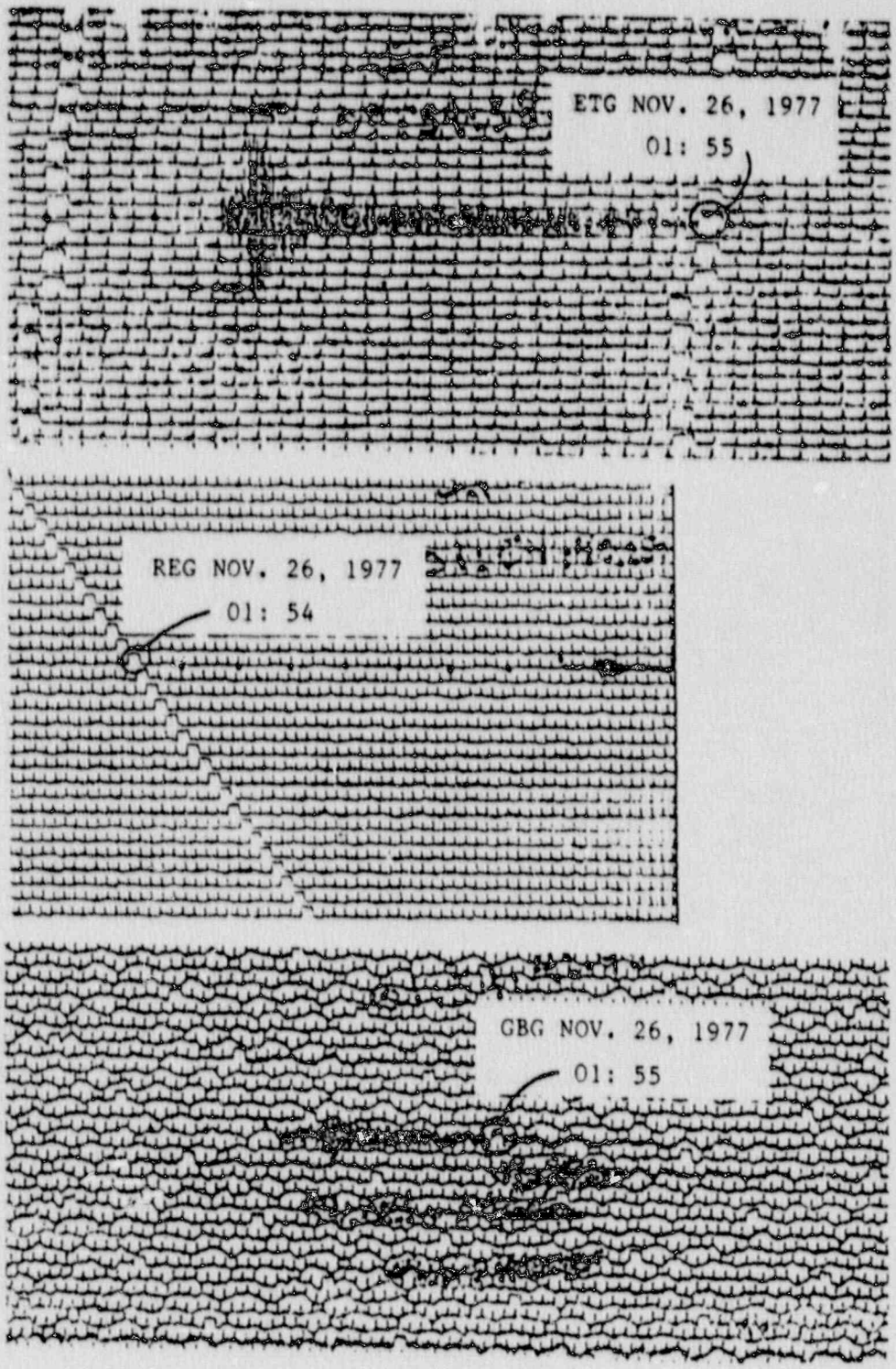

Figure 3. Typical traces of Lake Sinclair events.

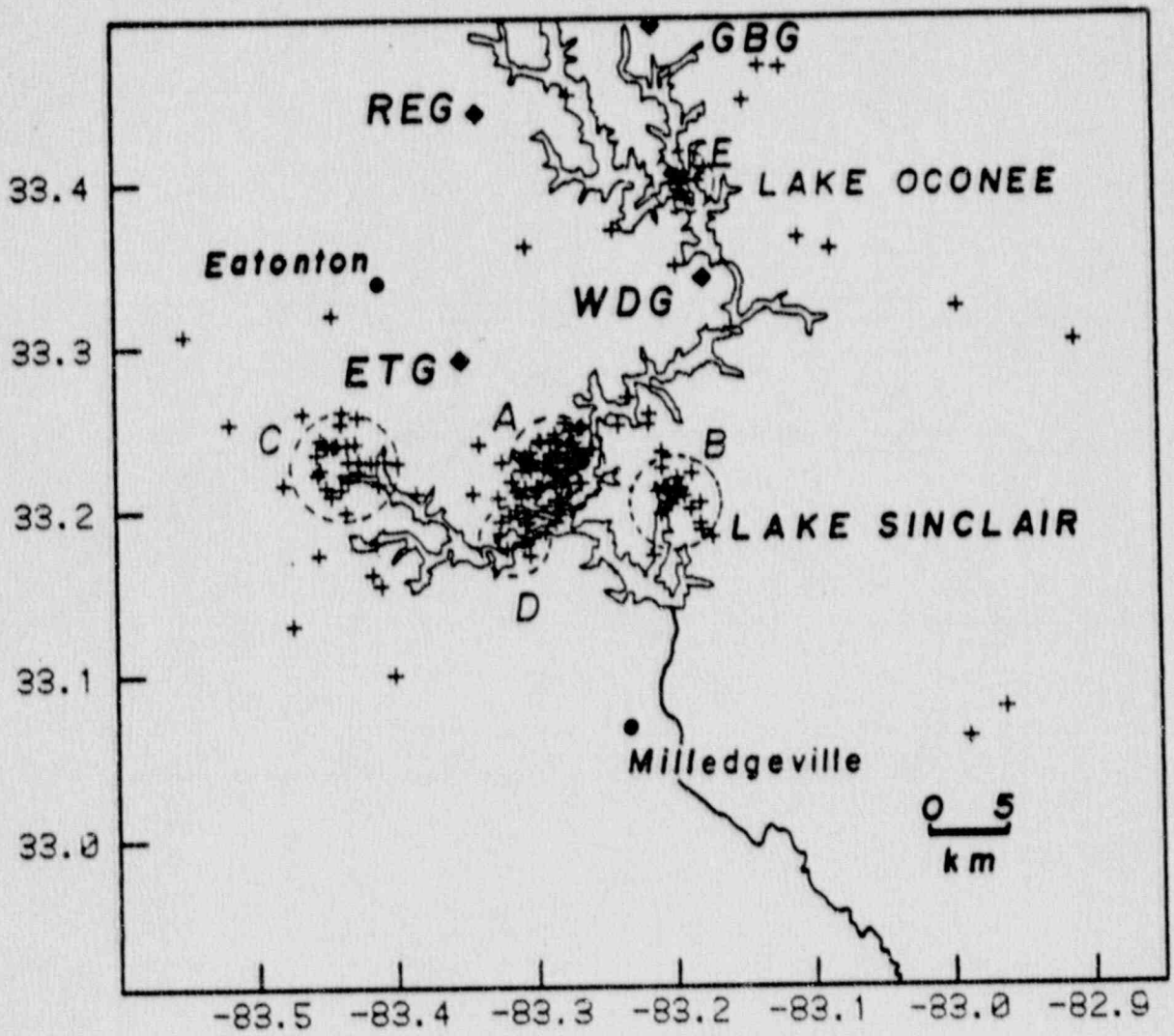

Figure 4. The 189 relocated epicenters of the Lake Sinclair and Lake Oconee areas. Dashed circles identify clusters A through E.

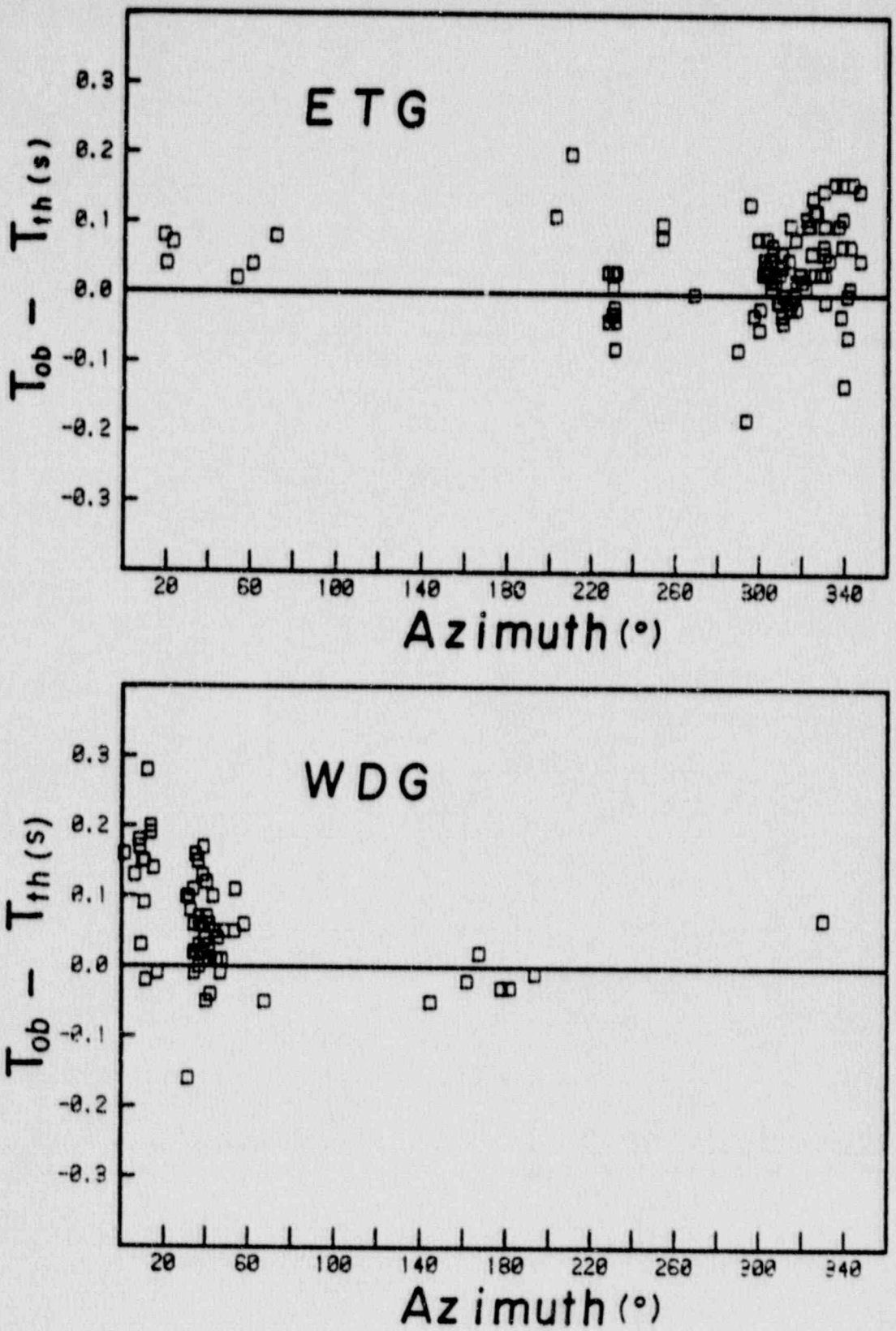

Figure 5. P-wave travel-time residuals for stations ETG and WDG plotted versus azimuth.

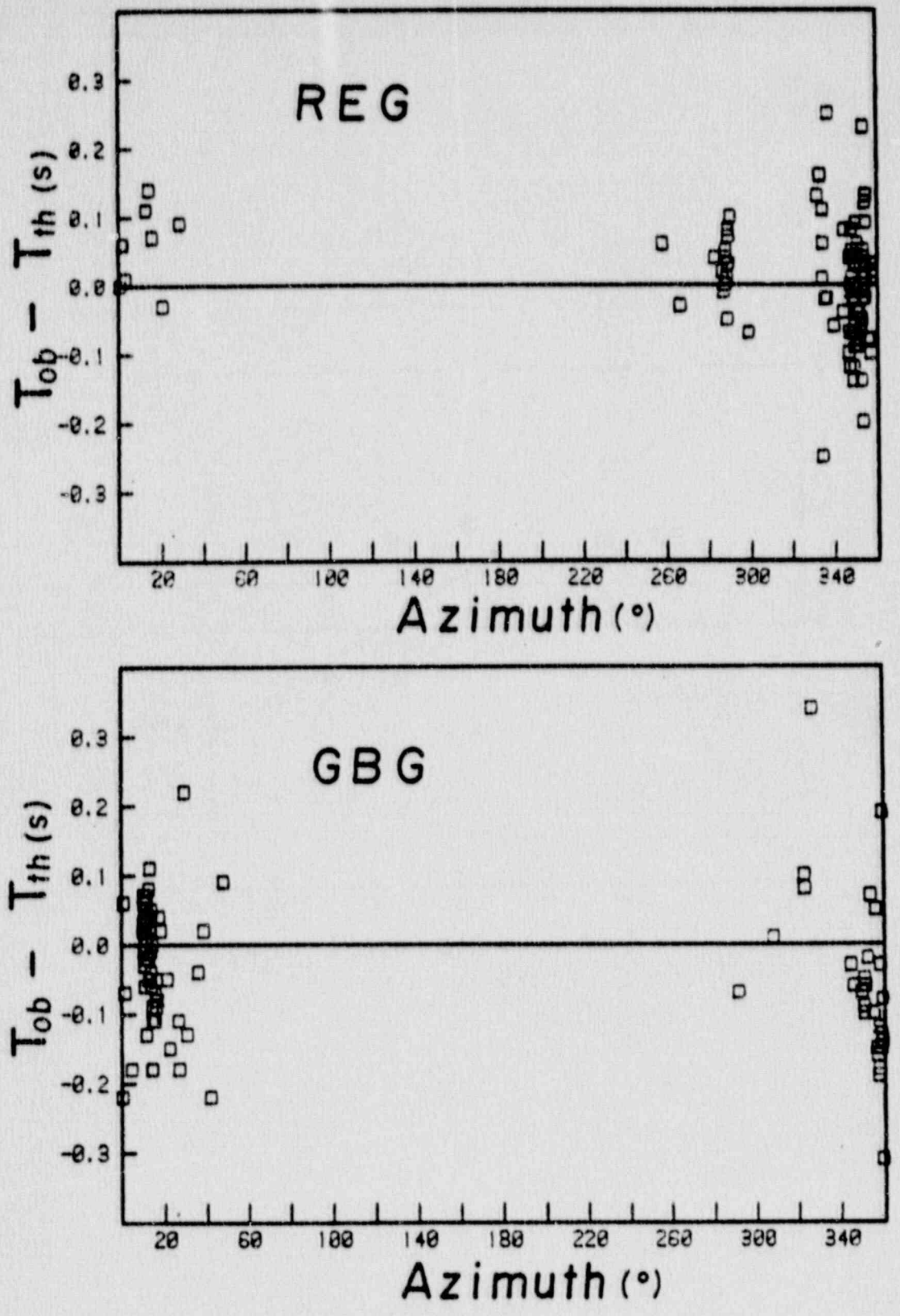

Figure 6. P-wave travel-time residuals for stations REG and GBG plotted versus azimuth.

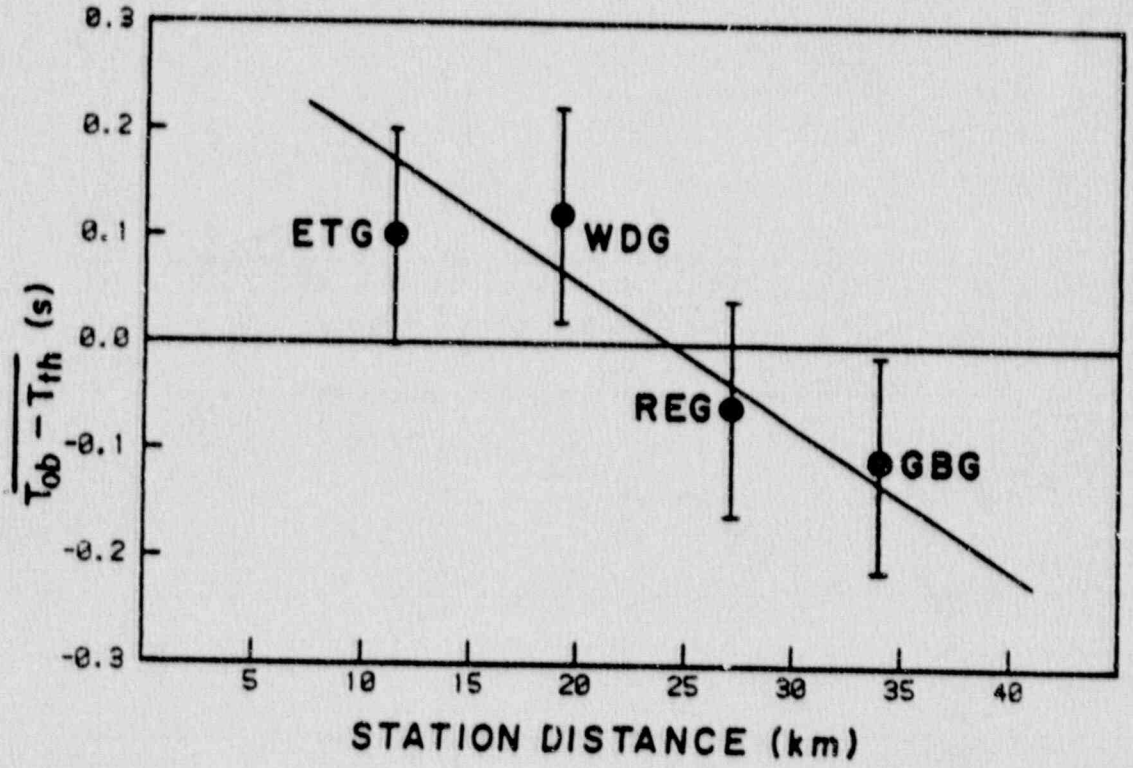

Figure 7. Mean P-wave residuals from a constant velocity model for cluster A events that were recorded on four stations.

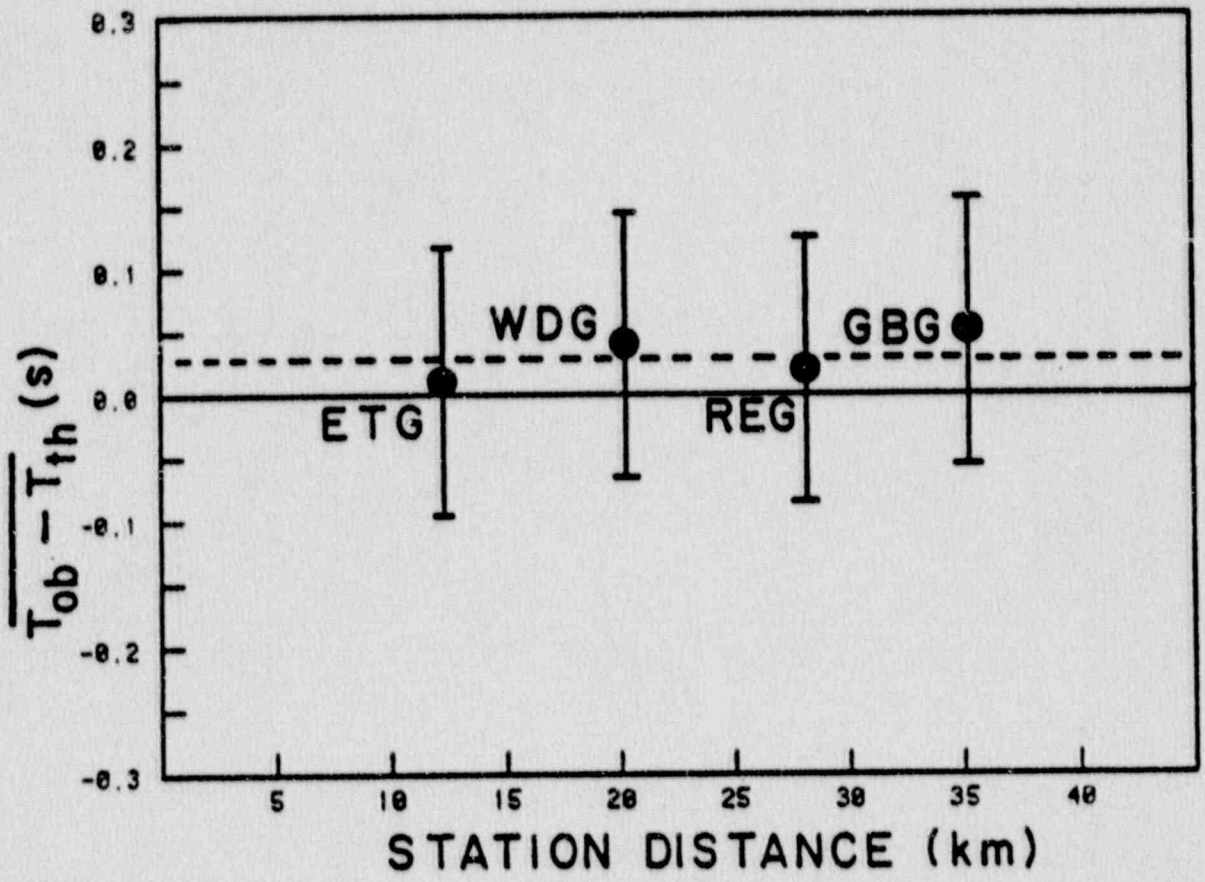

Figure 8. Mean P-wave residuals for a two-layer model for cluster A events that were recorded on four stations.

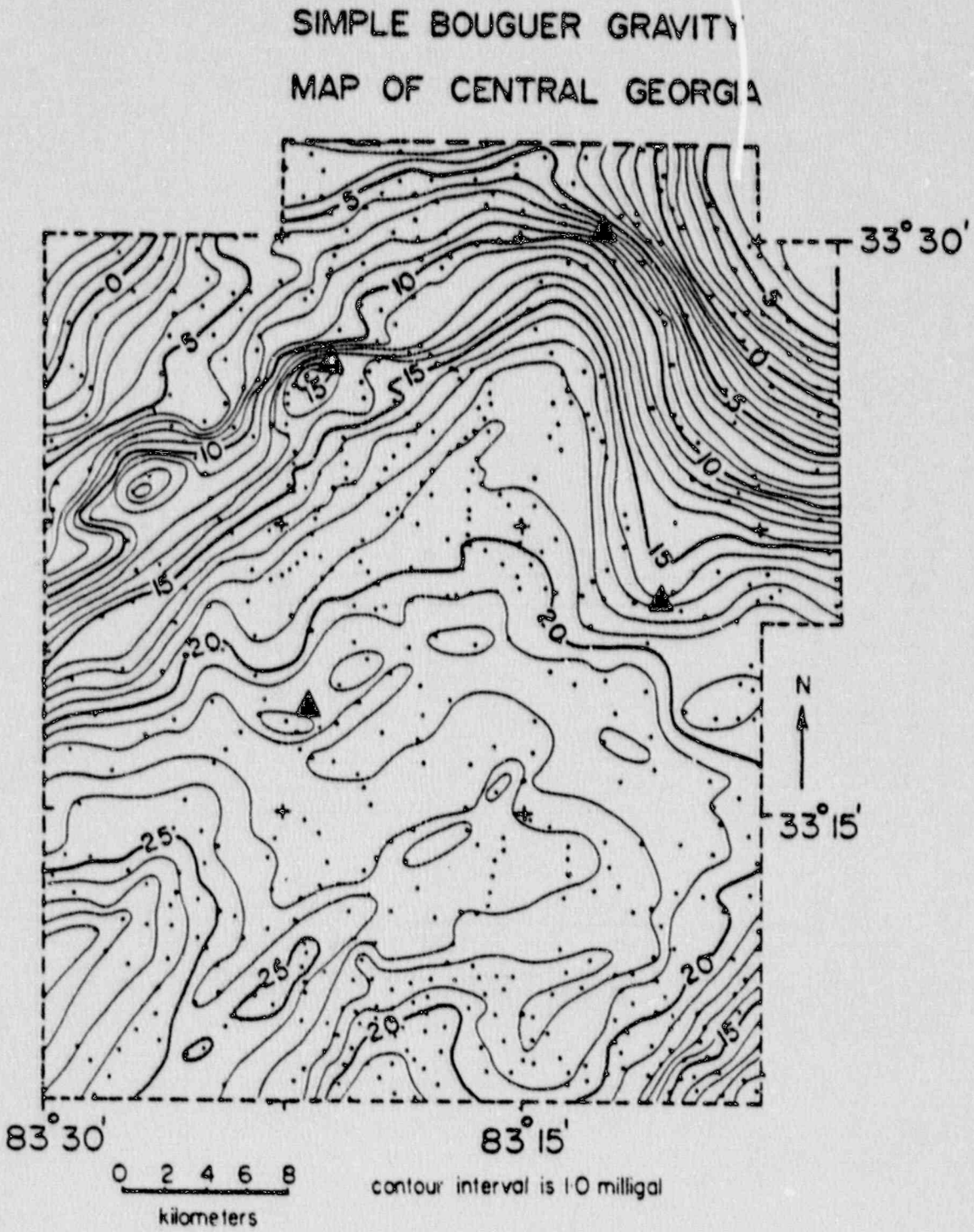

Figure 9. Bouguer Map of the Lake Sinclair area and Lake Oconee area (after O'Nour, 1982).

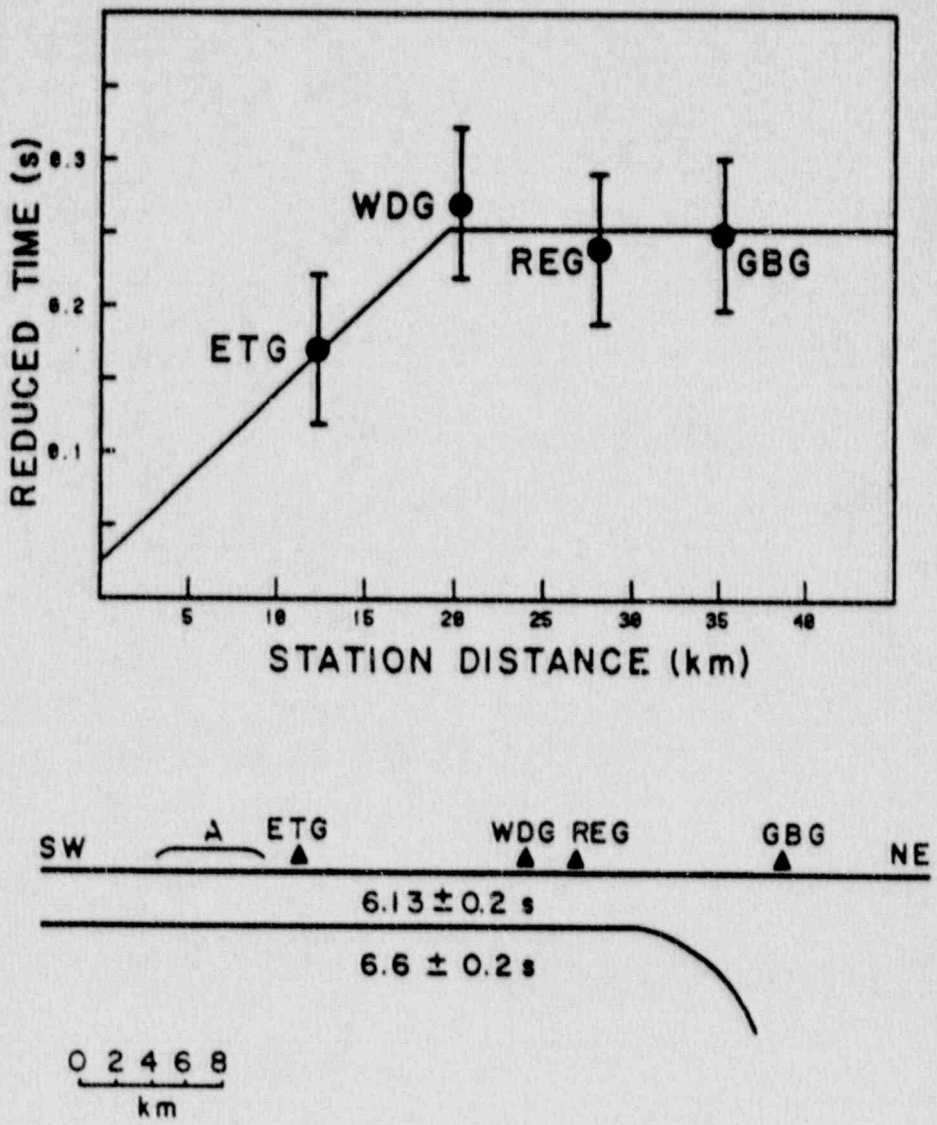

Figure 10. Reduced P-wave travel times for a two-layered model plotted versus station distance and a velocity model for the Lake Sinclair and Lake Oconee areas.

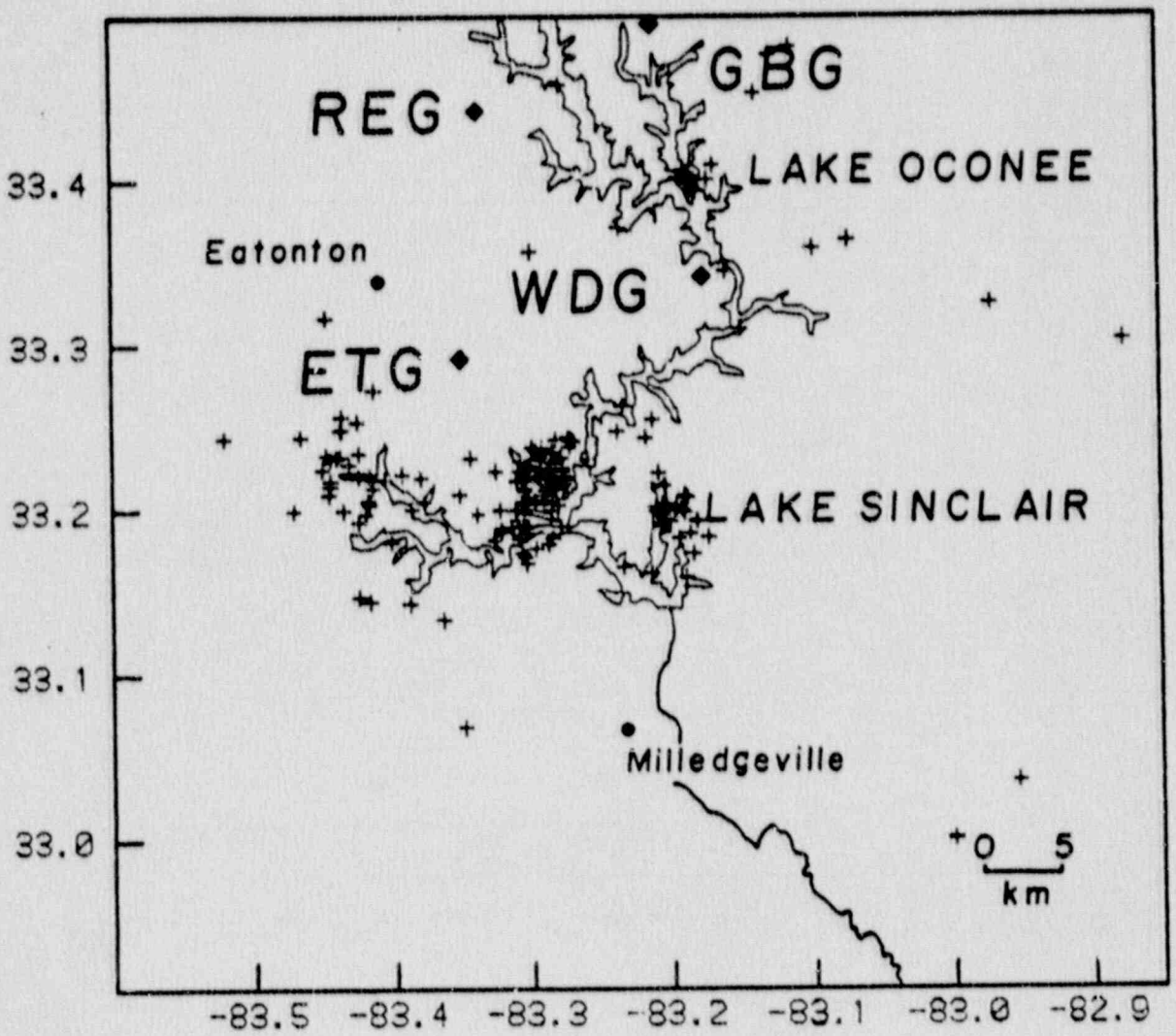

Figure 11. Epicenters for the Lake Sinclair and Lake Oconee areas using the two-layer velocity Model.

NRC FORM 335 (2-89) NRCM 1102, 3201, 3202

U.S. NUCLEAR REGULATORY COMMISSION

BIBLIOGRAPHIC DATA SHEET

(See instructions on the reverse)

1. REPORT NUMBER (Assigned by NRC, Add Vol., Supp., Rev., and Addendum Numbers, if any.)

NUREG/CR-5258, Vol. 3

2. TITLE AND SUBTITLE

Georgia/Alabama Regional Seismographic Network
Annual Report
July 1987 - June 1988

3. DATE REPORT PUBLISHED

MONTH: September | YEAR: 1990

4. FIN OR GRANT NUMBER

D1598

5. AUTHOR(S)

L. T. Long

6. TYPE OF REPORT

Annual Report

7. PERIOD COVERED (Inclusive Dates)

July 1987 - June 1988

8. PERFORMING ORGANIZATION - NAME AND ADDRESS (If NRC, provide Division, Office or Region, U.S. Nuclear Regulatory Commission, and mailing address; if contractor, provide name and mailing address.)

School of Earth and Atmospheric Sciences
Georgia Institute of Technology
Atlanta, Georgia 30332

9. SPONSORING ORGANIZATION - NAME AND ADDRESS (If NRC, type "Same as above"; if contractor, provide NRC Division, Office or Region, U.S. Nuclear Regulatory Commission, and mailing address.)

Division of Engineering
Office of Nuclear Regulatory Research
U.S. Nuclear Regulatory Commission
Washington, DC 20555

10. SUPPLEMENTARY NOTES

11. ABSTRACT (200 words or less)

A review of the historical seismicity of southeastern Tennessee suggests that the period of 1970 through 1988 was anomalously more active than before 1970. If this is true, then it represents a unique stress release event that would satisfy the model for major intraplate earthquakes proposed by Long (1988). First motion data and SV/P amplitude ratios were used to determine 36 single events and two composite focal mechanism solutions for earthquakes in southeastern Tennessee. The dominant focal mechanism is strike slip with reverse or normal fault components. Linearizing the relation between measured apparent coda Q and assumed constant coda Q for discrete zones of crust suggests an anomalously low (Q=50) region northeast of station CBT. Fracture density was mapped in an area of induced seismicity near Clarks Hill Reservoir. It appears that areas of higher joint spacing correspond to zones of induced seismicity. In this and other reservoirs, earthquakes tend to occur in granite gneiss where jointing is sparse and the rock is strong. Seismic activity is not often observed in foliated schists and altered mafic rocks, in which stress may be released through creep.

12. KEY WORDS/DESCRIPTORS (List words or phrases that will assist researchers in locating the report.)

Seismicity
Induced Seismicity
Focal Mechanisms
Coda Q
Georgia
Alabama
Tennessee

13. AVAILABILITY STATEMENT

Unlimited

14. SECURITY CLASSIFICATION

(This Page) Unclassified

(This Report) Unclassified

15. NUMBER OF PAGES

16. PRICE

UNITED STATES
NUCLEAR REGULATORY COMMISSION
WASHINGTON, D.C. 20555